Adam Can Converge Without Any Modification On Update Rules

Yushun Zhang[14], **Congliang Chen**[1], **Naichen Shi**[2], **Ruoyu Sun**[3]*, **Zhi-Quan Luo**[14]
[1]The Chinese University of Hong Kong, Shenzhen, China [2]University of Michigan, US
[3]University of Illnois at Urbna-Champaign, US [4]Shenzhen Research Institute of Big Data
{yushunzhang,congliangchen}@link.cuhk.edu.cn, naichens@umich.edu
ruoyus@illinois.edu, luozq@cuhk.edu.cn

Abstract

Ever since Reddi et al. (2018) pointed out the divergence issue of Adam, many new variants have been designed to obtain convergence. However, vanilla Adam remains exceptionally popular and it works well in practice. Why is there a gap between theory and practice? We point out there is a mismatch between the settings of theory and practice: Reddi et al. (2018) pick the problem after picking the hyperparameters of Adam, i.e., (β_1, β_2); while practical applications often fix the problem first and then tune (β_1, β_2). Due to this observation, we conjecture that the empirical convergence can be theoretically justified, only if we change the order of picking the problem and hyperparameter. In this work, we confirm this conjecture. We prove that, when the 2nd-order momentum parameter β_2 is large and 1st-order momentum parameter $\beta_1 < \sqrt{\beta_2} < 1$, Adam converges to the neighborhood of critical points. The size of the neighborhood is propositional to the variance of stochastic gradients. Under an extra condition (strong growth condition), Adam converges to critical points. As β_2 increases, our convergence result can cover any $\beta_1 \in [0, 1)$ including $\beta_1 = 0.9$, which is the default setting in deep learning libraries. To our knowledge, this is the first result showing that Adam can converge under a wide range of hyperparameters *without any modification* on its update rules. Further, our analysis does not require assumptions of bounded gradients or bounded 2nd-order momentum. When β_2 is small, we further point out a large region of (β_1, β_2) combinations where Adam can diverge to infinity. Our divergence result considers the same setting (fixing the optimization problem ahead) as our convergence result, indicating that there is a phase transition from divergence to convergence when increasing β_2. These positive and negative results provide suggestions on how to tune Adam hyperparameters: for instance, when Adam does not work well, we suggest tuning up β_2 and trying $\beta_1 < \sqrt{\beta_2}$.

1 Introduction

Modern machine learning tasks often aim to solve the following finite-sum problem.

$$\min_{x \in \mathbb{R}^d} f(x) = \sum_{i=0}^{n-1} f_i(x), \tag{1}$$

where n is the number of samples or mini-batches and x denotes the trainable parameters. In deep learning, Adam (Kingma & Ba, 2014) is one of the most popular algorithms for solving (1). It has been applied to various machine learning domains such as natural language processing (NLP) (Vaswani et al., 2017; Brown et al., 2020; Devlin et al., 2018), generative adversarial networks (GANs) (Radford et al., 2015; Isola et al., 2017; Zhu et al., 2017) and computer vision (CV) (Dosovitskiy et al., 2021). Despite its prevalence, Reddi et al. (2018) point out that Adam can diverge with a wide range of hyperparameters. A main result in (Reddi et al., 2018) states that [2]:

*Correspondence author

[2]We formally re-state their results in Appendix D.2.

36th Conference on Neural Information Processing Systems (NeurIPS 2022).

For any β_1, β_2 s.t. $0 \le \beta_1 < \sqrt{\beta_2} < 1$, there exists a problem such that Adam diverges.

Here, β_1 and β_2 are the hyperparameter to control Adam's 1st-order and 2nd-order momentum. More description of Adam can be seen in Algorithm 1 (presented later in Section 2.1). Ever since (Reddi et al., 2018) pointed out the divergence issue, many new variants have been designed. For instance, AMSGrad (Reddi et al., 2018) enforced the adaptor v_t (defined later in Algorithm 1) to be non-decreasing; AdaBound (Luo et al., 2019) imposed constraint $v_t \in [C_l, C_u]$ to ensure the boundedness on effective stepsize. We introduce more variants in Appendix D.1.

On the other hand, counter-intuitively, vanilla Adam remains exceptionally popular (see evidence at (Scholar)). Without any modification on its update rules, Adam works well in practice. Even more mysteriously, we find that the commonly reported hyperparameters actually satisfy the divergence condition stated earlier. For instance, Kingma & Ba (2014) claimed that $(\beta_1, \beta_2) = (0.9, 0.999)$ is a "good choice for the tested machine learning problems" and it is indeed the default setting in deep learning libraries. In super-large models GPT-3 and Megatron (Brown et al., 2020; Smith et al., 2022), (β_1, β_2) is chosen to be $(0.9, 0.95)$. GAN researchers (e.g. Radford et al. (2015); Isola et al. (2017)) use $(\beta_1, \beta_2) = (0.5, 0.999)$. All these hyperparameters live in the divergence region $\beta_1 < \sqrt{\beta_2}$. Surprisingly, instead of observing the divergence issue, these hyperparameters achieve good performances and they actually show the sign of convergence.

Why does Adam work well despite its theoretical divergence issue? Is there any mismatch between deep learning problems and the divergent example? We take a closer look into the divergence example and find out the mismatch *does* exist. In particular, we notice an important (but often ignored) characteristic of the divergence example: (Reddi et al., 2018) picks (β_1, β_2) *before* picking the sample size n. Put in another way, to construct the divergence example, they change n for different (β_1, β_2). For instance, for $(\beta_1, \beta_2) = (0, 0.99)$, they use one n to construct the divergent example; for $(\beta_1, \beta_2) = (0, 0.9999)$, they use another n to construct another divergent example. On the other hand, in practical applications of Adam listed above, practitioners tune the hyperparameters (β_1, β_2) *after* the sample size n is fixed. So there is a gap between the setting of theory and practice: the order of picking n and (β_1, β_2) is different.

Considering the good performance of Adam under fixed n, we conjecture that Adam can converge in this setting. Unfortunately, the behavior of vanilla Adam is far less studied than its variants (perhaps due to the criticism of divergence). To verify this conjecture, we run experiments for different choices of (β_1, β_2) on a few tasks. First, we run Adam for a convex function (2) with fixed n (see the definition in Section 3.2). Second, we run Adam for the classification problem on data MNIST and CIFAR-10 with fixed batchsize. We observe some interesting phenomena in Figure 1 (a), (b) and (c).

First, when β_2 is large, the optimization error is small for almost all values of β_1. Second, when $\beta_1,\ \beta_2$ are both small, there is a red region with relatively large error. On MNIST, CIFAR-10, the error in the red region is increased by 1.4 times than that in the blue region. The situation is a lot worse on function (2) (defined later in Section 3.2): the error in the red region is 70 times higher.

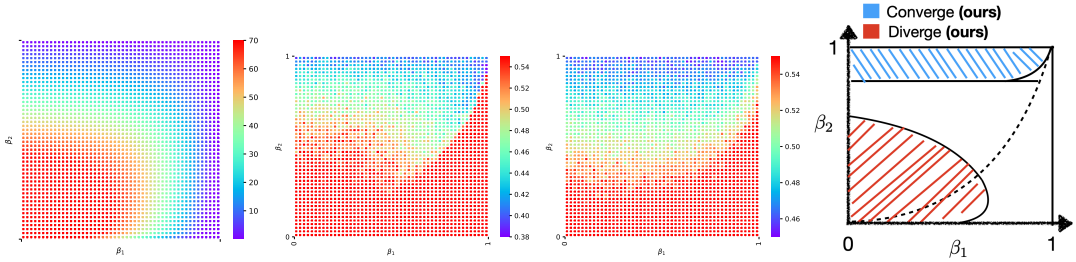

(a) Function (2) (b) MNIST (c) CIFAR-10 (d) Our contribution

Figure 1: **(a), (b), (c)**: The performance of Adam on different tasks. For each task, we show the results with β_1 and β_2 in grids $\{(k_1/50, k_2/50) | k_1 = 0, \cdots, 49, k_2 = 0, \cdots, 49\}$. **(a)**: the optimality gap $x - x^*$ on the convex function (2). **(b) (c)**: The training loss on MNIST and CIFAR-10. **(d)**: An illustration of our contribution in (β_1, β_2) phase diagram. The shape of the region follows the solution to our analytic conditions. The size of the region depends on n. The dotted curve satisfies $\beta_1 = \sqrt{\beta_2}$. In all figures, n is fixed before picking (β_1, β_2).

While Adam's performances seem unstable in the red region, we find that *Adam always performs well in the top blue region in Figure 1.* This seems to suggest that Adam can converge without any algorithmic modification, as long as β_1 and β_2 are chosen properly. We ask the following question:

In this work, we theoretically explore this question. Our contributions are visualized in Figure 1 (d). We prove the following results when n is fixed (or more rigorously, when the function class is fixed):

- We prove that when β_2 is large enough and $\beta_1 < \sqrt{\beta_2}$, Adam converges to the neighborhood of critical points. The size of the neighborhood is propositional to the variance of stochastic gradients. With an extra condition (so-called strong growth condition), we prove that Adam can converge to critical points. As β_2 increases, these results can cover any momentum parameter $\beta_1 \in [0, 1)$ including the default setting $\beta_1 = 0.9$. In particular, our analysis does *not* require bounded gradient assumption.
- We study the divergence issue of small-β_2 Adam. We prove that: for any fixed n (or more rigorously, for any fixed function class), there exists a function such that, Adam diverges to infinity when (β_1, β_2) is picked in the red region in Figure 1 (d). The size of the red region increases with n. The shape of the region follows the solution to our analytic conditions.
- We emphasize a few characteristics of our results. **(1) phase transition**. The divergence result considers the same setting as our convergence result, indicating that there is a phase transition from divergence to convergence when changing β_2. **(2) problem-dependent bounds**. Our convergence and divergence regions of (β_1, β_2) are problem-dependent, which is drastically different from (Reddi et al., 2018) which established the problem-independent worst-case choice of (β_1, β_2). **(3) non-asymptotic characterization**. the "divergence region" of (β_1, β_2) expands as n increases and converges to the whole region $[0, 1)^2$ as n goes to infinity, which recovers (actually stronger than) the problem-independent divergence result of (Reddi et al., 2018) that requires $\beta_1 < \sqrt{\beta_2}$. In this sense, we can view the divergence result of (Reddi et al., 2018) as an asymptotic characterization of the divergence region (as $n \to \infty$) and our divergence result as a non-asymptotic characterization (for any fixed n). We provide more discussion in Section 4.
- Our positive and negative results can provide suggestions for tuning β_1 and β_2: for instance,when Adam does not work well, we suggest tuning up β_2 and trying $\beta_1 < \sqrt{\beta_2}$. We provide more tuning suggestions in Appendix C.

We believe our results can boost new understandings for Adam. While Reddi et al. (2018) reveal that "Adam can diverge", our results show the other side of the coin: when n is fixed (or when function class is fixed), Adam can still converge without any modification on its update rules. Our results suggest that Adam is still a theoretically justified algorithm and practitioners can use it confidently.

We further emphasize that our convergence results can cover any $\beta_1 \in [0, 1)$, which allows the algorithm to bring arbitrarily heavy momentum signals. It turns out that large-momentum Adam is not easy to analyze. Even with stronger assumptions like bounded gradient ($\|\nabla f(x)\| < \mathrm{C}, \forall x$), its convergence is not well understood (see related works in Section 2.2). To our best knowledge, this is the first result that proves vanilla Adam with any β_1 can converge *without* any assumption of bounded gradient or bounded 2nd-order momentum. The proof contains a new method to handle unbounded momentum in the stochastic non-linear dynamics system. We will highlight our technical novelties in Section 5.

2 Preliminaries

2.1 Review of Adam

We consider finite-sum problem (1). We use x to denote the optimization variable. We denote ∇f_j as the gradient of f_j and let $\circ$ be the component-wise product. The division and square-root operator are component-wise as well. We present randomly shuffled Adam in Algorithm 1.

In Algorithm 1, m denotes the 1st-order momentum and v denotes the 2nd-order momentum. they are weighted averaged by hyperparameter β_1, β_2, respectively. Larger β_1, β_2 will adopt more history information. We denote $x_{k,i}, m_{k,i}, v_{k,i} \in \mathbb{R}^d$ as the value of x, m, v at the k-th outer loop (epoch) and i-th inner loop (batch), respectively. We choose $\eta_k = \frac{\eta_1}{\sqrt{nk}}$ as the stepsize. In practice, ϵ is adopted for numerical stability and it is often chosen to be 10^{-8}. In our theory, we allow ϵ to be an arbitrary non-negative constant including 0.

In the original version of Adam in (Kingma & Ba, 2014), it has an additional "bias correction" step. This "bias correction" step can be implemented by changing the stepsize η_k into $\hat{\eta}_k = \frac{\sqrt{1-\beta_2^k}}{1-\beta_1^k}\eta_k$

Algorithm 1 Adam

Initialize $x_{1,0} = x_0$, $m_{1,-1} = \nabla f(x_0)$ and $v_{1,-1} = \max_i \nabla f_i(x_0) \circ \nabla f_i(x_0)$.
for $k = 1 \to \infty$ **do**
  Sample $\{\tau_{k,0}, \tau_{k,1}, \cdots, \tau_{k,n-1}\}$ as a random permutation of $\{0, 1, 2, \cdots, n-1\}$
  for $i = 0 \to n-1$ **do**
    $m_{k,i} = \beta_1 m_{k,i-1} + (1-\beta_1) \nabla f_{\tau_{k,i}}(x_{k,i})$
    $v_{k,i} = \beta_2 v_{k,i-1} + (1-\beta_2) \nabla f_{\tau_{k,i}}(x_{k,i}) \circ \nabla f_{\tau_{k,i}}(x_{k,i})$
    $x_{k,i+1} = x_{k,i} - \frac{\eta_k}{\sqrt{v_{k,i}+\epsilon}} \circ m_{k,i}$
  end for
  $x_{k+1,0} = x_{k,n}$; $v_{k+1,-1} = v_{k,n-1}$; $m_{k+1,-1} = m_{k,n-1}$
end for

and using zero initialization. In Algorithm 1, the "bias correction" step is replaced by a special initialization, which also corrects the bias. Note that $\hat{\eta_k} \in [\sqrt{1-\beta_2}\eta_k, \frac{1}{1-\beta_1}\eta_k]$ is well-bounded near η_k, so η_k and $\hat{\eta_k}$ brings the same convergence rate. In addition, as the effect of initialization becomes negligible when the training progresses, Adam with zero & our initialization will have the same asymptotic behavior. We follow the form of Algorithm 1, which makes results cleaner. In our analysis, we make the assumptions below.

Assumption 2.1. we consider $x \in \mathbb{R}^d$ and $f_i(x)$ satisfies gradient Lipschitz continuous with constant L. We assume $f(x)$ is lower bounded by a finite constant f^*.

Assumption 2.2. $f_i(x)$ and $f(x)$ satisfy: $\sum_{i=0}^{n-1} \|\nabla f_i(x)\|_2^2 \leq D_1 \|\nabla f(x)\|_2^2 + D_0, \forall x \in \mathbb{R}^d$.

Assumption 2.2 is quite general. When $D_1 = 1/n$, it becomes the "constant variance" with constant D_0/n. "constant variance" condition is commonly used in both SGD and Adam analysis (e.g. (Ghadimi et al., 2016; Zaheer et al., 2018; Huang et al., 2021)). Assumption 2.2 allows more flexible choices of $D_1 \neq n$ and thus it is weaker than "constant variance".

When $D_0 > 0$, the problem instance is sometimes called "non-realizable" (Shi et al., 2020). In this case, adaptive gradient methods are not guaranteed to reach the exact critical points. Instead, they only converge to a bounded region (near critical points) (Zaheer et al., 2018; Shi et al., 2020). This phenomenon indeed occurs for Adam in experiments, even with diminishing stepsize (see Figure 4 (a)). The behavior of SGD is similar: constant stepsize SGD converges to a bounded region with its size propositional to the noise level D_0 (Yan et al., 2018; Yu et al., 2019; Liu et al., 2020b).

When $D_0 = 0$, Assumption 2.2 is often called "strong growth condition" (SGC) (Vaswani et al., 2019). When $\|\nabla f(x)\| = 0$, under SGC we have $\|\nabla f_j(x)\| = 0$ for all j. SGC is increasingly popular recently e.g.(Schmidt & Roux, 2013; Vaswani et al., 2019). This condition is known to be reasonable in the overparameterized regime where neural networks can interpolate all data points (Vaswani et al., 2019). We will show that Adam can converge to critical points if SGC holds.

When n, f^*, L, D_0, D_1 are fixed a priori, we use $\mathcal{F}^{n,f^*}_{L,D_0,D_1}(\mathbb{R}^d)$ to denote the function class containing $f(x)$ satisfying Assumption 2.1 and 2.2 with constant n, f^*, etc.. Since n is fixed when the function class $\mathcal{F}^{n,f^*}_{L,D_0,D_1}(\mathbb{R}^d)$, we introduce this notation to clearly present the divergence result in Proposition 3.3. Without this pre-defined function class, the claim of divergence might be confusing.

2.2 Related Works

Ever since Reddi et al. (2018) pointed out the divergence issue, there are many attempts on designing new variants of Adam. Since we focus on understanding Adam *without modification* on its update rules, we introduce more variants later in Appendix D.1.

Compared with proposing new variants, the convergence of vanilla Adam is far less studied than its variants (perhaps due to the criticism of divergence). There are only a few works analyzing vanilla Adam and they require extra assumptions. Zhou et al. (2018b) analyze the counter-example in (Reddi et al., 2018) and find certain hyperparameter can work. However, their analysis is restricted to the counter-example. Zaheer et al. (2018) study the relation between mini-batch sizes and (non-)convergence of Adam. However, this work require $\beta_1 = 0$ and Adam is reduced to RMSProp (Hinton et al., 2012). De et al. (2018) analyze RMSProp and non-zero-β_1 Adam, but they assume the sign of all stochastic gradients to keep the same. It seems unclear how to check this condition a priori.

Additionally, they require β_1 to be inversely related to the upper bound of gradient, which forces β_1 to be small (as a side note, this result only applies to full-batch Adam). Défossez et al. (2020) analyze Adam with $\beta_1 < \beta_2$ and provide some insights on the momentum mechanisms. However, their bound is inversely proportional to ϵ (the hyperparameter for numerical stability) and the bound goes to infinity when ϵ goes to 0. This is different from practical application since small ϵ such as 10^{-8} often works well. Further, using large ϵ is against the nature of adaptive gradient methods because $\sqrt{v}$ no longer dominates in the choice of stepsize. In this case, Adam is essentially transformed back to SGD. Two recent works (Huang et al., 2021) and (Guo et al., 2021) propose novel and simple frameworks to analyze Adam-family with large β_1. Yet, they require the effective stepsize of Adam to be bounded in certain interval, i.e., $\frac{1}{\sqrt{v_t}+\epsilon} \in [C_l, C_u]$ [3]. This boundedness condition changes Adam into AdaBound (Luo et al., 2019) and thus they cannot explain the observations on original Adam in Section 1. To summarize, all these works require at least one strong assumption (e.g. large ϵ). Additionally, they all (including those for new variants) require bounded gradient assumptions.

A recent work (Shi et al., 2020) takes the first attempt to analyze RMSProp without bounded gradient assumption. They show that RMSProp can converge to the neighborhood of critical points. [4] We believe it is important to study Adam rather than RMSProp: Numerically, Adam often outperforms RMSProp on complicated tasks (e.g. on Atari games, the mean reward is improved from 88% to 110% (Agarwal et al., 2020)). Theoretically, literature on RMSProp cannot reveal the interaction between β_1 and β_2; or how these hyperparameters jointly affect (or jeopardize) the convergence of Adam. However, it is non-trivial to jointly analyze the effect of β_1 and β_2. We point out there are at least three challenges. First, it seems unclear how to control the massive momentum m_t of Adam. Second, m_t is multiplied by $1/\sqrt{v_t}$, causing non-linear perturbation. Third, m_t and $1/\sqrt{v_t}$ are statistically dependent and cannot be decoupled. We propose new methods to resolve these issues. We highlight our technical novelties in Section 5.

2.3 The Importance and Difficulties of Removing Bounded Gradient Assumptions

Here, we emphasize the importance to remove bounded gradient assumption. First, unlike the assumptions in Section 2.1, bounded gradient is *not* common in SGD analysis. So it is of theoretical interests to remove this condition for Adam. Second, bounded gradient condition rules out the chances of gradient divergence a priori. However, there are numerical evidences showing that Adam's gradient can diverge (see Section 6 and Appendix B). Removing the boundedness assumption helps us point out the divergence and convergence phase transition in the (β_1, β_2) diagram.

However, it is often difficult to analyze convergence without bounded gradient assumption. First, it is non-trivial to control stochastic momentum. Even for SGD, this task is challenging. For instance, An early paper Bertsekas & Tsitsiklis (2000) analyzed SGD-type methods without any boundedness condition. But it is not until recently that Yu et al. (2019); Liu et al. (2020b); Jin et al. (2022) prove SGDM (SGD with momentum) converges without bounded gradient assumption. Such attempts of removing boundedness assumptions are often appreciated for general optimization problems where "bounded-assumption-free" is considered as a major contribution.

Secondly, for Adam, the role of momentum m_t is even more intricate since it is multiplied by $1/\sqrt{v_t}$. Combined with v_t, the impact of previous signals not only affect the update direction, but also change the stepsize for each component. Further, both momentum m_t and stepsize $1/\sqrt{v_t}$ are random variables and they are highly correlated. Such statistical dependency causes trouble for analysis. In summary, the role of momentum in Adam could be much different from that in SGDM or GDM. Even with boundedness conditions, the convergence of large-β_1 Adam is still not well understood (see related works in Section 2.2). In this work, we propose new techniques to handle Adam's momentum under any large β_1, regardless of the gradient magnitude. These techniques are not revealed in any existing works. We introduce our technical contribution in Section 5.

3 Main Results

3.1 Convergence Results

Here, we give the convergence results under large β_2.

[3] For completeness, we explain why they require this condition in Appendix D.1.

[4] They also provide a convergence result for Adam with β_1 close enough to 0. However, a simple calculation by Zhang et al. (2022) shows that they require $\beta_1 < 10^{-7}$. Thus their result does not provide much extra information other than RMSProp.

Theorem 3.1. *For any $f(x) \in \mathcal{F}^{n,f^*}_{L,D_0,D_1}(\mathbb{R}^d)$, we assume the hyperparameters in Algorithm 1 satisfy: $\beta_1 < \sqrt{\beta_2} < 1$; β_2 is greater or equal to a threshold $\gamma_1(n)$; and $\eta_k = \frac{\eta_1}{\sqrt{nk}}$. Let $k_m \in \mathbb{N}$ satisfies $k_m \geq 4$ and $\beta_1^{(k_m-1)n} \leq \frac{\beta_1^n}{\sqrt{k_m-1}}$,* [5] *we have the following results for any $T > k_m$:*

$$\min_{k\in[k_m,T]} \mathbb{E}\left\{\min\left[\sqrt{\frac{2D_1 d}{D_0}}\|\nabla f(x_{k,0})\|_2^2, \|\nabla f(x_{k,0})\|_2\right]\right\} = \mathcal{O}\left(\frac{\log T}{\sqrt{T}}\right) + \mathcal{O}(\sqrt{D_0}).$$

Remark 1: the choice of β_2. Our theory suggests that large β_2 should be used to ensure convergence. This message matches our experimental findings in Figure 1. We would like to point out that the requirement of "large β_2" is neccessary, because small β_2 will indeed lead to divergence (shown later in Section 3.2). We here comment a bit on the the threshold $\gamma_1(n)$. $\gamma_1(n)$ satisfies $\beta_2 \geq 1 - \mathcal{O}\left(\frac{1-\beta_1^n}{n^2\rho}\right)$ (see inequality (34) and Remark G.7), where ρ is a constant that depends on the training trajectory. In worst cases, ρ is upper bounded by $n^{2.5}$, but we find the practical ρ to be much smaller. In Appendix B, we estimate ρ on MNIST and CIFAR-10. In practical training process, we empirically observe that $\rho \approx \mathcal{O}(n)$, thus the required $\gamma_1(n) \approx 1 - \mathcal{O}\left(n^{-3}\right)$. Note that our threshold of β_2 is a sufficient condition for convergence, so there may be a gap between the practical choices and the theoretical bound of β_2. Closing the gap will be an interesting future direction.

We find that $\gamma_1(n)$ increases with n. This property suggests that larger β_2 should be used when n is large. This phenomenon is also verified by our experiments in Appendix B. We also remark that $\gamma_1(n)$ slowly increases with β_1. This property is visualized in Figure 1 (d) where the lower boundary of blue region slightly lifts up when β_1 increases.

Remark 2: the choice of β_1. Theorem 3.1 requires $\beta_1 < \sqrt{\beta_2}$. Since β_2 is suggested to be large, our convergence result can cover flexible choice of $\beta_1 \in [0, 1)$. For instance, $\beta_2 = 0.999$ brings the threshold of $\beta_1 < 0.9995$, which covers basically all practical choices of β_1 reported in the literature (see Section 1), including the default setting $\beta_1 = 0.9$. This result is much stronger than those in the RMSProp literature (e.g. (Shi et al., 2020; Zaheer et al., 2018)). To our knowledge, we are the first to prove convergence of Adam under any $\beta_1 \in [0, 1)$ without bounded gradient assumption.

Remark 3: convergence to a bounded region. When $D_0 > 0$, Adam converges to a bounded region near critical points. As discussed in Section 2.1, converging to bounded region is common for stochastic methods including constant-stepsize SGD (Yan et al., 2018; Yu et al., 2019; Liu et al., 2020b) and diminishing-stepsize RMSProp (Zaheer et al., 2018; Shi et al., 2020). This phenomenon is also observed in practice: even for convex quadratic function with $D_0 > 0$, Adam with diminishing stepsize *cannot* reach exactly zero gradient (see Figure 4 (a) in Section 6). This is because: even though η_k is decreasing, the effective stepsize $\eta_k/\sqrt{v_{k,i}}$ might not decay. The good news is that, the constant $\mathcal{O}(\sqrt{D_0})$ vanishes to 0 as β_2 goes to 1 (both in theory and experiments). The relation between β_2 and constant $\mathcal{O}(\sqrt{D_0})$ are introduced in Remark G.14 in Appendix G.9. The size shrinks to 0 because the movement of $\sqrt{v_{k,i}}$ shrinks as β_2 increases.

As a corollary of Theorem 3.1, we have the following result under SGC (i.e., $D_0 = 0$).

Corollary 3.2. *Under the setting in Theorem 3.1. When $D_0 = 0$ for Assumption 2.2, we have*

$$\min_{k\in[k_m,T]} \mathbb{E}\|\nabla f(x_{k,0})\|_2 = \mathcal{O}\left(\frac{\log T}{\sqrt{T}}\right).$$

Under SGC (i.e. $D_0 = 0$), Corollary 3.2 states that Adam can converge to critical points. This is indeed the case in practice. For instance, function (2) satisfies SGC and we observe 0 gradient norm after Adam converges (see Section 6 and Appendix B). The convergence rate in Corollary 3.2 is comparable to that of SGD under the same condition in (Vaswani et al., 2019).

3.2 Divergence Results

Theorem 3.1 shows that when β_2 is large, any $\beta_1 < \sqrt{\beta_2}$ ensures convergence. Now we consider the case where β_2 is small. We will show that in this case, a wide range of β_1 is facing the risk of diverging to infinity. The divergence of small-β_2 Adam suggests that "large β_2" is necessary in

[5] When $\beta_1 = 0.9$, $k_m = 15$ for any $n \geq 1$.

the convergence result Theorem 3.1. We construct a counter-example in $\mathcal{F}^{n,f^*}_{L,D_0,D_1}(\mathbb{R}^d)$. Consider $f(x) = \sum_{i=0}^{n-1} f_i(x)$ for $x \in \mathbb{R}$, we define $f_i(x)$ as:

$$
\begin{aligned}
f_i(x) &= \begin{cases} nx, & x \geq -1 \\ \frac{n}{2}(x+2)^2 - \frac{3n}{2}, & x < -1 \end{cases} \quad \text{for } i = 0, \\
f_i(x) &= \begin{cases} -x, & x \geq -1 \\ -\frac{1}{2}(x+2)^2 + \frac{3}{2}, & x < -1 \end{cases} \quad \text{for } i > 0.
\end{aligned} \tag{2}
$$

Summing up all the $f_i(x)$, we can see that

$$
f(x) = \begin{cases} x, & x \geq -1 \\ \frac{1}{2}(x+2)^2 - \frac{3}{2}, & x < -1 \end{cases}
$$

is a lower bounded convex smooth function with optimal solution $x^* = -2$. Function (2) allows both iterates and gradients to diverge to infinity. As shown in Figure 1 (a), when running Adam on (2), there exists a red large-error region. This shows the sign of divergence. We further theoretically verify the conjecture in Proposition 3.3.

Proposition 3.3. *For any function class $\mathcal{F}^{n,f^*}_{L,D_0,D_1}(\mathbb{R}^d)$, there exists a $f(x) \in \mathcal{F}^{n,f^*}_{L,D_0,D_1}(\mathbb{R}^d)$, s.t. when (β_1, β_2) satisfies analytic condition* (12), (13), (14) *in Appendix E, Adam's iterates and function values diverge to infinity. By solving these conditions in* `NumPy`*, we plot the orange region in Figure 2. The size of the region depends on n and it expands to the whole region when n goes to infinity.*

The proof can be seen in Appendix E. We find the "divergence region" always stays below the "convergence threshold" $\gamma_1(n)$ in Theorem 3.1, so the two results are self-consistent (see the remark in Appendix E). Proposition 3.3 states the divergence of iterates and function values. Consistently, our experiments also show the divergence of gradient (see Section 6 and Appendix B). These results characterize Adam's divergence behavior both numerically and theoretically.

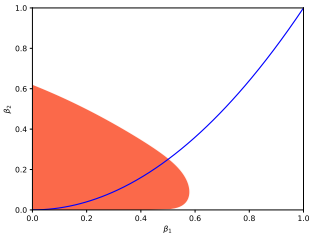

Figure 2: On function (2) with $n = 20$, Adam diverges in the colored region. The region is plotted by solving condition (12), (13), (14) in `NumPy`. The blue curve satisfies $\beta_1 = \sqrt{\beta_2}$.

We emphasize that the orange region is *not* discussed in (Reddi et al., 2018) because we consider n fixed while they allow n changing. When n is allowed to increase, our orange region will expand to the whole region and thus we can derive a similar (actually stronger) result as (Reddi et al., 2018). We provide more explanation in Section 4. Combining Theorem 3.1 and Proposition 3.3, we establish a clearer image on the relation between (β_1, β_2) and qualitative behavior of Adam.

4 Reconciling Our Results with (Reddi et al., 2018)

We discuss more on the relation between (Reddi et al., 2018) and our results. The divergence result shown in Section 1 does not contradict with our convergence results in Theorem 3.1. Further, it is different from our divergence result in Proposition 3.3. The key difference lies in whether (β_1, β_2) is picked *before or after* picking the function class $\mathcal{F}^{n,f^*}_{L,D_0,D_1}(\mathbb{R}^d)$. We discuss the following two cases.

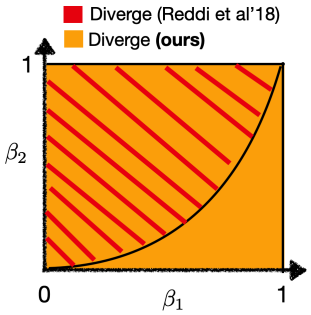

Figure 3: Adam's behavior when (β_1, β_2) in **Case I**.

Case I: When (β_1, β_2) is picked before picking $\mathcal{F}^{n,f^*}_{L,D_0,D_1}(\mathbb{R}^d)$. As discussed in Section 1, the divergence result requires different n for different (β_1, β_2). In this sense, the considered function class is constantly changing. It does *not* contradict with our Theorem 3.1 which considers a fixed function class with fixed n. For **Case I**, we illustrate Adam's behavior in Figure 3. The red region is proved by (Reddi et al., 2018). For completeness, we remove the condition "$\beta_1 < \sqrt{\beta_2}$" and further prove that Adam will diverge to infinity for *any* $(\beta_1, \beta_2) \in [0, 1)^2$. The result is shown in the following Corollary 4.1.

Corollary 4.1. *For any $(\beta_1, \beta_2) \in [0, 1)^2$, there exists a function satisfying Assumption 2.1 and 2.2 that the Adam's iterates and function values diverge to infinity.*

Proof of Corollary 4.1 can be seen in the final paragraph in Appendix E. In the proof, we also require different n to cause divergence for different (β_1, β_2). So the function class is constantly changing. As a result, in **Case I**, we cannot prove any convergence result.

Table 1: Possible algorithmic behaviors of Adam in **Case II**.

Setting	Hyperparameters	Adam's behavior
$\forall f \in \mathcal{F}^{n,f^*}_{L,D_0,D_1}(\mathbb{R}^d)$ with $D_0 = 0$	β_2 is large and $\beta_1 < \sqrt{\beta_2}$	converge to critical points **(Ours)**
$\forall f \in \mathcal{F}^{n,f^*}_{L,D_0,D_1}(\mathbb{R}^d)$ with $D_0 \neq 0$	β_2 is large and $\beta_1 < \sqrt{\beta_2}$	converge to a bounded region with size $\mathcal{O}(D_0)$ **(Ours)**
$\exists f \in \mathcal{F}^{n,f^*}_{L,D_0,D_1}(\mathbb{R}^d)$	The orange region in Figure 2	diverge to infinity **(Ours)**

Case II: When (β_1, β_2) is picked after picking $\mathcal{F}^{n,f^*}_{L,D_0,D_1}(\mathbb{R}^d)$. When the function class is picked in advance, sample size n will also be fixed. This case is closer to most practical applications. In this case, we find that Adam's behavior changes significantly in the different region of Figure 3. First, $\forall f(x) \in \mathcal{F}^{n,f^*}_{L,D_0,D_1}(\mathbb{R}^d)$ will converge when $\beta_1 < \sqrt{\beta_2}$ and β_2 is large. Second, $\exists f(x) \in \mathcal{F}^{n,f^*}_{L,D_0,D_1}(\mathbb{R}^d)$ will diverge to infinity when (β_1, β_2) are in the orange region in Figure 2. Since **Case II** is closer to practical scenarios, these results can provide better guidance for hyperparameter tuning for Adam users. We provide some suggestions for practitioners in Appendix C.

For **Case II**, we summarize the possible behaviors of Adam in Table 1. We also illustrate our convergence and divergence results in Figure 1 (d). Note that there are some blanket areas where Adam's behavior remains unknown, this part will be left as interesting future work.

5 Proof Ideas for the Convergence Result

We now (informally) introduce our proof ideas for the convergence result in Theorem 3.1. Simply put, we want to control the update direction $m_{k,i}/\sqrt{v_{k,i}}$ inside the dual cone of gradient direction. Namely:

$$\mathbb{E}\langle \nabla f(x_{k,0}), \sum_{i=0}^{n-1} \frac{m_{k,i}}{\sqrt{v_{k,i}}} \rangle > 0. \tag{3}$$

However, directly proving (3) could be difficult because both $m_{k,i}$ and $v_{k,i}$ distort the trajectory. To start with, we try to control the movement of $v_{k,i}$. We use a standard approach for Adam-type algorithms: use large or increasing β_2 (e.g. (Shi et al., 2020; Zou et al., 2019; Chen et al., 2018b)). Recall $v_{k,i} = (1-\beta_2)\sum_{j=1}^{i} \beta_2^{i-j} \nabla f_{\tau_{k,j}}(x_{k,j}) \circ \nabla f_{\tau_{k,j}}(x_{k,j}) + \beta_2^i v_{k,0}$, we have $v_{k,i} \approx v_{k,0}$ when β_2 is large. In this case, we have:

$$\mathbb{E}\left\langle \nabla f(x_{k,0}), \sum_{i=0}^{n-1} \frac{m_{k,i}}{\sqrt{v_{k,i}}} \right\rangle \approx \mathbb{E}\left\langle \frac{\nabla f(x_{k,0})}{\sqrt{v_{k,0}}}, \sum_{i=0}^{n-1} m_{k,i} \right\rangle \approx \mathbb{E}\left\langle \frac{\nabla f(x_{k,0})}{\sqrt{v_{k,0}}}, \nabla f(x_{k,0}) \right\rangle > 0,$$

where the first "$\approx$" is due to the large β_2 and the second "$\approx$" is our goal. Now we need to show:

$$\mathbb{E}\left\langle \frac{\nabla f(x_{k,0})}{\sqrt{v_{k,0}}}, \left(\sum_{i=0}^{n-1} m_{k,i}\right) - \nabla f(x_{k,0}) \right\rangle \overset{(*)}{=} \mathbb{E}\left(\sum_{l=1}^{d}\sum_{i=0}^{n-1} \frac{\partial_l f(x_{k,0})}{\sqrt{v_{l,k,0}}} \left(m_{l,k,i} - \partial_l f_{\tau_{k,i}}(x_{k,0})\right)\right) \approx 0, \tag{4}$$

where $\partial_l f(x_{k,0})$ is the l-th component of $\nabla f(x_{k,0})$, similarly for $m_{l,k,0}$ and $v_{l,k,0}$. $(*)$ is due to the finite-sum structure. However, it is not easy to prove (4). We point out some technical issues below.

Issue I: massive momentum. Directly proving (4) is still not easy. We need to first consider a simplified problem: for every $l \in [d]$, assume we treat $\partial_l f(x_{k,0})/\sqrt{v_{l,k,0}}$ as a constant, how to bound $\mathbb{E}\sum_{i=0}^{n-1}\left(m_{l,k,i} - \partial_l f_{\tau_{k,i}}(x_{k,0})\right)$?

It turns out that this simplified problem is still non-trivial. When β_1 is large, $m_{l,k,i}$ contains heavy historical signals which significantly distort the trajectory from gradient direction. Existing literature (Zaheer et al., 2018; De et al., 2018; Shi et al., 2020) take a naive approach: they set $\beta_1 \approx 0$ so that $m_{l,k,i} \approx \partial_l f_{\tau_{k,i}}(x_{k,i})$. Then we get (4) ≈ 0. However, this method cannot be applied here since we are interested in practical cases where β_1 is large in $[0, 1)$.

Issue II: stochastic non-linear dynamics. Even if we solve **Issue I**, it is still unclear how to prove (4). This is because: for every $l \in [d]$, $\partial_l f(x_{k,0})/\sqrt{v_{l,k,0}}$ is a r.v. instead of a constant. With this term involved, we are facing with a stochastic non-linear dynamics, which could be difficult to analyze. Further, $\partial_l f(x_{k,0})/\sqrt{v_{l,k,0}}$ is statistically dependent with $\big(m_{l,k,i} - \partial_l f_{\tau_{k,i}}(x_{k,0})\big)$, so we are not allowed to handle the expectation $\mathbb{E}(\partial_l f(x_{k,0})/\sqrt{v_{l,k,0}})$ separately .

Unfortunately, even with additional assumptions like bounded gradient, there is no general approach to tackle the above issues. In this work, we propose solutions regardless of gradient magnitude.

Solution to Issue I. We prove the following Lemma to resolve **Issue I**.

Lemma 5.1. *(Informal) Consider Algorithm 1. For every $l \in [d]$ and any $\beta_1 \in [0, 1)$, we have the following result under Assumption 2.1.*

$$\delta(\beta_1) := \mathbb{E} \sum_{i=0}^{n-1} \big(m_{l,k,i} - \partial_l f_{\tau_{k,i}}(x_{k,0})\big) = \mathcal{O}\left(\frac{1}{\sqrt{k}}\right),$$

where $\partial_l f(x_{k,0})$ is the l-th component of $\nabla f(x_{k,0})$; $m_{l,k,i} = (1-\beta_1)\partial_l f_{\tau_{k,i}}(x_{k,i}) + \beta_1 m_{l,k,i-1}$.

We present the proof idea in Appendix A. Simply put, we construct a simple toy example called "color-ball" model (of the 1st kind). This toy model shows a special property of $\delta(\beta_1)$. We find out: for Algorithm 1, error terms from successive epochs can be canceled, which keeps the momentum roughly in the descent direction. This important property is not revealed in any existing work.

Remark 4: When assuming bounded gradient $\|\nabla f(x)\| \leq G$, a naive upper bound would be $\delta(\beta_1) = \mathcal{O}(G)$. However, such constant upper bound does not imply $\delta(\beta_1)$ is close to 0. It will not help prove the convergence. This might be partially the reason why large-β_1 Adam is hard to analyze even under bounded gradient (see related works in Section 2.2). We emphasize Lemma 5.1 holds true regardless of gradient norm, so it could be deployed in both bounded or unbounded gradient analysis.

Solution to Issue II. We try to show (4) by adopting Lemma 5.1. However, the direct application cannot work since $\frac{\partial_l f(x_{k,0})}{\sqrt{v_{l,k,0}}}$ is random. Despite its randomness, we find out that when β_2 is large, the changes of $\frac{\partial_l f(x_{k,0})}{\sqrt{v_{l,k,0}}}$ shrinks along iteration. As such, although $\frac{\partial_l f(x_{k,0})}{\sqrt{v_{l,k,0}}}$ brings extra perturbation, the quantity in (4) share the similar asymptotic behavior as $\delta(\beta_1)$. We prove the following Lemma 5.2.

Lemma 5.2. *(Informal) Under Assumption 2.1 and 2.2, consider Algorithm 1 with large β_2 and $\beta_1 < \sqrt{\beta_2}$. For those l with gradient component larger than certain threshold, we have:*

$$\left| \frac{\partial_l f(x_{k,0})}{\sqrt{v_{k,0}}} - \frac{\partial_l f(x_{k-1,0})}{\sqrt{v_{k-1,0}}} \right| = \mathcal{O}\left(\frac{1}{\sqrt{k}}\right); \tag{5}$$

$$\mathbb{E}\left(\frac{\partial_l f(x_{k,0})}{\sqrt{v_{l,k,0}}} \sum_{i=0}^{n-1} (m_{l,k,i} - \partial_l f_{\tau_{k,i}}(x_{k,0})) \right) = \mathcal{O}\left(\frac{1}{\sqrt{k}}\right). \tag{6}$$

In Appendix A, we introduce how to derive (6) from (5). To do so, we introduce a new type of "color-ball" model (we call it color-ball of the 2nd kind) which adopts the random perturbation of $\frac{\partial_l f(x_{k,0})}{\sqrt{v_{l,k,0}}}$. Understanding color-ball model of the 2nd kind is crucial for proving Lemma 5.2.

We conclude the proof of (4) by some additional analysis on "those l with small gradient component". This case is a bit easier since it reduces to bounded gradient case. For readers who wants to learn more about the idea of tackling **Issue I** and **II**, please refer to Appendix A where we formally introduce the 1st and 2nd kind of color-ball models. Since the whole proof is quite long, we provide a proof sketch in Appendix G.1. The whole proof is presented in Appendix G.

6 Experiments

To support our theory, we provide more simulations and real-data experiments. All the experimental settings and hyperparameters are presented in Appendix B.1. We aim to show:

(I). When β_2 is large, a large range of β_1 gives good performance, including all $\beta_1 < \sqrt{\beta_2}$.

(II). When β_2 is small, a large range of β_1 performs relatively badly.

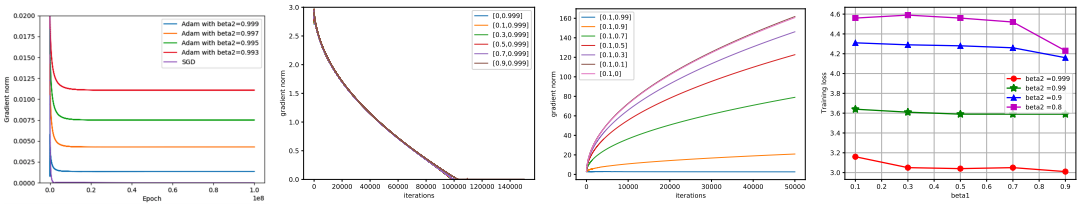

(a) Function (9) with $D_0 > 0$ (b) Function (2) with $D_0 = 0$ (c) The trajectories of small-β_2 Adam (d) WikiText-103

Figure 4: The performance of Adam on different tasks. **(a) (b):** large-β_2 Adam converges to bounded region when $D_0 > 0$ and converges to critical points when $D_0 = 0$. We use diminishing stepsize $\eta_k = 0.1/\sqrt{k}$. **(c):** When β_2 is small, gradient norm of Adam iterates can be unbounded. We use function 2 with initialization $x = -5$ and $n = 20$. The legends in (b) and (c) stand for $[\beta_1, \beta_2]$. **(d):** The training loss under different (β_1, β_2) on NLP tasks. We use Adam to train Transformer XL on WikiText-103 dataset.

Convergence to bounded region when $D_0 > 0$. In Figure 4, we run large-β_2 Adam on function (9) (defined later in Appendix B). This function satisfies with $D_0 > 0$. We find that even with diminishing stepsize $\eta_k = 1/\sqrt{k}$, Adam may not converge to an exact critical point. Instead, it converges to a bounded region. This is because: even though η_k is decreasing, the effective stepsize $\eta_k/\sqrt{v_{k,i}}$ might not decay. Further, the size of the region shrinks when β_2 increases. This is because the movement of $\sqrt{v_{k,i}}$ shrinks as β_2 increases. These phenomena match **Remark 3** and claim **(I)**.

Convergence to critical points when $D_0 = 0$ Since function (2) satisfies $D_0 = 0$, we run more experiments on (2) with initialization $x = -5$ and $n = 5, 10, 15, 20$. We show the result of $n = 20$ in Figure 4 (a), (b); the rest are shown in Appendix B. We find that: when β_2 is large, Adam converges to critical points for $\beta_1 < \sqrt{\beta_2}$. These phenomena match claim **(I)**.

Gradient norm of iterates can be unbounded when β_2 is small. On function (2), We further run Adam with small β_2 at initialization $x = -5$. In this case, gradient norms of iterates increase dramatically. This emphasizes the importance of discarding bounded gradient assumptions. These phenomena match claim **(II)**.

MNIST and CIFAR-10. As shown in Figure 1 (b)& (c) in Section 1, the training results match both claim **(I)** and **(II).** In addition, there is a convex-shaped boundary on the transition from low loss to higher loss, this boundary roughly matches the condition in Theorem 3.1.

NLP. We use Adam to train Transformer XL (Dai et al., 2019) on the WikiText-103 dataset (Merity et al., 2016). This architecture and dataset is widely used in NLP tasks (e.g. (Howard & Ruder, 2018; See et al., 2017)). As shown in Figure 4 (d), the training results match both claim **(I)** and **(II).**

7 Conclusions

In this work, we explore the (non-)convergence of Adam. When β_2 is large, we prove that Adam can converge with any $\beta_1 < \sqrt{\beta_2}$. When β_2 is small, we further show that Adam might diverge to infinity for a wide range of β_1. One interesting question is to verify the advantage of Adam over SGD. In this work, we focus on the fundamental issue of convergence. Proving faster convergence of Adam would be our future work.

Acknowledgments and Disclosure of Funding

Yushun Zhang would like to thank Bohan Wang, Reviewer xyuf and Reviewer UR9H for the careful proof reading. Yushun Zhang would like to thank Bohan Wang for the valuable discussions around Lemma G.3. Yushun Zhang would also like to thank Reviewer UR9H for the valuable discussions around Lemma G.13.

References

Agarwal, R., Schuurmans, D., and Norouzi, M. An optimistic perspective on offline reinforcement learning. In International Conference on Machine Learning, pp. 104–114. PMLR, 2020.

Bertsekas, D. P. and Tsitsiklis, J. N. Gradient convergence in gradient methods with errors. SIAM Journal on Optimization, 10(3):627–642, 2000.

Brown, T. B., Mann, B., Ryder, N., Subbiah, M., Kaplan, J., Dhariwal, P., Neelakantan, A., Shyam, P., Sastry, G., Askell, A., et al. Language models are few-shot learners. arXiv preprint arXiv:2005.14165, 2020.

Chen, C., Shen, L., Zou, F., and Liu, W. Towards practical adam: Non-convexity, convergence theory, and mini-batch acceleration. arXiv preprint arXiv:2101.05471, 2021.

Chen, J., Zhou, D., Tang, Y., Yang, Z., Cao, Y., and Gu, Q. Closing the generalization gap of adaptive gradient methods in training deep neural networks. arXiv preprint arXiv:1806.06763, 2018a.

Chen, X., Liu, S., Sun, R., and Hong, M. On the convergence of a class of adam-type algorithms for non-convex optimization. arXiv preprint arXiv:1808.02941, 2018b.

Dai, Z., Yang, Z., Yang, Y., Carbonell, J., Le, Q. V., and Salakhutdinov, R. Transformer-xl: Attentive language models beyond a fixed-length context. arXiv preprint arXiv:1901.02860, 2019.

De, S., Mukherjee, A., and Ullah, E. Convergence guarantees for rmsprop and adam in non-convex optimization and an empirical comparison to nesterov acceleration. arXiv preprint arXiv:1807.06766, 2018.

Défossez, A., Bottou, L., Bach, F., and Usunier, N. On the convergence of adam and adagrad. arXiv e-prints, pp. arXiv–2003, 2020.

Deng, L. The mnist database of handwritten digit images for machine learning research. IEEE Signal Processing Magazine, 29(6):141–142, 2012.

Devlin, J., Chang, M.-W., Lee, K., and Toutanova, K. Bert: Pre-training of deep bidirectional transformers for language understanding. arXiv preprint arXiv:1810.04805, 2018.

Dosovitskiy, A., Beyer, L., Kolesnikov, A., Weissenborn, D., Zhai, X., Unterthiner, T., Dehghani, M., Minderer, M., Heigold, G., Gelly, S., Uszkoreit, J., and Houlsby, N. An image is worth 16x16 words: Transformers for image recognition at scale. In International Conference on Learning Representations, 2021. URL https://openreview.net/forum?id=YicbFdNTTy.

Dozat, T. Incorporating nesterov momentum into adam. 2016.

Gadat, S. and Gavra, I. Asymptotic study of stochastic adaptive algorithm in non-convex landscape. arXiv preprint arXiv:2012.05640, 2020.

Ghadimi, S., Lan, G., and Zhang, H. Mini-batch stochastic approximation methods for nonconvex stochastic composite optimization. Mathematical Programming, 155(1):267–305, 2016.

Guo, Z., Xu, Y., Yin, W., Jin, R., and Yang, T. A novel convergence analysis for algorithms of the adam family. arXiv preprint arXiv:2112.03459, 2021.

He, K., Zhang, X., Ren, S., and Sun, J. Deep residual learning for image recognition. In Proceedings of the IEEE conference on computer vision and pattern recognition, pp. 770–778, 2016.

Hinton, G., Srivastava, N., and Swersky, K. Neural networks for machine learning lecture 6a overview of mini-batch gradient descent. Cited on, 14(8):2, 2012.

Howard, J. and Ruder, S. Universal language model fine-tuning for text classification. arXiv preprint arXiv:1801.06146, 2018.

Huang, F., Li, J., and Huang, H. Super-adam: Faster and universal framework of adaptive gradients. arXiv preprint arXiv:2106.08208, 2021.

Iiduka, H. Theoretical analysis of adam using hyperparameters close to one without lipschitz smoothness. arXiv preprint arXiv:2206.13290, 2022.

Isola, P., Zhu, J.-Y., Zhou, T., and Efros, A. A. Image-to-image translation with conditional adversarial networks. In Proceedings of the IEEE conference on computer vision and pattern recognition, pp. 1125–1134, 2017.

Jin, R., Xing, Y., and He, X. On the convergence of msgd and adagrad for stochastic optimization. arXiv preprint arXiv:2201.11204, 2022.

Kingma, D. P. and Ba, J. Adam: A method for stochastic optimization. arXiv preprint arXiv:1412.6980, 2014.

Krizhevsky, A., Hinton, G., et al. Learning multiple layers of features from tiny images. 2009.

Liu, L., Jiang, H., He, P., Chen, W., Liu, X., Gao, J., and Han, J. On the variance of the adaptive learning rate and beyond. In International Conference on Learning Representations, 2020a. URL https://openreview.net/forum?id=rkgz2aEKDr.

Liu, Y., Gao, Y., and Yin, W. An improved analysis of stochastic gradient descent with momentum. arXiv preprint arXiv:2007.07989, 2020b.

Luo, L., Xiong, Y., and Liu, Y. Adaptive gradient methods with dynamic bound of learning rate. In International Conference on Learning Representations, 2019. URL https://openreview.net/forum?id=Bkg3g2R9FX.

Merity, S., Xiong, C., Bradbury, J., and Socher, R. Pointer sentinel mixture models. arXiv preprint arXiv:1609.07843, 2016.

Radford, A., Metz, L., and Chintala, S. Unsupervised representation learning with deep convolutional generative adversarial networks. arXiv preprint arXiv:1511.06434, 2015.

Reddi, S. J., Kale, S., and Kumar, S. On the convergence of adam and beyond. In International Conference on Learning Representations, 2018. URL https://openreview.net/forum?id=ryQu7f-RZ.

Schmidt, M. and Roux, N. L. Fast convergence of stochastic gradient descent under a strong growth condition. arXiv preprint arXiv:1308.6370, 2013.

Scholar, G. Adam: A method for stochastic optimization. https://scholar.google.nl/citations?view_op=view_citation&hl=en&user=yyIoQu4AAAAJ&citation_for_view=yyIoQu4AAAAJ:RGFaLdJalmkC. 2022.

See, A., Liu, P. J., and Manning, C. D. Get to the point: Summarization with pointer-generator networks. arXiv preprint arXiv:1704.04368, 2017.

Shi, N., Li, D., Hong, M., and Sun, R. Rmsprop converges with proper hyper-parameter. In International Conference on Learning Representations, 2020.

Smith, S., Patwary, M., Norick, B., LeGresley, P., Rajbhandari, S., Casper, J., Liu, Z., Prabhumoye, S., Zerveas, G., Korthikanti, V., et al. Using deepspeed and megatron to train megatron-turing nlg 530b, a large-scale generative language model. arXiv preprint arXiv:2201.11990, 2022.

Vaswani, A., Shazeer, N., Parmar, N., Uszkoreit, J., Jones, L., Gomez, A. N., Kaiser, Ł., and Polosukhin, I. Attention is all you need. In Advances in neural information processing systems, pp. 5998–6008, 2017.

Vaswani, S., Bach, F., and Schmidt, M. Fast and faster convergence of sgd for over-parameterized models and an accelerated perceptron. In The 22nd International Conference on Artificial Intelligence and Statistics, pp. 1195–1204. PMLR, 2019.

Yan, Y., Yang, T., Li, Z., Lin, Q., and Yang, Y. A unified analysis of stochastic momentum methods for deep learning. arXiv preprint arXiv:1808.10396, 2018.

Yu, H., Jin, R., and Yang, S. On the linear speedup analysis of communication efficient momentum sgd for distributed non-convex optimization. In International Conference on Machine Learning, pp. 7184–7193. PMLR, 2019.

Zaheer, M., Reddi, S., Sachan, D., Kale, S., and Kumar, S. Adaptive methods for nonconvex optimization. In Bengio, S., Wallach, H., Larochelle, H., Grauman, K., Cesa-Bianchi, N., and Garnett, R. (eds.), Advances in Neural Information Processing Systems, volume 31. Curran Associates, Inc., 2018. URL https://proceedings.neurips.cc/paper/2018/file/90365351ccc7437a1309dc64e4db32a3-Paper.pdf.

Zhang, Y., Chen, C., and Luo, Z.-Q. Does adam converge and when? In ICLR Blog Track, 2022. URL https://iclr-blog-track.github.io/2022/03/25/does-adam/. https://iclr-blog-track.github.io/2022/03/25/does-adam/.

Zhou, D., Chen, J., Cao, Y., Tang, Y., Yang, Z., and Gu, Q. On the convergence of adaptive gradient methods for nonconvex optimization. arXiv preprint arXiv:1808.05671, 2018a.

Zhou, Z., Zhang, Q., Lu, G., Wang, H., Zhang, W., and Yu, Y. Adashift: Decorrelation and convergence of adaptive learning rate methods. arXiv preprint arXiv:1810.00143, 2018b.

Zhu, J.-Y., Park, T., Isola, P., and Efros, A. A. Unpaired image-to-image translation using cycle-consistent adversarial networks. In Proceedings of the IEEE international conference on computer vision, pp. 2223–2232, 2017.

Zou, F., Shen, L., Jie, Z., Zhang, W., and Liu, W. A sufficient condition for convergences of adam and rmsprop. In Proceedings of the IEEE/CVF Conference on Computer Vision and Pattern Recognition, pp. 11127–11135, 2019.

Negative Social Impact

This script may provide better guidance for neural nets training. It would have certain negative social impact if neural nets are deployed for illegal usage.

Appendix Organization

The Appendix is organized as follows.

- Appendix A introduces two “color-ball" models and their applications in proving Lemma 5.1 and Lemma 5.2. This part is important for proving Theorem 3.1.
- Appendix B introduces more experiments to support our theory.
- Appendix C provide some suggestions for hyperparameter tuning of Adam.
- Appendix D.1 provide more discussions on some recent related works. Appendix D.2 re-state the non-convergence results in (Reddi et al., 2018).
- Appendix E provides detailed proof for Proposition 3.3.
- Appendix F provides some more notations and technical lemmas that serve for the proof of Theorem 3.1.
- Appendix G provides detailed proof for Theorem 3.1. Especially, Appendix G.1 provide a proof roadmap.

A Introduction to the “Color-Ball” Models: the Key Ingredients to Prove Theorem 3.1

We now introduce two “color-ball" models and their applications in tackling **Issue I** and **Issue II** mentioned in Section 5. These two color-ball models are important for proving Theorem 3.1.

Solution to Issue I. As discussed in Section 5, we wish to show that $\delta(\beta_1)$ vanishes with k. Formally, we wish to get the following equation (7) for every $l \in [d]$.

$$\delta(\beta_1) = \left| \mathbb{E}\left[\sum_{i=0}^{n-1} \left(m_{l,k,i} - \partial_l f_i\left(x_{k,0}\right) \right) \right] \right| = \mathcal{O}(\beta_1^{nk}), \quad \forall \beta_1 \in [0,1) \tag{7}$$

When k is large, $\mathcal{O}(\beta_1^{nk})$ vanishes faster than $\mathcal{O}(\frac{1}{\sqrt{k}})$ and thus Lemma 5.1 can be proved. In the following context, we will carefully quantify the mismatch between $m_{l,k,i}$ and the $\partial_l f(x_{k,0})$. We find out that the error terms from successive epochs can be cancelled, which keeps the momentum roughly in the descent direction. To help readers understand our idea, we introduce the “color-ball " model (of the 1st kind) as follows.

The color-ball model of the 1st kind. Consider a box containing two balls labeled with constant $c_0, c_1 \in \mathbb{R}$, respectively. In each round (epoch), we randomly sample balls from the box without replacement, then we put them back. We denote the 1st sampled label in the k-th epoch as a_k and the 2nd sampled one as b_k; $a_k, b_k \in \{c_0, c_1\}$. We define two random variables m_0 and m_1 as follows (assume $\beta \in [0,1)$):

$$m_1 = \underbrace{b_k + \beta a_k}_{m_{1,k}} + \underbrace{\beta^2 b_{k-1} + \beta^3 a_{k-1}}_{m_{1,k-1}} + \cdots + \underbrace{\beta^{2(k-1)} b_1 + \beta^{2(k-1)+1} a_1}_{m_{1,1}};$$

$$m_0 = \underbrace{\qquad a_k}_{m_{0,k}} + \underbrace{\beta^1 b_{k-1} + \beta^2 a_{k-1}}_{m_{0,k-1}} + \cdots + \underbrace{\beta^{2(k-1)-1} b_1 + \beta^{2(k-1)} a_1}_{m_{1,1}};$$

where $m_{0,k}$ denotes the summand of m_0 in k-th epoch, similarly for $m_{1,k}$. Note that in each epoch, m_0 and m_1 share the same sample order. Further, we introduce the following deterministic constants.

$$f_1 = c_1(\underbrace{1+\beta}_{f_{1,k}} + \underbrace{\beta^2+\beta^3}_{f_{1,k-1}} \cdots + \underbrace{\beta^{2(k-1)}+\beta^{2(k-1)+1}}_{f_{1,1}});$$

$$f_0 = c_0(\underbrace{1+\beta}_{f_{0,k}} + \underbrace{\beta^2+\beta^3}_{f_{0,k-1}} \cdots + \underbrace{\beta^{2(k-1)}+\beta^{2(k-1)+1}}_{f_{0,1}});$$

where $f_{0,k}$ denotes the summand of f_0 in k-th epoch, similarly for $f_{1,k}$. Now we prove the following Lemma A.1.

Lemma A.1. *In the color-ball model of the 1st kind, we have*

$$\left|\mathbb{E}\left[\sum_{i=0}^{1} m_i - \sum_{i=0}^{1} f_i\right]\right| = \beta^{2(k-1)+1}\left(\frac{c_0}{2}+\frac{c_1}{2}\right),$$

where the expectation is taken on all the possible draws. For the color-ball example with $n \geq 2$ balls, we have

$$\left|\mathbb{E}\left[\sum_{i=0}^{n-1} m_i - \sum_{i=0}^{n-1} f_i\right]\right| = \beta^{n(k-1)}\sum_{i=0}^{n-1} c_i(\frac{1}{n}\beta^1 \cdots + \frac{n-1}{n}\beta^{n-1}).$$

How is Lemma A.1 related to (7)**?** In this color-ball toy example, m_i mimics the possible realization of momentum up to the i-th inner loop in k-th epoch. f_i mimics the stochastic gradient $\nabla f_i(x_{k,0})$. This is because we can expand $\nabla f_i(x_{k,0})$ into an infinite-sum sequence $\nabla f_i(x_{k,0}) = (1-\beta_1)\nabla f_i(x_{k,0})\sum_{j=0}^{\infty}\beta_1^j$, which shares a similar structure as f_i. In this sense, Lemma A.1 may provide ideas to prove (7). Nevertheless, there are still gap between these two, we will explain the gap later.

Proof. We use $\mathbb{E}_k[\cdot]$ to denote the conditional expectation given all the history up to the beginning of k-th epoch. Since $\mathbb{E}[\cdot] = \mathbb{E}[\mathbb{E}_k[\cdot]]$, we first calculate $\mathbb{E}_k\left[\sum_{i=0}^{1} m_i\right]$. Since all the history before k-th epoch is fixed, we relegate this part to later discussion and first focus on the expectation of $\sum_{i=0}^{1} m_{i,k}$. As shown in Figure 5 (upper part), there are 2 possible realization.

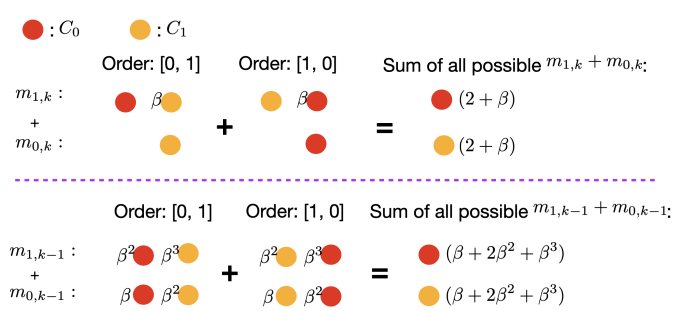

Figure 5: All possible realization of $\sum_{i=0}^{1} m_{i,k}$ and $\sum_{i=0}^{1} m_{i,k-1}$.

With the help of Figure 5 (upper part), we have the following result.

$$\begin{aligned}\mathbb{E}_k\left[\sum_{i=0}^{1} m_{i,k} - \sum_{i=0}^{1} f_{i,k}\right] &= \mathbb{E}_k\left[\sum_{i=0}^{1} m_{i,k}\right] - (1+\beta)(c_0+c_1) \\ &= -\frac{\beta}{2}(c_0+c_1) \qquad (8)\end{aligned}$$

Now we move one step further to calculate $\mathbb{E}_{k-1}\mathbb{E}_k\left[\sum_{i=0}^{1} m_i - \sum_{i=0}^{1} f_i\right]$. Using the similar strategy as (8), we have the following result. The calculation is illustrated in Figure 5 (lower part) and Figure 6.

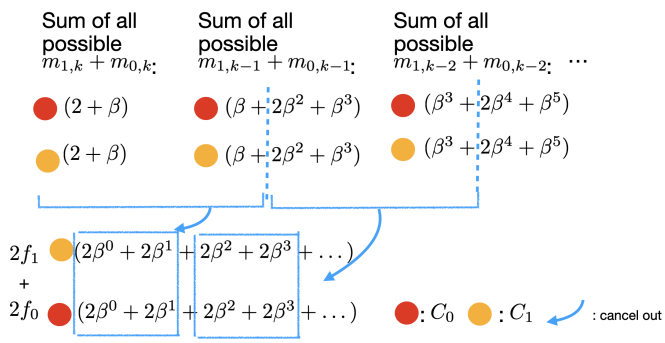

Figure 6: For every k, $\mathbb{E}_k\left[\sum_{i=0}^{1} m_{i,k} - \sum_{i=0}^{1} f_{i,k}\right]$ will create residues, while these residues will be canceled out in the $(k-1)$-th epoch.

$$
\begin{aligned}
& \mathbb{E}_{k-1}\left\{\mathbb{E}_k\left[\sum_{i=0}^{1} m_{i,k} - \sum_{i=0}^{1} f_{i,k} + \sum_{i=0}^{1} m_{i,k-1} - \sum_{i=0}^{1} f_{i,k-1}\right]\right\} \\
\overset{(8)}{=} \quad & -\frac{\beta}{2}(c_0 + c_1) + \mathbb{E}_{k-1}\left\{\sum_{i=0}^{1} m_{i,k-1}\right\} - \sum_{i=0}^{1} f_{i,k-1} \\
\overset{\text{Figure 5 and 6}}{=} \quad & -\frac{\beta}{2}(c_0 + c_1) + \frac{1}{2}(\beta + 2\beta^2 + \beta^3)(c_0 + c_1) - (\beta^2 + \beta^3)(c_0 + c_1) \\
= \quad & -\frac{\beta^3}{2}(c_0 + c_1)
\end{aligned}
$$

We observe that *only the highest order term remains in the calculation.* Repeat this process until $k = 1$, we will get the results in Lemma A.1. The above analysis also holds for general $n \geq 2$.

□

The gap between Lemma A.1 and Equation (7)**.** Lemma A.1 shows the key idea of proving equation (7). However, due to its idealized setting, the color-ball toy example is still far from our real goal (7). We list some of the gaps here.

- In each possible trajectory: $x_{k,i}$ is changing with k and i, while the balls are fixed in the color-ball example.
- When taking expectation: x is changing in different trajectory, while the balls is fixed in the color-ball example.
- x is a vector in $\mathbb{R}^d$ while the label of the balls are constant in $\mathbb{R}$.

It requires extra technical lemmas to handle these differences. We provide more discussions in Appendix G.1.

Solution to Issue II. We now discuss how to resolve **Issue II** mentioned in Section 5. The solution contains two parts. First, we need to prove (5). Second, we derive (6) from (5). Due to the limited space, we relegate the first part to Appendix G.1 (related to Lemma G.2). Now, we discuss the second part: Assume we have (5), how do we use it to prove (6)? To answer this question, we introduce the color-ball model of the 2nd kind.

The color-ball model of the 2nd kind. Consider the same setting as the color-ball model in **Step 1**. We define a sequence of real random variable $\{r_j\}_{j=1}^k$ with the following relation.

$$|r_j - r_{j-1}| = \frac{1}{\sqrt{j}}, \quad j = 1, \cdots k.$$

Further, we assume r_j is fixed when fixing the history up to j-th round. The sequence $\{r_j\}_{j=1}^k$ mimics the sequence $\{\frac{\partial_l f(x_{k,0})}{\sqrt{v_{l,k,0}}}\}_{k=1}^\infty$ in (5). Now, we consider the following quantities.

$$r_k m_1 = r_k \left(\underbrace{b_k + \beta a_k}_{m_{1,k}} + \underbrace{\beta^2 b_{k-1} + \beta^3 a_{k-1}}_{m_{1,k-1}} + \cdots + \underbrace{\beta^{2(k-1)} b_1 + \beta^{2(k-1)+1} a_1}_{m_{1,1}} \right);$$

$$r_k m_0 = r_k \left(\underbrace{a_k}_{m_{0,k}} + \underbrace{\beta^1 b_{k-1} + \beta^2 a_{k-1}}_{m_{0,k-1}} + \cdots + \underbrace{\beta^{2(k-1)-1} b_1 + \beta^{2(k-1)} a_1}_{m_{1,1}} \right);$$

$$r_k f_1 = r_k \left(c_1 (\underbrace{1+\beta}_{f_{1,k}} + \underbrace{\beta^2 + \beta^3}_{f_{1,k-1}} \cdots + \underbrace{\beta^{2(k-1)} + \beta^{2(k-1)+1}}_{f_{1,1}}) \right);$$

$$r_k f_0 = r_k \left(c_0 (\underbrace{1+\beta}_{f_{0,k}} + \underbrace{\beta^2 + \beta^3}_{f_{0,k-1}} \cdots + \underbrace{\beta^{2(k-1)} + \beta^{2(k-1)+1}}_{f_{0,1}}) \right);.$$

We now prove the following Lemma A.2.

Lemma A.2. *Consider the color-ball model of the 2nd kind, we have*

$$\mathbb{E}\left[\sum_{i=0}^{1} r_k m_i - \sum_{i=0}^{1} r_k f_i\right] = \beta^{2(k-1)+1}\left(-\frac{c_0}{2} - \frac{c_1}{2}\right) + \mathcal{O}(\frac{1}{\sqrt{k}}).$$

For general $n = 1, 2, 3, \cdots$, we have

$$\mathbb{E}\left[\sum_{i=0}^{n-1} r_k m_i - \sum_{i=0}^{n-1} r_k f_i\right] = \sum_{i=0}^{n-1} c_i \beta^{(k-1)n}(-\frac{1}{n}\beta^1 \cdots - \frac{n-1}{n}\beta^{n-1}) + \mathcal{O}(\frac{1}{\sqrt{k}}).$$

Proof. We only describe the proof idea here. The proof contains the following 4 steps.

Step 2.1. We firstly take $\mathbb{E}_k[\cdot]$ and thus r_k can be viewed as a constant. We use the color-ball procedure as in Figure 7 to calculate $\mathbb{E}_k\left[r_k \sum_{i=0}^1 m_{i,k} - r_k \sum_{i=0}^1 f_i\right]$.

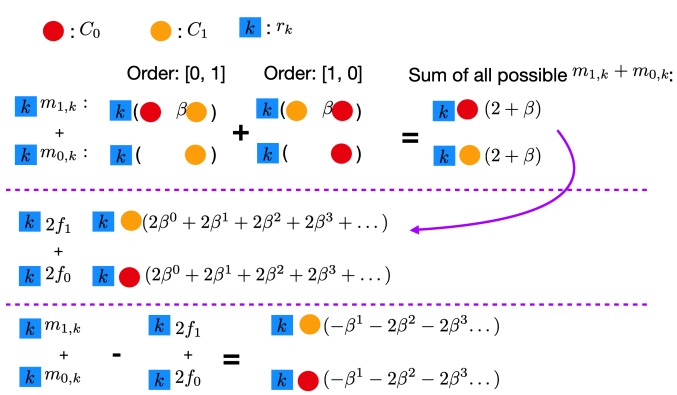

Figure 7: **Step 2.1** in the new color-ball model.

Step 2.2. We change $\mathbb{E}_k\left[r_k \sum_{i=0}^{1} m_{i,k-1}\right]$ into $\mathbb{E}_k\left[r_{k-1} \sum_{i=0}^{1} m_{i,k-1}\right]$ + Error; where Error $= \mathcal{O}(1/\sqrt{k})$.

Step 2.3. We calculate $\mathbb{E}_{k-1}\mathbb{E}_k\left[r_{k-1} \sum_{i=0}^{1} m_{i,k-1}\right] = \mathbb{E}_{k-1}\left[r_{k-1} \sum_{i=0}^{1} m_{i,k-1}\right]$. This part is illustrated in the top row in Figure 8

Step 2.4. For the leftovers in **Step 2.1**, we change all r_k into r_{k-1}. Then we do the cancellation to calculate $\mathbb{E}_{k-1}\mathbb{E}_k\left[r_{k-1} \sum_{i=0}^{1} m_{i,k-1} + r_{k-1} \sum_{i=0}^{1} m_{i,k} - r_{k-1} \sum_{i=0}^{1} f_i\right]$. This step is shown in the second and third row in Figure 8.

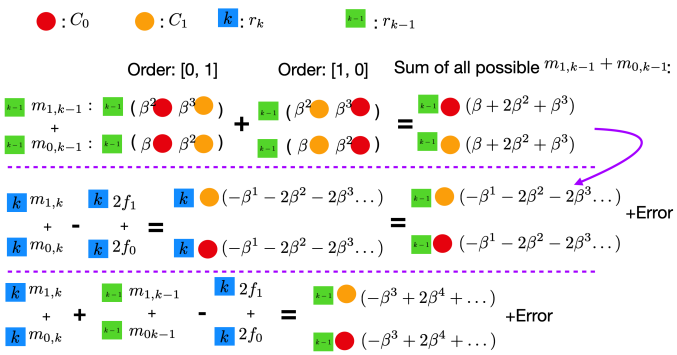

Figure 8: **Step 2.3 and 2.4** in the new color-ball model.

Repeat this process to the 1st epoch. We can prove the Lemma A.2.

□

We emphasize that here are still some gap between Lemma A.2 and our goal in (6) in Lemma 5.2. First, we have the similar gap as discussed at the end of the **Solution to Issue I**. Second, the condition in Lemma 5.2 has requirement on the gradient norm, while this requirement is temporarily ignored in the color-ball method of the 2nd kind. It requires some technical lemmas to handle these gaps.

For more details, please refer to the complete proof in Appendix G.

B More experiments

Estimation on ρ in Theorem 3.1. To ensure convergence, Theorem 3.1 requires $\beta_2 \geq \gamma_1(n) = 1 - \mathcal{O}((1-\beta_1^n)/n^2\rho)$. Now we estimate the constant ρ. According to our definition in Remark G.7 in Appendix G.1, $\rho = \rho_1\rho_2\rho_3$, where ρ_1, ρ_2, ρ_3 are defined as follows.

$$\rho_1 \geq \frac{\sum_{i=1}^{n} |\partial_l f_i(x_{k,0})|}{\sqrt{\sum_{i=1}^{n} |\partial_l f_i(x_{k,0})|^2}};$$

$$\rho_2 \geq \frac{|\max_i \partial_l f_i(x_{k,0})|^2}{\frac{1}{n}\sum_{i=1}^{n} |\partial_l f_i(x_{k,0})|^2};$$

$$\rho_3 \geq \frac{|\sum_{i=1}^{n} \partial_l f_i(x_{k,0})|}{\sqrt{\frac{1}{n}\sum_{i=1}^{n} |\partial_l f_i(x_{k,0})|^2}}.$$

These definitions can also be seen in Appendix F.1. In worst case, we have $0 \leq \rho_3 \leq \sqrt{n}\rho_1 \leq n$. However, ρ is highly dependent on the problem instance $f(x)$ and training process. We now estimate how ρ changes with Adam's trajectory on MNIST and CIFAR-10. We use $\beta_1 = 0.9$, $\beta_2 = 0.99$. On both datasets, we set batchsize to be 64, which brings $n = 937$ on MNIST and $n = 781$ on

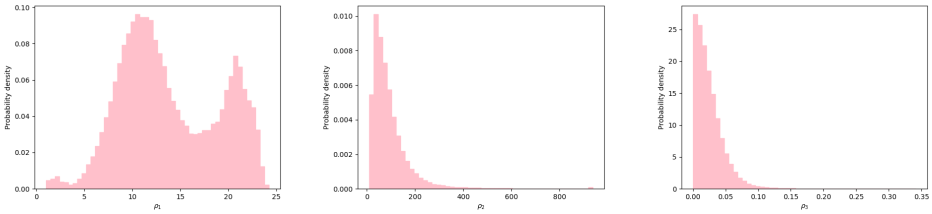

(a) Histogram of ρ_1 (b) Histogram of ρ_2 (c) Histogram of ρ_3

Figure 9: Histograms of ρ_1, ρ_2, ρ_3 along the training process on MNIST.

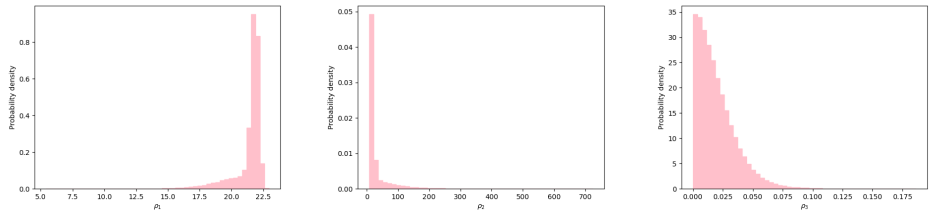

(a) Histogram of ρ_1 (b) Histogram of ρ_2 (c) Histogram of ρ_3

Figure 10: Histograms of ρ_1, ρ_2, ρ_3 along the training process on CIFAR-10.

CIFAR-10. We collect ρ_1, ρ_2, ρ_3 along the training process and estimate their distribution density. The results are shown in Figure 9 and 10.

On both CIFAR-10 and MNIST, we observe that the maximal $\rho_1 < 25 \approx \mathcal{O}(\sqrt{n})$, $\rho_2 < 400 \approx \mathcal{O}(n)$, $\rho_3 < 0.1 \approx \mathcal{O}(1/\sqrt{n})$. Therefore, $\rho = \rho_1\rho_2\rho_3 \approx \mathcal{O}(n)$.

Batchsize and β_2. As shown in Figure 11: on MNIST, smaller batchsize requires larger β_2 to reach small loss. Since batchsize equals to (number of total sample)/(number of batches). In the context of finite-sum setting with n summand, n usually stands for the number of batches (e.g., In the extreme case when batchsize $= 1$, n equals to the number of total samples). Therefore, smaller batchsize brings larger n. As such, Figure 11 matches the message by Theorem 3.1: the threshold of β_2 increases with n.

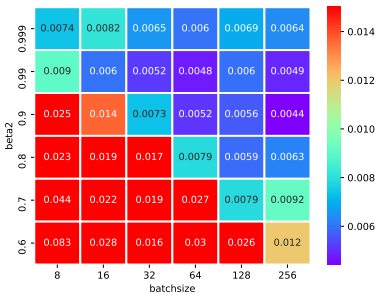

Figure 11: The training loss on MNIST under different batchsize and β_2. Here, β_1 is fixed to be 0.9

More experiments on function (2)**.** Figure 1 (a) shows the optimality gap after 50k iterations when $n = 10$ and initialization $x = 1$. Here, we provide more relevant experiments. First, when initialized at $x = 1$, we run experiments with $n = 5, 10, 15, 20$. The results are shown in Figure 12. We observe that the blue region shrinks as n increases. This matches our conclusion in Theorem 3.1: when n increases, the convergent threshold of β_2 increases, which means we need larger β_2 to ensure convergence. It also matches the conclusion in Theorem 3.3: when n increases, the divergence region will expand (more evidence can be seen in Appendix E).

When initializing at $x = -5$, we further demonstrate that the gradient norm of $f(x)$ can dramatically increase. All the setting is the same as that in Figure 12 except for the change of initialization.

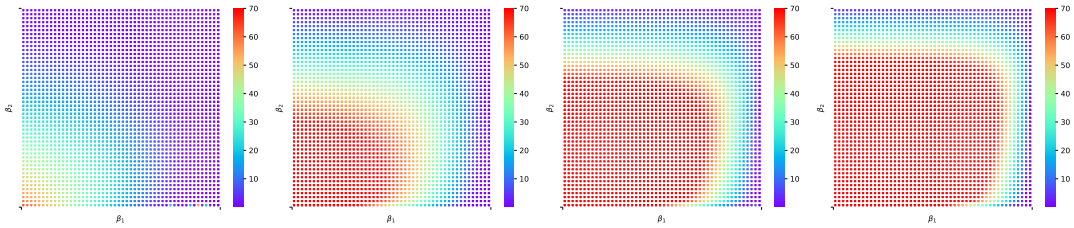

(a) $n = 5$ (b) $n = 10$ (c) $n = 15$ (d) $n = 20$

Figure 12: The optimality gap $x - x^*$ after running 50k iterations of Adam on function (2). We use initialization $x = 1$.

Starting at $x = -5$, the algorithm can touch the "quadratic" side of function (2) where the gradient is unbounded. The results are shown in Figure 13. We observe a similar pattern as that in Figure 12. As a result, the gradient norm of $f(x)$ is large in the left bottom corner.

We further plot the change of gradient norm along the iterations. We pick $\beta_1 = 0.1$ and $\beta_2 = 0, 0.1, 0.3, 0.5, 0.7, 0.9, 0.99$ to see the phase transition when increasing β_2. The result is shown in Figure 14. When β_2 is small, the gradient norm of $f(x)$ increases rapidly along the iteration. Most of them are even much larger than the upper bound of color bar in Figure 13. As a result, there is a phase transition from diverge to converge when increasing β_2 from 0 to 1.

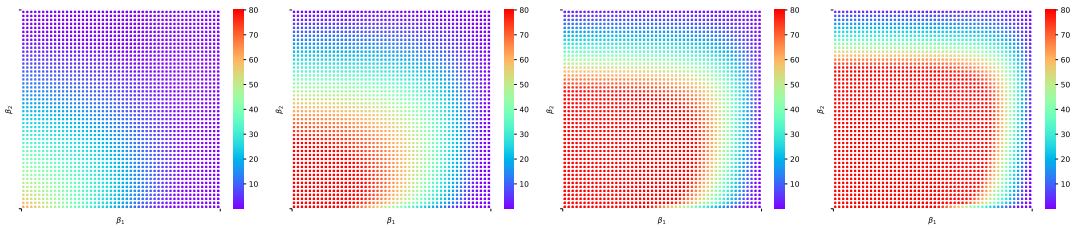

(a) $n = 5$ (b) $n = 10$ (c) $n = 15$ (d) $n = 20$

Figure 13: The gradient norm of $f(x)$ after running 50k iterations of Adam on function (2). We use initialization $x = -5$.

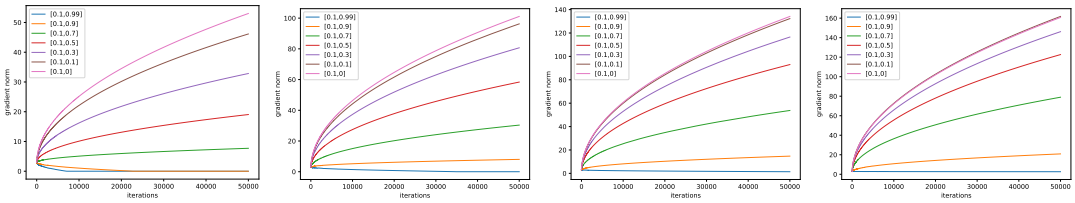

(a) $n = 5$ (b) $n = 10$ (c) $n = 15$ (d) $n = 20$

Figure 14: The change of gradient norm along the iterations of Adam on function (2). We use initialization $x = -5$. We use $[\beta_1, \beta_2]$ to label the curves trained with corresponding hyperparameters.

Adam converges to a exact critical point when $D_0 = 0$. Since function (2) satisfies $D_0 = 0$, we further provide empirical evidence that Adam converges to a exact critical point when $D_0 = 0$. We use function (2) $n = 20$ and initialization $x = -5$. We choose some large enough β_2 to ensure the convergence. As shown in Figure 15, We observe 0 gradient norm after Adam converges. All the hyperparameter setting is the same as before.

Adam converges to a bounded region when $D_0 > 0$. Now we show that Adam may not converge to an exact critical point when $D_0 > 0$. Instead, it converges to a bounded region near the critical point. For this part, we re-state the example from (Shi et al., 2020). Consider the following function.

$$f_j(x) = \begin{cases} (x-a)^2 \text{ if } j = 0 \\ -0.1\left(x - \frac{10}{9}a\right)^2 \text{ if } 1 \le j \le 9 \end{cases} \tag{9}$$

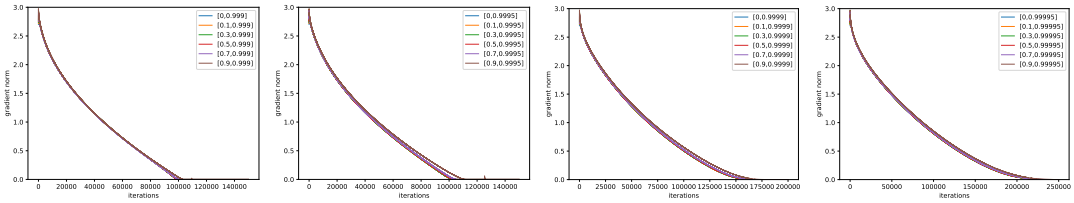

(a) $\beta_2 = 0.999$ (b) $\beta_2 = 0.9995$ (c) $\beta_2 = 0.9999$ (d) $\beta_2 = 0.99995$

Figure 15: Under SGC (When $D_0 = 0$), we observe 0 gradient norm after Adam converges. We use function (2) with $n = 20$ and initialization $x = -5$. We use $[\beta_1, \beta_2]$ to label the curves trained with corresponding hyperparameters.

Summing up $f_j(x)$ we get

$$f(x) = \sum_{j=0}^{9} f_j(x) = \frac{1}{10}x^2 - \frac{1}{9}a^2.$$

This $f(x)$ is lower bounded by $\frac{-a^2}{9}$ with optimal solution $x^* = 0$. At the optimal point $x^* = 0$, $\nabla f_j(x^*) \neq 0$ so we have $D_0 > 0$. When running Algorithm 1 on this function, we observe that Adam with diminishing stepsize does not converge to 0 gradient norm. Instead, it converge to a bounded region. Further, the size of the region shrinks when β_2 increases. These phenomena matches our discussion in **Remark 3.** The result is shown in Figure 4 (a). In the experiment, we choose $\beta_1 = 0.9$, $a = 3$, $x_0 = -2$ and diminishing stepsize $\eta_k = \frac{0.1}{\sqrt{k}}$.

B.1 Experimental Settings

Here, we introduce our experimental settings.

- **Experiments on function** (2)**.** We use Algorithm 1 with cyclic order f_0, f_1, f_2 and so on. We report the optimality gap $x - x^*$ after 50k iteration, or equivalently $50000/n$ epochs. We use $\epsilon = 10^{-8}$ for numerical stability. We use diminishing stepsize $\eta_k = 0.1/\sqrt{k}$, where k is the index of epoch. Unless otherwise stated, this setting applies to all the other experiments on function (2).

  In Figure 1 (a), we use $n = 10$ and initialization $x = 1$. We will report more results with different n and different initialization in Appendix B.
- **MNIST (Deng, 2012).** We use one-hidden-layer neural network with width =16. We set batchsize =1, weight decay =0, stepsize =0.0001 and train for 20 epochs. We use $\epsilon = 10^{-8}$ for numerical stability.
- **CIFAR-10 (Krizhevsky et al., 2009).** We use ResNet-18 (He et al., 2016) as the architecture. We choose batchsize =16, weight decay =5e-4 , initial stepsize=1e-3. We use a stage-wise constant learning rate scheduling with a multiplicative factor of 0.1 on epoch 30, 60 and 90. We use $\epsilon = 10^{-8}$ for numerical stability.

  For MNIST and CIFAR-10, larger batchsize will bring similar pattern as that in Figure 1, but the phase transition will occur at some smaller β_2.
- **NLP.** The WikiText-103 dataset is a collection of over 100 million tokens extracted from the set of verified 'Good' and 'Featured' articles on Wikipedia. The base model of Transformer XL contains 16 self-attention layers. In each self-attention layer, there are 10 heads. The encoding dimension of each head is set to be 41. We set batchsize = 60, number of iteration = 200k, and initial stepsize = 0.00025. We use cosine learning rate scheduler, which is a popular choice for training Transformer. We use $\epsilon = 10^{-8}$ for numerical stability.

C Some Potential Implications for Practical Users

Theorem 3.1 and Proposition 3.3 establish a clearer image on the relation between (β_1, β_2) and qualitative behavior of Adam, which may have certain implication for practical users. Many practitioners

are still doing grid or random search over (β_1, β_2), which could be costly. The following advice may cut down a large portion of search space. Suppose we start with some random point (β_1^*, β_2^*), we provide the following suggestions for tuning β_1 and β_2.

Case 1: If (β_1^*, β_2^*) lies above the blue curve in Figure 2. We point out two sub-cases. First, if Adam with (β_1^*, β_2^*) diverges, then any points with "$\beta_1 < \sqrt{\beta_2}$" and "$\beta_2 < \beta_2^*$" shall not be tried due to the risk of divergence. Second, if Adam with (β_1^*, β_2^*) converges, then any points above this point will converge. You may either fix $\beta_1 = \beta_1^*$ and increase β_2, or fix $\beta_2 = \beta_2^*$ and try smaller β_1. Both ways have convergence guarantee.

Case 2: If (β_1^*, β_2^*) lies below the blue curve in Figure 2. We still discuss two sub-cases. First, if you observe divergence at (β_1^*, β_2^*), then do not further try any point on the left. We do not suggest exploring the points in below either, since the majority of them will still face the risk of divergence. Instead, we suggest fix $\beta_1 = \beta_1^*$ and increase β_2. Since our Theorem 3.1 applies for any $\beta_1 < \sqrt{\beta_2}$, algorithm will converge when β_2 is large enough.

Second, if you observe convergence at (β_1^*, β_2^*) (which is also possible according to Figure 1 (a)), then we suggest: (i) either fix $\beta_1 = \beta_1^*$ and increase β_2, or (ii) fix $\beta_2 = \beta_2^*$ and try smaller β_1. Both ways push (β_1, β_2) into the region of Theorem 3.1 with convergence guarantee.

D More Discussion on Related Works.

D.1 More Related Works on the Convergence Analysis of Adam Family

New variants of Adam. Ever since Reddi et al. (2018) pointed out the non-convergence issue of Adam, one active line of work has tried to design new variants of Adam that can be proved to converge. For instance, Zou et al. (2019); Gadat & Gavra (2020); Chen et al. (2018b, 2021) replace the constant hyperparameters by iterate-dependent ones e.g. β_{1t} or β_{2t}. AMSGrad (Reddi et al., 2018) and AdaFom (Chen et al., 2018b) modify $\{v_t\}$ to be an non-decreasing sequence. Similarly, AdaBound (Luo et al., 2019) impose lower and upper bounds on $\{v_t\}$ to prevent the effective stepsize from vanishing or exploding. Zhou et al. (2018b) also adopt a new estimate of v_t to correct the bias. There are also attempts to combine Adam with Nesterov momentum (Dozat, 2016) as well as warm-up techniques (Liu et al., 2020a). Padam (Chen et al., 2018a) also introduce a partial adaptive parameter to improve the generalization performance. There are also some works providing theoretical analysis on the variants of Adam. For instance, Zhou et al. (2018a) study the convergence of AdaGrad and AMSGrad under bounded gradient condition. Gadat & Gavra (2020) study the asymptotic behavior of a subclass of adaptive gradient methods from landscape point of view. Their analysis applies to Adam-variants with $\beta_1 = 0$ and β_2 increasing along the iterates (it could also be understood as RMSProp with increasing β_2). When this script is under review, a new work (Iiduka, 2022) appear on line. Iiduka (2022) analyze the convergence of AMSGrad by relaxing the Lipschitz-gradient condition. However, their analysis requires extra conditions on both bounded gradient and bounded domain.

Some more discussions on (Guo et al., 2021) and (Huang et al., 2021). Here, we discuss more on two recent works Guo et al. (2021) and Huang et al. (2021). As mentioned in Section 2.2, they both require some extra conditions. First, both Guo et al. (2021) and Huang et al. (2021) requires bounded gradient assumption. This can be seen in Assumption 2 in (Guo et al., 2021). In (Huang et al., 2021), they require bounded iterates (their Theorem 1) or change Adam into AdaBound (Luo et al., 2019) by clipping (their Remark 2, Corollary 1). Both settings inherent boundedness on gradient.

Besides bounded gradient, both (Huang et al., 2021) and (Guo et al., 2021) requires $1/(\sqrt{v_t}+\epsilon) \leq C_u$. This condition is stated in Assumption 2 in (Guo et al., 2021) and Assumption 3 in (Huang et al., 2021) (they presented it as $H_t \succeq \rho I_d \succ 0$, where matrix $H_t = \text{diag}(\sqrt{v_t} + \epsilon)$). Combining these two conditions, the effective stepsize of Adam will be bounded in certain interval $\frac{1}{\sqrt{v_t}+\epsilon} \in [C_l, C_u]$. Such boundedness condition changes Adam into AdaBound (Luo et al., 2019) and thus cannot explain the observations of Adam in Section 1.

D.2 A Brief Introduction to (Reddi et al., 2018)

Here, we re-state two counter examples by (Reddi et al., 2018). For the consistence of notation, we will re-state their results under our notation in the full script. They consider the convex problem ((Reddi et al., 2018)): $\min \sum_{i=0}^{n-1} f_i(x)$ where $x \in [-1, 1]$, $n \geq 3$:

$$f_i(x) = \begin{cases} nx, & \text{for } i = 0 \\ -x, & \text{otherwise,} \end{cases} \tag{10}$$

Note that (10) satisfy both Assumption 2.1 and 2.2 (with $D_1 = n^2 + n - 1$ and $D_0 = 0$), so our assumptions do not rule out this counter-example a priori. This is a constrained problem with feasible set $x \in [-1, 1]$, the optimal solution is $x^* = -1$. Since they consider constrained problems, their claimed "divergence" actually means the iterates will stay in a huge region with the size of whole feasible set. Here, we call it "non-convergence" to distinguish from our result of "diverge to infinity" in Proposition 3.3.

They consider sampling f_i in the cyclic order: f_0, f_1, f_2. In (Reddi et al., 2018), Function (10) is presented as an "online optimization problem with non-zero average regret". We choose to use the form of (10) since it is more consistent with our notation in Algorithm 1. We re-state their results as follows.

Theorem D.1 (Theorem 2 in (Reddi et al., 2018))**.** *For any fixed (β_1, β_2) s.t. $\beta_1 < \sqrt{\beta_2}$, there exists function* (10) *with large enough n, s.t. Adam will converge to highly sub-optimal solution $x = 1$.*

We briefly re-state the non-convergent condition for this Theorem. As stated in Equation (7), Appendix B in (Reddi et al., 2018), for every fixed (β_1, β_2), they need a "constant n that depends on β_1 and β_2". As such, they require different n to cause non-convergence on different (β_1, β_2). So the considered function class is constantly changing.

For completeness, we further re-state Theorem 1 in (Reddi et al., 2018).

Theorem D.2 (Theorem 1 in (Reddi et al., 2018))**.** *For function* (10)*, when $\beta_1 = 0$ and $\beta_2 = 1/(n^2 + 1)$, Adam will converge to highly sub-optimal solution $x = 1$.*

This theorem considers choosing (β_1, β_2) after n. However, this result only show non-convergence on *a single point* $(\beta_1, \beta_2) = (0, 1/(n^2 + 1))$. This point lies somewhere on the left boundary of Figure 3. It seems unclear how Adam's behavior would change as we change the (β_1, β_2) to anywhere else.

E Proof of Proposition 3.3

We restate our counter-example here. Consider $f(x) = \sum_{i=0}^{n-1} f_i(x)$ for $x \in \mathbb{R}$, we define $f_i(x)$ as follows:

$$\begin{aligned} f_i(x) &= \begin{cases} nx, & x \geq -1 \\ \frac{n}{2}(x+2)^2 - \frac{3n}{2}, & x < -1 \end{cases} \text{ for } i = 0, \\ f_i(x) &= \begin{cases} -x, & x \geq -1 \\ -\frac{1}{2}(x+2)^2 + \frac{3}{2}, & x < -1 \end{cases} \text{ for } i > 0. \end{aligned} \tag{11}$$

Summing up all the $f_i(x)$, we can see that

$$f(x) = \begin{cases} x, & x \geq -1 \\ \frac{1}{2}(x+2)^2 - \frac{3}{2}, & x < -1 \end{cases}$$

is a convex smooth function with optimal solution $x^* = -2$ and optimal value $f(x^*) = -3/2$.

However, we are going to show that, for any fixed $n > 2$, there exists an orange region shown in Figure 2, s.t., Adam with any (β_1, β_2) combination in the yellow region diverge to $x = \infty$ rather than the optimal solution $x = -2$, causing the divergence. Now we introduce the formal statement of Proposition 3.3.

Proposition E.1. (Formal statement of Proposition 3.3.) *Consider the convex function* (11) *for a fixed n. Starting at the initialization $x = 1$ and initial stepsize η_1, the iterates of Adam diverge to infinity if the following holds:*

$$(\mathbf{C1}) : \left(n - 1 - \min\left\{n-1, \log_{\beta_2}(\frac{1}{10n^2})\right\}\right) \frac{1-\beta_1^{\min\left\{n-1, \log_{\beta_2}(\frac{1}{10n^2})\right\}}}{\sqrt{1+\max\left\{0.1, \beta_2^{n-1}n^2\right\}}} \geq \frac{1-\beta_1}{\sqrt{1-\beta_2}} + \frac{\beta_1}{\sqrt{1-\beta_2}}n; \tag{12}$$

$$(\mathbf{C2}) : (1-\beta_1^{n-1}) > (1-\beta_1)\beta_1^{n-1}n. \tag{13}$$

$$(\mathbf{C3}) : \eta_1 \leq 2\sqrt{(1-\beta_2)\beta_2^n}. \tag{14}$$

The analysis is motivated by that in (Reddi et al., 2018, Theorem 1). However, (Reddi et al., 2018, Theorem 1) considers a simplified case with $\beta_1 = 0$. Here, we consider non-zero β_1, especially for those $\beta_1 > \sqrt{\beta_2}$. To show the divergence, we aim to prove the following claim: (we denote $x_{k,i}$ as the value of x at the k-th outer loop and i-th inner loop)

Claim: for any fixed $n > 2$, there exists an orange region shown in Figure 2 s.t., Adam with any β_1-β_2 combination in the orange region gives $x_{k+1,0} > 1$ as long as $x_{k,0} = 1$.

Since the gradient stays constant when $x > 1$, so x will go to infinity if the claim holds. To prove this claim, we only need to analyze the trajectory of Adam within one particular outer loop, e.g., the k-th outer loop. We will show that $x_{k+1,0} > 1$ if this outer loop is initialized with $x_{k,0} = 1$. Similarly as (Reddi et al., 2018), we assume $f_i(x)$ are sampled in the order of $f_0(x), f_1(x), \cdots, f_{n-1}(x)$ within the k-th outer loop.

Now let us prove the claim. For function (11), the update rule of Adam is shown as follows.

$$x_{k,1} = (x_{k,0} + \delta_{k,0}), \quad \delta_{k,0} = -\frac{\eta_1}{\sqrt{k}}\left(\frac{n(1-\beta_1) + \beta_1 m_{k-1,n-1}}{\sqrt{(1-\beta_2)n^2 + \beta_2 v_{k-1,n-1}}}\right) \tag{15}$$

$$x_{k,i+1} = (x_{k,i} + \delta_{k,i}), \quad i = 1, \cdots, n-1; \tag{16}$$

where $\delta_{k,i} = -\frac{\eta_1}{\sqrt{k}}\left(\frac{(1-\beta_1)\sum_{j=0}^{i-1}(-1)\beta_1^j + (1-\beta_1)\beta_1^i n + \beta_1^{i+1} m_{k-1,n-1}}{\sqrt{(1-\beta_2)+\beta_2 v_{k,i-1}}}\right)$.

We decompose the total movement $\sum_{i=0}^{n-1}\delta_{k,i}$ into three terms as follows.

$$\begin{aligned}
\sum_{i=0}^{n-1}\delta_{k,i} \quad = \quad & \frac{\eta_1}{\sqrt{k}}\underbrace{\left(-\frac{\beta_1 m_{k-1,n-1}}{\sqrt{(1-\beta_2)n^2+\beta_2 v_{k-1,n-1}}} - \frac{\beta_1^2 m_{k-1,n-1}}{\sqrt{(1-\beta_2)+\beta_2 v_{k,0}}} - \cdots - \frac{\beta_1^n m_{k-1,n-1}}{\sqrt{(1-\beta_2)+\beta_2 v_{k,n-2}}}\right)}_{(I)} \\
& + \frac{\eta_1}{\sqrt{k}}\underbrace{\left(\frac{1-\beta_1}{\sqrt{(1-\beta_2)+\beta_2 v_{k,0}}} + \frac{(1-\beta_1)+\beta_1(1-\beta_1)}{\sqrt{(1-\beta_2)+\beta_2 v_{k,1}}} + \cdots + \frac{(1-\beta_1)\sum_{j=0}^{n-2}\beta_1^j}{\sqrt{(1-\beta_2)+\beta_2 v_{k,n-2}}}\right)}_{(II)} \\
& + \frac{\eta_1}{\sqrt{k}}\underbrace{\left(-\frac{n(1-\beta_1)}{\sqrt{(1-\beta_2)n^2+\beta_2 v_{k-1,n-1}}} - \frac{n(1-\beta_1)\beta_1}{\sqrt{(1-\beta_2)+\beta_2 v_{k,0}}} - \cdots - \frac{n(1-\beta_1)\beta_1^{n-1}}{\sqrt{(1-\beta_2)+\beta_2 v_{k,n-2}}}\right)}_{(III)}.
\end{aligned}$$

We will show that for some β_1 and β_2: (I), $(II) > 0$ and $(III) < 0$. However, (I) and (II) outweigh (III), causing the divergence.

First, we show that $m_{k-1,n-1} < 0$ when β_1 is small.

$$
\begin{aligned}
-m_{k-1,n-1} &= (1-\beta_1)\sum_{j=0}^{n-2}\beta_1^j - (1-\beta_1)\beta_1^{n-1}n - \beta_1^n m_{k-2,n-1} \\
&= (1-\beta_1^{n-1}) - (1-\beta_1)\beta_1^{n-1}n - \beta_1^n m_{k-2,n-1} \\
&= \left[(1-\beta_1^{n-1}) - (1-\beta_1)\beta_1^{n-1}n\right]\sum_{j=0}^{k}(\beta_1^n)^j .
\end{aligned}
$$

when β_1 is small,we have $(1-\beta_1^{n-1}) > (1-\beta_1)\beta_1^{n-1}n$, which implies $-m_{k-1,n-1} > 0$. For these choices of β_1, we have $(I) > 0$. Now we derive a lower bound for (II).

$$
\begin{aligned}
(II) &\geq \frac{1-\beta_1}{\sqrt{1+\beta_2 n^2}} + \frac{(1-\beta_1)+\beta_1(1-\beta_1)}{\sqrt{1+\beta_2^2 n^2}} + \cdots + \frac{(1-\beta_1)\sum_{j=0}^{n-2}\beta_1^j}{\sqrt{1+\beta_2^{n-1}n^2}} \\
&= \frac{1-\beta_1}{\sqrt{1+\beta_2 n^2}} + \frac{1-\beta_1^2}{\sqrt{1+\beta_2^2 n^2}} + \cdots + \frac{1-\beta_1^{n-1}}{\sqrt{1+\beta_2^{n-1}n^2}}.
\end{aligned}
$$

The inequality is due to the fact that $v_{k,0} \leq n^2$. Since $\beta_2^j n^2$ is small when β_2 is small and j is close to n, there exists some small β_2 such that $\beta_2^j n^2 \leq 0.1$ for at least one $j < n$. For these small enough β_2, we keep the summand with $j \geq \log_{\beta_2}(0.1/n^2)$ and drop the rest. We have the following lower bound for (II).

$$
(II) \geq \left(n-1-\log_{\beta_2}(\frac{1}{10n^2})\right)\frac{1-\beta_1^{\log_{\beta_2}(\frac{1}{10n^2})}}{\sqrt{1+0.1}}
$$

However, this lower bound only holds for the small β_2. With simple modification, we derive a universal lower bound of (II) for any $\beta_2 \in (0,1)$.

$$
(II) \geq \left(n-1-\min\left\{n-1, \log_{\beta_2}(\frac{1}{10n^2})\right\}\right)\frac{1-\beta_1^{\min\left\{n-1,\log_{\beta_2}(\frac{1}{10n^2})\right\}}}{\sqrt{1+\max\left\{0.1, \beta_2^{n-1}n^2\right\}}}
$$

Now we derive a lower bound for (III).

$$
\begin{aligned}
(III) &= -\frac{n(1-\beta_1)}{\sqrt{(1-\beta_2)n^2+\beta_2 v_{k-1,n-1}}} - \frac{n(1-\beta_1)\beta_1}{\sqrt{(1-\beta_2)+\beta_2 v_{k,0}}} - \cdots - \frac{n(1-\beta_1)\beta_1^{n-1}}{\sqrt{(1-\beta_2)+\beta_2 v_{k,n-2}}} \\
&\geq -\frac{1-\beta_1}{\sqrt{1-\beta_2}}\left(1+n(\sum_{j=1}^{n-1}\beta_1^j)\right) \\
&= -\frac{1-\beta_1}{\sqrt{1-\beta_2}} - \frac{\beta_1(1-\beta_1^{n-1})}{\sqrt{1-\beta_2}}n \\
&\geq -\frac{1-\beta_1}{\sqrt{1-\beta_2}} - \frac{\beta_1}{\sqrt{1-\beta_2}}n.
\end{aligned}
$$

The remaining step is to show for small enough step size η_1, the iterates will stay in the linear region, thus the above gradient holds for all iterates in the trajectory.

As we initial x as $x_0 = 1$, if for all $m < n$ and $k > 0$, $\sum_{i=0}^{m}\delta_{k,i} \geq -2$, we can conclude all iterates in the trajectory stay in the linear region.

Because it holds that $m_{k-1,n-1} \leq 0$ and $v_{k-1,n-1} \geq 0$, we have the following result after dropping most negative terms in the definition of $\delta_{k,i}$:

$$\delta_{k,i} \geq -\frac{\eta_1}{\sqrt{k}} \frac{n(1-\beta_1)\beta_1^i}{\sqrt{n^2(1-\beta_2)\beta_2^i}} \geq -\eta_1 \frac{(1-\beta_1)\beta_1^i}{\sqrt{(1-\beta_2)\beta_2^n}}.$$

Therefore, to make $\sum_{i=0}^m \delta_{k,i} \geq \sum_{i=0}^m -\eta_1 \frac{(1-\beta_1)\beta_1^i}{\sqrt{(1-\beta_2)\beta_2^n}} \geq -2$, we have

$$\eta_1 \leq 2\sqrt{(1-\beta_2)\beta_2^n}.$$

To show the divergence, we want to show that there exists some β_1 and β_2 s.t. the both of the following conditions hold:

$$(\mathbf{C1}) : \left(n-1-\min\left\{n-1, \log_{\beta_2}(\frac{1}{10n^2})\right\}\right) \frac{1-\beta_1^{\min\left\{n-1, \log_{\beta_2}(\frac{1}{10n^2})\right\}}}{\sqrt{1+\max\left\{0.1, \beta_2^{n-1}n^2\right\}}} \geq \frac{1-\beta_1}{\sqrt{1-\beta_2}} + \frac{\beta_1}{\sqrt{1-\beta_2}}n;$$

$$(\mathbf{C2}) : \beta_1 \text{ is small s.t. } (1-\beta_1^{n-1}) > (1-\beta_1)\beta_1^{n-1}n.$$

$$(\mathbf{C3}) : \eta_1 \leq 2\sqrt{(1-\beta_2)\beta_2^n}.$$

The proof of Theorem 3.3 is completed. With the help of Python, we visualize the region where $(\mathbf{C1})$ and $(\mathbf{C2})$ hold. The results are shown in Figure 16. We use orange color to indicate the region where $(\mathbf{C1})$ holds. White color is used for the counter part. As for $(\mathbf{C2})$, we use the gray vertical line to indicate the line where $(1-\beta_1^{n-1}) = (1-\beta_1)\beta_1^{n-1}n$. Note that there are two solutions to this equation: one solution is $\beta_1 = 1$ and the other solution lies in $0 < \beta_1 < 1$, this is why there are two vertical lines in the figure. $(\mathbf{C2})$ holds on the left hand side of the left gray vertical line.

The intersection of two regions will be the region where Adam diverges, which is actually the orange region in Figure 16. As n increases, $(\mathbf{C2})$ holds for a wide range of β_1, so the grey vertical lines move towards $\beta_1 = 1$ and finally get overlapped. In addition, the size of divergence region increases with n

Relation with $\gamma_1(n)$ in Theorem 3.1 According to Theorem 3.1, $\gamma_1(n)$ is at least in the order of $1 - \mathcal{O}(n^{-2})$. Combining with Figure 16. It is not hard to see that $\gamma_1(n)$ is always larger than the upper boundary of the orange region, so there is no contradiction.

Proof of Corollary 4.1. For any $(\beta_1, \beta_2) \in [0,1)^2$, condition **(C1), (C2)** and **(C3)** can be satisfied by some sufficiently large n. Therefore, Adam will diverge and the proof is concluded.

F Some More Notations and Useful Lemmas for Convergence Analysis

F.1 More notations

- We denote $x_{k,i}, m_{k,i}, v_{k,i} \in \mathbb{R}^d$ as the value of x, m, v at the k-th outer loop and i-th inner loop. Further, we denote $x_{l,k,i}, m_{l,k,i}, v_{l,k,i} \in \mathbb{R}$ as the l-th component of $x_{k,i}, m_{k,i}, v_{k,i}$.
- We denote η_k as the stepsize at the k-th epoch (outer loop). We will focus mainly on diminishing step size, especially $\eta_k = \frac{\eta_1}{\sqrt{nk}}$, where n is the number of batches (inner loop).
- We denote $\partial_l f(x) = \frac{\partial}{\partial x_l} f(x)$, $\partial_l f_j(x) = \frac{\partial}{\partial x_l} f_j(x)$. Further, we will use $\tau_{k,i}$ to index the i-th randomly chosen batch in the k-th epoch. In this sense, we denote $\partial_l f_{\tau_{k,i}}(x)$ as $\frac{\partial}{\partial x_l} f_{\tau_{k,i}}(x)$.
- Given an epoch k, we denote α as the index of the coordinate with the greatest gradient:

$$\alpha = \arg\max_{l=1,2,\cdots,d} \left|\partial_l f\left(x_{k,0}\right)\right|.$$

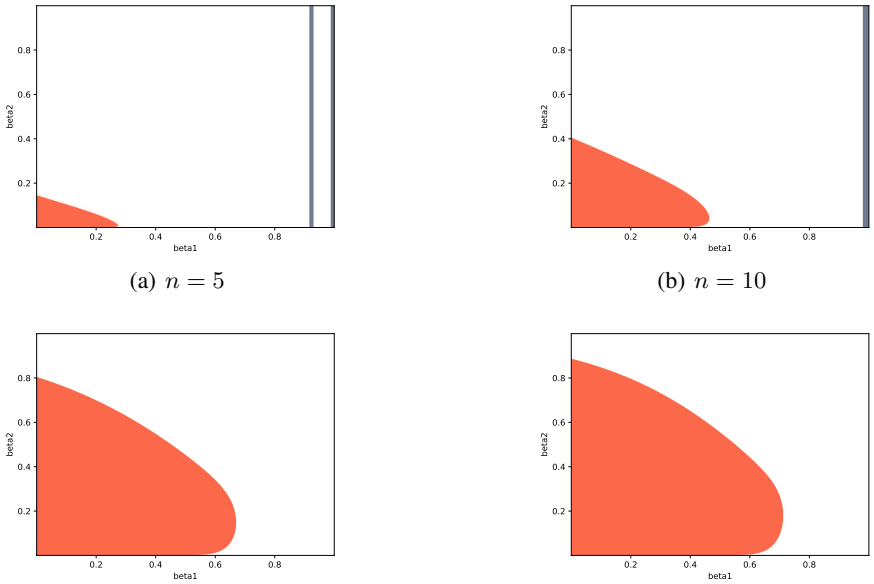

(a) $n = 5$ (b) $n = 10$

(c) $n = 50$ (d) $n = 100$

Figure 16: This figure illustrates the region where both $(\mathbf{C1})$ and $(\mathbf{C2})$ in Proposition E.1 hold. The orange color indicates the region where $(\mathbf{C1})$ holds. White color is used for the counter part. The gray vertical lines are used to indicate the boundary of $(\mathbf{C2})$. Note that there are two solutions to the equation in $(\mathbf{C2})$: one solution is $\beta_1 = 1$ and the other solution lies in $0 < \beta_1 < 1$, this is why there are two vertical lines in the figure. $(\mathbf{C2})$ holds on the left hand side of the left gray vertical line. This figure is visualized in Python.

- We define ρ_1, ρ_2, ρ_3 as constants satisfying the following condition for any $l = 1, \cdots, d$:

$$\rho_1 \geq \frac{\sum_{i=1}^n |\partial_l f_i(x_{k,0})|}{\sqrt{\sum_{i=1}^n |\partial_l f_i(x_{k,0})|^2}};$$

$$\rho_2 \geq \frac{|\max_i \partial_l f_i(x_{k,0})|^2}{\frac{1}{n}\sum_{i=1}^n |\partial_l f_i(x_{k,0})|^2};$$

$$\rho_3 \geq \frac{|\sum_{i=1}^n \partial_l f_i(x_{k,0})|}{\sqrt{\frac{1}{n}\sum_{i=1}^n |\partial_l f_i(x_{k,0})|^2}}.$$

  ρ_1, ρ_2, ρ_3 are problem-dependent constants. In worst case, we have $0 \leq \rho_3 \leq \sqrt{n}\rho_1 \leq n$.
- We define the constant $\triangle_x := \frac{\eta_0}{\sqrt{x}} \frac{L\sqrt{d}}{\sqrt{1-\beta_2}} \frac{1-\beta_1}{1-\frac{\beta_1}{\sqrt{\beta_2}}}$. This constant will be used repeatedly, especially in Lemma F.2.
- We define $Q_k := \triangle_1 \frac{n\sqrt{n}}{\sqrt{k}} \frac{32\sqrt{2}}{(1-\beta_2)^n \beta_2^n}$. This constant will be used repeatedly.
- We define

$$\delta_1 = \frac{(1-\beta_2)4n\rho_2}{\beta_2^n} + \left(\frac{1}{\sqrt{\beta_2^n}} - 1\right). \tag{17}$$

  This constant will be used repeatedly. Note that $\delta_1 \to 0$ when $\beta_2 \to 1$.
- $\mathbb{E}(\cdot)$ means taking expectation over the whole trajectory.
- We will use $\mathbb{E}_k[\cdot]$ as a shorthand for $\mathbb{E}[\cdot \mid x_{k,0}, x_{k-1,n-1}, \cdots, x_{1,0}]$, i.e. the conditional expectation given all the history up to $x_{k,0}$. Similarly, $\mathbb{E}_{k-1}$ stands for the conditional expectation given all the history up to $x_{k-1,0}$.

We further introduce some 'index' notation of the stochastic gradients, these notations will be useful in the proof. For all the stochastic gradient, we have

- **True index:** every stochastic gradient has its own true index: $f_1(\cdot), f_2(\cdot), \cdots, f_{n-1}(\cdot)$. All these $\{f_i(\cdot)\}_{i=0}^{n-1}$ are fixed once the optimization problem is formulated.
  Note that for a fixed x, we have the following relationship between f_i and f:
$$\sum_{i=0}^{n-1} \partial_l f_i(x) = \partial_l f(x). \tag{18}$$
- **Random-shuffle index:** At the k-th epoch, all the stochastic gradients are sampled in the order of $f_{\tau_{k,0}}(\cdot), f_{\tau_{k,1}}(\cdot), \cdots, f_{\tau_{k,n-1}}(\cdot)$.
  Since Algorithm 1 is sampling without replacement, there is an implicit bijective mapping between $\{f_i(\cdot)\}_{i=0}^{n-1}$ and $\{f_{\tau_{k,i}}(\cdot)\}_{i=0}^{n-1}$. Further, for a fixed x, we have the following useful property:
$$\sum_{i=0}^{n-1} \partial_l f_{\tau_{k,i}}(x) = \partial_l f(x). \tag{19}$$
- **Index for m and v:** As shown in Algorithm 1, we denote :
$$m_{l,k,i} = (1-\beta_1)\{\partial_l f_{\tau_{k,i}}(x_{k,i}) + \cdots + \beta_1^i \partial_l f_{\tau_{k,0}}(x_{k,0})\} + \beta_1^{i+1} m_{l,k,0},$$
$$v_{l,k,i} = (1-\beta_2)\{\partial_l f_{\tau_{k,i}}(x_{k,i})^2 + \cdots + \beta_1^i \partial_l f_{\tau_{k,0}}(x_{k,0})^2\} + \beta_2^{i+1} v_{l,k,0}.$$

F.2 Some useful lemmas

We begin with proving some useful lemmas.

Lemma F.1. *For any $\beta \neq 1$, we have*
$$(1-\beta)\sum_{j=1}^{\infty} \beta^{j-1} = 1,$$
$$(1-\beta)\sum_{j=1}^{\infty} j\beta^{j-1} = \frac{1}{1-\beta},$$
$$(1-\beta)\sum_{j=1}^{\infty} j^2\beta^{j-1} = \frac{1+\beta}{(1-\beta)^2}.$$

Proof. Proof only involves basic calculation, we omit the proof here. □

Lemma F.2. *Under Assumption 2.1, if $\beta_1 < \sqrt{\beta_2}$, we have*
$$\left|\partial_l f_{\tau_{k,i}}(x_{k,i+1}) - \partial_l f_{\tau_{k,i}}(x_{k,i})\right| \leq \frac{\eta_0}{\sqrt{nk}} \frac{L\sqrt{d}}{\sqrt{1-\beta_2}} \frac{1-\beta_1}{1-\frac{\beta_1}{\sqrt{\beta_2}}} = \triangle_{nk}. \tag{20}$$

Proof. We start with bounding $|x_{l,k,i+1} - x_{l,k,i}|$. By the update formula of Adam, we have

$$\begin{aligned}
|x_{l,k,i+1} - x_{l,k,i}| &= \eta_k \frac{|m_{l,k,i}|}{\sqrt{v_{l,k,i}}} \\
&\leq \eta_k(1-\beta_1)\left\{\beta_1^0 \frac{|\partial_l f_{\tau_{k,i}}(x_{k,i})|}{\sqrt{v_{l,k,i}}} + \beta_1 \frac{|\partial_l f_{\tau_{k,i-1}}(x_{k,i-1})|}{\sqrt{v_{l,k,i}}} + \dots\right\} \\
&\leq \eta_k(1-\beta_1)\left\{\beta_1^0 \frac{|\partial_l f_{\tau_{k,i}}(x_{k,i})|}{\sqrt{(1-\beta_2)\beta_2^0}|\partial_l f_{\tau_{k,i}}(x_{k,i})|} + \beta_1 \frac{|\partial_l f_{\tau_{k,i-1}}(x_{k,i-1})|}{\sqrt{(1-\beta_2)\beta_2}|\partial_l f_{\tau_{k,i-1}}(x_{k,i-1})|} + \dots\right\} \\
&\leq \eta_k \frac{(1-\beta_1)}{\sqrt{1-\beta_2}}\left((\frac{\beta_1}{\sqrt{\beta_2}})^0 + (\frac{\beta_1}{\sqrt{\beta_2}})^1 + (\frac{\beta_1}{\sqrt{\beta_2}})^2 + \dots\right) \\
&= \eta_k \frac{(1-\beta_1)}{\sqrt{1-\beta_2}} \frac{1}{1-\frac{\beta_1}{\sqrt{\beta_2}}}.
\end{aligned} \tag{21}$$

Now, by Assumption 2.1, we have

$$\begin{aligned}
\left|\partial_l f_{\tau_{k,i}}(x_{k,i+1}) - \partial_l f_{\tau_{k,i}}(x_{k,i})\right| &\leq \|\nabla f_{\tau_{k,i}}(x_{k,i+1}) - \nabla f_{\tau_{k,i}}(x_{k,i})\|_2 \\
&\leq L\|x_{k,i+1} - x_{k,i}\|_2 \\
&\leq L\sqrt{d}\max_l |x_{l,k,i+1} - x_{l,k,i}| \\
&\leq \eta_k \frac{L\sqrt{d}}{\sqrt{1-\beta_2}} \frac{1-\beta_1}{1-\frac{\beta_1}{\sqrt{\beta_2}}} \\
&= \frac{\eta_0}{\sqrt{nk}} \frac{L\sqrt{d}}{\sqrt{1-\beta_2}} \frac{1-\beta_1}{1-\frac{\beta_1}{\sqrt{\beta_2}}} \qquad (22)
\end{aligned}$$

Proof is completed.

□

Lemma F.3. *Under Assumption 2.1 and 2.2, for any integer $i \in [0, n-1]$, we have the following two results,*

$$|\partial_l f_{\tau_{k,i}}(x_{k,i})| \leq i\triangle_{nk} + \sqrt{D_1}\rho_1 d\left(|\partial_\alpha f(x_{k,0})| + \sqrt{\frac{D_0}{D_1 d}}\right), \qquad (23)$$

$$|\partial_l f_{\tau_{k,i}}(x_{k,0})| \leq \sum_{i=0}^{n-1} |\partial_l f_{\tau_{k,i}}(x_{k,0})| \leq \sum_{l=1}^{d}\sum_{i=0}^{n-1} |\partial_l f_{\tau_{k,i}}(x_{k,0})| \leq \sqrt{D_1}\rho_1 d\left(|\partial_\alpha f(x_{k,0})| + \sqrt{\frac{D_0}{D_1 d}}\right), \qquad (24)$$

where $|\partial_\alpha f(x_{k,0})| = \max_{l\in[1,d]} |\partial_l f(x_{k,0})|$.

Proof.

$$\begin{aligned}
|\partial_l f_{\tau_{k,j}}(x_{k,j})| &\overset{\text{Lemma } F.2}{\leq} j\triangle_{nk} + |\partial_l f_{\tau_{k,j}}(x_{k,0})| \\
&\leq j\triangle_{nk} + \sum_{l=1}^{d}\sum_{j=0}^{n-1} |\partial_l f_{\tau_{k,j}}(x_{k,0})| \\
&\overset{(*)}{\leq} j\triangle_{nk} + \rho_1 \sum_{l=1}^{d} \sqrt{\sum_{i=0}^{n-1} |\partial_l f_i(x_{k,0})|^2} \\
&\overset{\text{Cauchy-Swartz inequality}}{\leq} j\triangle_{nk} + \rho_1\sqrt{d}\sqrt{\sum_{l=1}^{d}\sum_{i=0}^{n-1} |\partial_l f_i(x_{k,0})|^2} \\
&\overset{\text{Assumption 2.2}}{\leq} j\triangle_{nk} + \rho_1\sqrt{d}\sqrt{D_1\|\nabla f(x_{k,0})\|_2^2 + D_0} \\
&\overset{(**)}{\leq} j\triangle_{nk} + \sqrt{D_1}\rho_1 d\sqrt{|\partial_\alpha f(x_{k,0})|^2 + \frac{D_0}{D_1 d}} \\
&\leq j\triangle_{nk} + \sqrt{D_1}\rho_1 d\left(|\partial_\alpha f(x_{k,0})| + \sqrt{\frac{D_0}{D_1 d}}\right)
\end{aligned}$$

where $(*)$ is because of the definition (see Appendix F.1): ρ_1 is a constant satisfying $\rho_1 \geq \frac{\sum_{i=1}^n |\partial_l f_i(x_{k,0})|}{\sqrt{\sum_{i=1}^n |\partial_l f_i(x_{k,0})|^2}}$; $(**)$ is due to $\|\nabla f(x_{k,0})\|_2^2 \leq d\,|\partial_\alpha f(x_{k,0})|^2$. The proof of (24) follows the same procedure as above. □

G Proof of Theorem 3.1

G.1 A roadmap of the proof

Our proof is based on the Descent Lemma:

$$\mathbb{E}f(x_{k+1,0}) - \mathbb{E}f(x_{k,0}) \quad \leq \quad \mathbb{E}\langle \nabla f(x_{k,0}), x_{k+1,0} - x_{k,0}\rangle + \frac{L}{2}\mathbb{E}\|x_{k+1,0} - x_{k,0}\|_2^2$$

The expectation $\mathbb{E}(\cdot)$ is taken on the whole trajectory. Summing both sides from the initialization $k = t_0$ to $k = T$, we have the following re-arranged inequality: (usually we set $t_0 = 1$.)

$$\mathbb{E}\sum_{k=t_0}^{T}\langle \nabla f(x_{k,0}), x_{k,0} - x_{k+1,0}\rangle \quad \leq \quad \frac{L}{2}\sum_{k=t_0}^{T}\mathbb{E}\|x_{k+1,0} - x_{k,0}\|_2^2 + \mathbb{E}f(x_{t_0,0}) - \mathbb{E}f(x_{T+1,0}). \quad (25)$$

To prove the convergence, we need an upper bound for $\frac{L}{2}\mathbb{E}\|x_{k+1,0} - x_{k,0}\|_2^2$, as well as a lower bound for $\mathbb{E}\langle \nabla f(x_{k,0}), x_{k,0} - x_{k+1,0}\rangle$ (and such a lower bound should be in the order of $\frac{1}{\sqrt{k}}\mathbb{E}\|\nabla f(x_{k,0})\|$).

The upper bound for $\frac{L}{2}\mathbb{E}\|x_{k+1,0} - x_{k,0}\|_2^2$ is relatively easy to get: according to the update rule of Adam, this term is in the order of $\mathcal{O}(\eta_k^2 m_{l,k,i}/v_{l,k,i}) = \mathcal{O}(\eta_k^2\|\nabla f(x_{k,0})\|/\|\nabla f(x_{k,0})\|) = \mathcal{O}(\frac{1}{k})$. Further, recall $\sum_{k=t_0}^{T}\frac{1}{k} \leq \log\frac{T+1}{t_0}$, so $\frac{L}{2}\mathbb{E}\|x_{k+1,0} - x_{k,0}\|_2^2$ contributes to the $\log$ term in Theorem 3.1. The proof is shown in Lemma F.2.

However, the lower bound for $\mathbb{E}\langle \nabla f(x_{k,0}), x_{k,0} - x_{k+1,0}\rangle = \mathbb{E}\left[\sum_{l=1}^{d}\sum_{i=0}^{n-1}\partial_l f(x_{k,0})\frac{m_{l,k,i}}{\sqrt{v_{l,k,i}}}\right]$ requires sophisticated derivation, we explain as follows. Before taking the expectation, we first work on every possible realization of $\sum_{l=1}^{d}\sum_{i=0}^{n-1}\partial_l f(x_{k,0})\frac{m_{l,k,i}}{\sqrt{v_{l,k,i}}}$. We perform the following decomposition for every $l \in [1, d]$.

$$\begin{aligned}\sum_{i=0}^{n-1}\partial_l f(x_{k,0})\frac{m_{l,k,i}}{\sqrt{v_{l,k,i}}} &= \sum_{i=0}^{n-1}\frac{\partial_l f(x_{k,0})}{\sqrt{v_{l,k,i}}}\left(\partial_l f_i(x_{k,0}) + m_{l,k,i} - \partial_l f_i(x_{k,0})\right) \\ &= \underbrace{\left[\sum_{i=0}^{n-1}\frac{\partial_l f(x_{k,0})}{\sqrt{v_{l,k,i}}}\partial_l f_i(x_{k,0})\right]}_{(a)} + \underbrace{\left[\partial_l f(x_{k,0})\sum_{i=0}^{n-1}\frac{1}{\sqrt{v_{l,k,i}}}(m_{l,k,i} - \partial_l f_i(x_{k,0}))\right]}_{(b)}.\end{aligned} \quad (26)$$

First of all, we introduce the following Lemma G.1 to further decompose (a) and (b). The intuition of this decomposition is as follows: by increasing β_2, we can control the movement of the moving average factor $v_{l,k,i}$, so the trajectory of Adam is easier to control.

Lemma G.1. *Under Assumption 2.1, for those l satisfying $\max_i|\partial_l f_i(x_{k,0})| \geq Q_k := \triangle_1\frac{n\sqrt{n}}{\sqrt{k}}\frac{32\sqrt{2}}{(1-\beta_2)^n\beta_2^n}$, we have the following lower bound for (a) in (26):*

$$\sum_{i=0}^{n-1}\frac{\partial_l f(x_{k,0})}{\sqrt{v_{l,k,i}}}\partial_l f_i(x_{k,0}) \quad \geq \quad \frac{\partial_l f\left(x_{k,0}\right)^2}{\sqrt{v_{l,k,0}}} - \delta_1\left|\frac{\partial_l f(x_{k,0})}{\sqrt{v_{l,k,0}}}\right|\sum_i\left|\partial_l f_i\left(x_{k,0}\right)\right|, \quad (27)$$

where $\delta_1 = \frac{(1-\beta_2)4n\rho_2}{\beta_2^n} + \left(\frac{1}{\sqrt{\beta_2^n}} - 1\right)$. ρ_2, ρ_3 are constants satisfying $\rho_2 \geq \frac{|\max_i\partial_l f_i(x_{k,0})|^2}{\frac{1}{n}\sum_{i=1}^{n}|\partial_l f_i(x_{k,0})|^2}$, $\rho_3 \geq \frac{\left|\sum_{i=1}^{n}\partial_l f_i(x_{k,0})\right|}{\sqrt{\frac{1}{n}\sum_{i=1}^{n}|\partial_l f_i(x_{k,0})|^2}}$. Note that $\delta_1 \to 0$ when $\beta_2 \to 1$.

Under the same condition, we also have a lower bound for (b) in (26):

$$
\begin{aligned}
&\sum_{i=0}^{n-1} \frac{\partial_l f\left(x_{k,0}\right)}{\sqrt{v_{l,k,i}}}\left(m_{l,k,i}-\partial_l f_i\left(x_{k,0}\right)\right) \\
\geq\quad & \frac{\partial_l f(x_{k,0})}{\sqrt{v_{l,k,0}}} \sum_{i=0}^{n-1}\left(m_{l,k,i}-\partial_l f_i\left(x_{k,0}\right)\right)-\delta_1\left|\frac{\partial_l f(x_{k,0})}{\sqrt{v_{l,k,0}}}\right| \sum_{i=0}^{n-1}\left|m_{l,k,i}-\partial_l f_i\left(x_{k,0}\right)\right|. \quad (28)
\end{aligned}
$$

The proof can be seen in Appendix G.2. Lemma G.1 decomposes both (a) and (b): in the denominator, we approximate $v_{l,k,i}$ (which is changing with i) by $v_{l,k,0}$ (which is fixed). Accordingly, the approximation error can be controlled by increasing β_2 (since $\delta_1 \to 0$ when $\beta_2 \to 1$). However, Lemma G.1 can only be applied to those l with $\max_i |\partial_l f_i(x_{k,0})| \geq Q_k$, so we need to discuss the following two cases to complete the whole picture.

Case 1: unbounded gradient. Given $x_{k,0}$, consider those l with $\max_i |\partial_l f_i(x_{k,0})| \geq Q_k$, we have the following decomposition:

$$
\begin{aligned}
\sum_{i=0}^{n-1} \partial_l f(x_{k,0}) \frac{m_{l,k,i}}{\sqrt{v_{l,k,i}}} \overset{(26)}{\geq}\quad & \underbrace{\left[\sum_{i=0}^{n-1} \frac{\partial_l f(x_{k,0})}{\sqrt{v_{l,k,i}}} \partial_l f_i(x_{k,0})\right]}_{(a)}+\underbrace{\left[\partial_l f(x_{k,0}) \sum_{i=0}^{n-1} \frac{1}{\sqrt{v_{l,k,i}}}\left(m_{l,k,i}-\partial_l f_i(x_{k,0})\right)\right]}_{(b)}. \\
\overset{\text{Lemma G.1}}{\geq}\quad & \frac{\partial_l f\left(x_{k,0}\right)^2}{\sqrt{v_{l,k,0}}}-\delta_1\left|\frac{\partial_l f(x_{k,0})}{\sqrt{v_{l,k,0}}}\right| \sum_{i=0}^{n-1}\left|\partial_l f_i\left(x_{k,0}\right)\right| \\
& +\frac{\partial_l f(x_{k,0})}{\sqrt{v_{l,k,0}}} \sum_{i=0}^{n-1}\left(m_{l,k,i}-\partial_l f_i(x_{k,0})\right)-\delta_1\left|\frac{\partial_l f(x_{k,0})}{\sqrt{v_{l,k,0}}}\right| \sum_{i=0}^{n-1}\left|m_{l,k,i}-\partial_l f_i(x_{k,0})\right| \\
\overset{\text{Lemma G.10}}{\geq}\quad & \underbrace{\left[\frac{\partial_l f\left(x_{k,0}\right)^2}{\sqrt{v_{l,k,0}}}\right]}_{(a_1)}-\underbrace{\left[\delta_1 \sqrt{\frac{2 \rho_3^2}{\beta_2^n}} \sum_{i=0}^{n-1}\left|\partial_l f_i\left(x_{k,0}\right)\right|\right]}_{(a_2)} \\
& +\underbrace{\left[\frac{\partial_l f(x_{k,0})}{\sqrt{v_{l,k,0}}} \sum_{i=0}^{n-1}\left(m_{l,k,i}-\partial_l f_i(x_{k,0})\right)\right]}_{(b_1)}-\underbrace{\left[\delta_1 \sqrt{\frac{2 \rho_3^2}{\beta_2^n}} \sum_{i=0}^{n-1}\left|m_{l,k,i}-\partial_l f_i(x_{k,0})\right|\right]}_{(b_2)},
\end{aligned}
\quad (29)
$$

Case 2: bounded gradient. Given $x_{k,0}$, consider those l with $\max_i |\partial_l f_i(x_{k,0})| \leq Q_k$, the analysis degenerates to the "bounded gradient" scenario, we have the following lower bound:

$$
\begin{aligned}
\sum_{i=0}^{n-1} \partial_l f(x_{k,0}) \frac{m_{l,k,i}}{\sqrt{v_{l,k,i}}} \quad & \geq \quad -\sum_{i=0}^{n-1}\left|\partial_l f(x_{k,0})\right|\left|\frac{m_{l,k,i}}{\sqrt{v_{l,k,i}}}\right| \\
& \overset{(21)}{\geq} \quad -|\partial_l f(x_{k,0})| \frac{1-\beta_1}{\sqrt{1-\beta_2}} \frac{1}{1-\frac{\beta_1}{\sqrt{\beta_2}}} n \\
& \overset{(*)}{\geq} \quad -n Q_k \frac{1-\beta_1}{\sqrt{1-\beta_2}} \frac{1}{1-\frac{\beta_1}{\sqrt{\beta_2}}} n \\
& = \quad -\triangle_1 \frac{n^2 \sqrt{n}}{\sqrt{k}} \frac{32 \sqrt{2}}{(1-\beta_2)^n \beta_2^n} \frac{1-\beta_1}{\sqrt{1-\beta_2}} \frac{1}{1-\frac{\beta_1}{\sqrt{\beta_2}}} n \\
& := \quad -F_1 \frac{1}{\sqrt{k}},
\end{aligned}
$$

where $F_1 := \triangle_1 n^2 \sqrt{n} \frac{32\sqrt{2}}{(1-\beta_2)^n \beta_2^n} \frac{1-\beta_1}{\sqrt{1-\beta_2}} \frac{1}{1-\frac{\beta_1}{\sqrt{\beta_2}}} n$, $(*)$ is due to the fact that $|\partial_l f(x_{k,0})| \leq n \max_i |\partial_l f_i(x_{k,0})| \leq nQ_k$.

Combining **Case 1 & 2** together, we have the following result (note that $(a_1), (a_2), (b_1), (b_2)$ vary with l. A more precise notation will be $(a_1)_l$, etc. We drop the subscript for brevity).

$$\begin{aligned}
\sum_{l=1}^{d} \sum_{i=0}^{n-1} \partial_l f(x_{k,0}) \frac{m_{l,k,i}}{\sqrt{v_{l,k,i}}} &\geq \underbrace{\sum_{l \text{ large}} \{(a_1) - (a_2) + (b_1) - (b_2)\}}_{\text{unbounded gradient}} - \underbrace{\sum_{l \text{ small}} F_1 \frac{1}{\sqrt{k}}}_{\text{bounded gradient}} \\
&\geq \underbrace{\sum_{l \text{ large}} \{(a_1) - (a_2) + (b_1) - (b_2)\}}_{\text{unbounded gradient}} - \underbrace{\sum_{l=1}^{d} \left\{ F_1 \frac{1}{\sqrt{k}} \right\}}_{\text{bounded gradient}} \\
&\geq \left\{ \sum_{l \text{ large}} (a_1) \right\} + \left\{ \sum_{l \text{ large}} (b_1) \right\} - \left\{ \sum_{l \text{ large}} \{(a_2) + (b_2)\} \right\} - dF_1 \frac{1}{\sqrt{k}},
\end{aligned} \tag{30}$$

where "l large" stands for the gradient component in **Case 1** and "l small" indicates those in **Case 2**. We assume "l large" is not an empty set, otherwise the analysis degenerates to the proof with bounded gradient assumption.

Now we take expectation on (30). The expectation is taken on all the possible trajectories up to the i-th iteration in k-th epoch.

$$\mathbb{E}\left[\sum_{l=1}^{d} \sum_{i=0}^{n-1} \partial_l f(x_{k,0}) \frac{m_{l,k,i}}{\sqrt{v_{l,k,i}}} \right] \overset{(30)}{\geq} \mathbb{E}\left\{ \sum_{l \text{ large}} (a_1) + \sum_{l \text{ large}} (b_1) - \sum_{l \text{ large}} \{(a_2) + (b_2)\} \right\} - dF_1 \frac{1}{\sqrt{k}}, \tag{31}$$

In the following context, we will discuss how to bound all terms in (31), respectively. First and foremost, we derive a lower bound for $\mathbb{E}\left[\sum_{l \textbf{ large}} (b_1)\right]$. Since $\mathbb{E}\left[\sum_{l \textbf{ large}} (b_1)\right]$ contains all the historical gradient information, it involves great effort to handle it. We will show that the lower bound of $\mathbb{E}\left[\sum_{l \textbf{ large}} (b_1)\right]$ will vanish when β_2 is large and k goes to infinity.

Recall $\mathbb{E}\left[\sum_{l \text{ large}} (b_1)\right] = \mathbb{E}\left[\sum_{l \text{ large}} \frac{\partial_l f(x_{k,0})}{\sqrt{v_{l,k,0}}} \sum_{i=0}^{n-1} (m_{l,k,i} - \partial_l f_i(x_{k,0}))\right]$. When β_1 is large, $m_{l,k,i}$ contains heavy historical signals. It seems unclear how large $\mathbb{E}\left[\sum_{l \text{ large}} (b_1)\right]$ would be when β_1 goes to 1. Existing literatures (Zaheer et al., 2018; De et al., 2018; Shi et al., 2020) take a naive approach: they set $\beta_1 \approx 0$ so that $m_{k,i} \approx \nabla f_{\tau_{k,i}}(x_{k,i})$. Then we get $\delta(\beta_1) \approx 0$. However, this naive method cannot be applied here since we are interested in practical cases where β_1 is large in $[0, 1)$. We emphasize the following technical difficulties in bounding $\mathbb{E}\left[\sum_{l \text{ large}} (b_1)\right]$ for any $\beta_1 \in [0, 1)$:

- **Issue (i)** In order to bound $\mathbb{E}\left[\sum_{l \text{ large}} (b_1)\right]$, we need to first know how to bound its simpler version: $\mathbb{E}\left[\sum_{i=0}^{n-1} (m_{l,k,i} - \partial_l f_i(x_{k,0}))\right]$. This term measures the difference between the current gradient and weighted historical gradients. It seems unclear that how large this term could be when β_1 goes to 1.

- **Issue (ii)** Even if we can bound $\mathbb{E}\left[\sum_{i=0}^{n-1}\left(m_{l,k,i}-\partial_l f_i(x_{k,0})\right)\right]$, it is still unclear how to bound $\mathbb{E}\left[\frac{\partial_l f(x_{k,0})}{\sqrt{v_{l,k,0}}}\sum_{i=0}^{n-1}\left(m_{l,k,i}-\partial_l f_i(x_{k,0})\right)\right]$, which is further multiplied by a random variable $\frac{\partial_l f(x_{k,0})}{\sqrt{v_{l,k,0}}}$.
- **Issue (iii)** Even if we can bound $\mathbb{E}\left[\frac{\partial_l f(x_{k,0})}{\sqrt{v_{l,k,0}}}\sum_{i=0}^{n-1}\left(m_{l,k,i}-\partial_l f_i(x_{k,0})\right)\right]$, it is still different from $\mathbb{E}\left[\sum_{l\text{ large}}(b_1)\right]$ which contains additional operation "$\sum_{l\text{ large}}$" inside the expectation. Note that the set "l large" is a random variable which changes along different trajectories, so there is still non-negligible gap between bounding $\mathbb{E}\left[\sum_{l\text{ large}}(b_1)\right]$ and $\mathbb{E}\left[\frac{\partial_l f(x_{k,0})}{\sqrt{v_{l,k,0}}}\sum_{i=0}^{n-1}\left(m_{l,k,i}-\partial_l f_i(x_{k,0})\right)\right]$.

To our best knowledge, there is no general approach to tackle the above issues. In the following content, we will overcome difficulties (i), (ii) and (iii) in Step 1, 2 and 3 respectively. In Step 1, we will discuss how to bound $\mathbb{E}\left[\sum_{i=0}^{n-1}\left(m_{l,k,i}-\partial_l f_i(x_{k,0})\right)\right]$, which is a simplified version of $\mathbb{E}\left[(b_1)\right]$. Bounding this term will shed light on bounding the whole term $\mathbb{E}\left[\sum_{l\text{ large}}(b_1)\right]$. Then in Step 2 and 3, we will prove several technical lemmas to handle the effect of $\frac{\partial_l f(x_{k,0})}{\sqrt{v_{l,k,0}}}$ and "$\sum_{l\text{ large}}$", by which we can tackle **(ii)** and **(iii)**. Combining all together we can bound $\mathbb{E}\left[\sum_{l\text{ large}}(b_1)\right]$.

Bounding $\mathbb{E}\left[\sum_{l\text{ large}}(b_1)\right]$: Step 1. We now introduce the key idea of bounding $\mathbb{E}\left[\sum_{i=0}^{n-1}\left(m_{l,k,i}-\partial_l f_i(x_{k,0})\right)\right]$. In Appendix A, we distill our idea into a toy example called "the color-ball model of the 1st kind" and thus we prove Lemma A.1. This lemma is crucial for bounding $\mathbb{E}\left[\sum_{i=0}^{n-1}\left(m_{l,k,i}-\partial_l f_i(x_{k,0})\right)\right]$. We refer the readers to Appendix A for more explanation.

Lemma A.1 can provide insights in bounding $\mathbb{E}\left[\sum_{i=0}^{n-1}\left(m_{l,k,i}-\partial_l f_i(x_{k,0})\right)\right]$. However, there is still certain gap between $\mathbb{E}\left[\sum_{i=0}^{n-1}\left(m_{l,k,i}-\partial_l f_i(x_{k,0})\right)\right]$ and the quantities in Lemma A.1. We elaborate as follows:

- To mimic the color-ball example, we need to expand $\sum_{i=0}^{n-1}\partial_l f_i(x_{k,0})$ into an *infinite* sum sequence: $\sum_{i=0}^{n-1}\partial_l f_i(x_{k,0})(1-\beta_1)(1+\beta_1+\cdots\beta_1^{\infty})$. However, $\sum_{i=0}^{n-1} m_{l,k,i}$ is a *finite* sum sequence up to the order of β^{kn}. In contrast, both sequences in the color-ball example are "finite sum". As such, there is an error term caused by "finite sum v.s. infinite sum".
- When taking the expectation, the variable x in each possible trajectory is different. In contrast, in the color-ball example, $\{a_i\}_{i=0}^2$ are fixed in all shuffling order (so it is much easier to calculate the expectation by summing them up).

  To mimic the color-ball example, we repeatedly take conditional expectation at the beginning of each k-th epoch. In this way, $x_{k,0}$ will be fix. Despite $x_{k,i}$ is still changing across the trajectory, we can transform $x_{k,i}$ into $x_{k,0}$ by using Lipschitz property.
- In each trajectory of $\sum_{i=0}^{n-1} m_{l,k,i}$, the variable x in the summand of $m_{l,k,i}$ varies with k and i; while the variable in $\partial_l f_i(x_{k,0})$ is fixed to be $x_{k,0}$. In contrast, in the color-ball example, $\{a_i\}_{i=0}^2$ are the same across the epoch.

  To mimic the final step in the color-ball example (Figure 6), at each step of conditional expectation, we need to simultaneously move the variables in $m_{l,k,i}$ and $\partial_l f_i(x_{k,0})$ (using Lipschitz property) so that they can match and cancel out with each other. This operation will introduce new error terms and it is our duty to put them under control.

We omit the proof for bounding $\mathbb{E}\left[\sum_{i=0}^{n-1}\left(m_{l,k,i}-\partial_l f_i(x_{k,0})\right)\right]$ since this is not our actual goal. Instead, we will directly use the above ideas to bound $\mathbb{E}\left[(b_1)\right]$. To do so, we need to further tackle the issue **(ii)** and **(iii)** mentioned before. We explain as follows.

Bounding $\mathbb{E}\left[\sum_{l \text{ large}}(b_1)\right]$: Step 2. We now resolve issue **(ii)**, i.e., handle the effect of $\frac{\partial_l f(x_{k,0})}{\sqrt{v_{l,k,0}}}$. The key idea is as follows: when we calculate $\mathbb{E}\left[(b_1)\right]$, we sequentially take conditional expectation $\mathbb{E}_k(\cdot)$, $\mathbb{E}_{k-1}(\cdot)$, etc.. When taking $\mathbb{E}_k(\cdot)$, we will fix all the historical information up to k-th epoch, so $\frac{\partial_l f(x_{k,0})}{\sqrt{v_{l,k,0}}}$ can be regarded as a constant. In this sense, $\mathbb{E}_k\left[\frac{\partial_l f(x_{k,0})}{\sqrt{v_{l,k,0}}}\sum_{i=0}^{n-1}\left(m_{l,k,i}-\partial_l f_i(x_{k,0})\right)\right]$ can be calculated following the same idea as color-ball toy example.

However, when taking $\mathbb{E}_{k-1}(\cdot)$, $\frac{\partial_l f(x_{k,0})}{\sqrt{v_{l,k,0}}}$ will become a random variable which changes with different trajectories. In this case, the color-ball method *cannot* be applied. To fix this issue, we introduce the following lemma to change $\frac{\partial_l f(x_{k,0})}{\sqrt{v_{l,k,0}}}$ into $\frac{\partial_l f(x_{k-1,0})}{\sqrt{v_{k-1,0}}}$, which can again be regarded as a fixed constant when taking $\mathbb{E}_{k-1}(\cdot)$.

Lemma G.2. *Suppose Assumption 2.1 holds and $\beta_1 < \sqrt{\beta_2}$. For any integer $j \in [0,k]$, if $\max_i |\partial_l f_i(x_{k,0})| \geq Q_k$, $\max_i |\partial_l f_i(x_{k-1,0})| \geq Q_{k-1}$, $\cdots$, $\max_i |\partial_l f_i(x_{k-j,0})| \geq Q_{k-j}$ (where $Q_k := \triangle_1 \frac{n\sqrt{n}}{\sqrt{k}} \frac{32\sqrt{2}}{(1-\beta_2)^n \beta_2^n}$), then we have the following result:*

$$\left|\frac{\partial_l f(x_{k,0})}{\sqrt{v_{l,k,0}}} - \frac{\partial_l f(x_{k-j,0})}{\sqrt{v_{l,k-j,0}}}\right| \leq \frac{1}{1-\frac{1}{\sqrt{\beta_2^n}}} \frac{n^2 \triangle_{n(k-j)}}{\sqrt{v_{l,k-j,0}}} + j\sqrt{\frac{2\rho_3^2}{\beta_2^n}} \frac{1}{\left(1-\frac{(1-\beta_2)4n\rho_2}{\beta_2^n}\right)}\delta_1,$$

where δ_1 is defined in (17).

The proof of Lemma G.2 can be seen in Appendix G.3. To proceed, we combine Lemma G.2 and the "color-ball method of the 2nd kind", and thus we can prove Lemma A.2. This lemma is crucial for our current goal: bounding $\mathbb{E}(b_1)$. We refer the readers to Appendix A for more information.

We emphasize that here are still the following gap between Lemma A.2 and our goal $\mathbb{E}(b_1)$.

- We have the similar gap as discussed at the end of the **Step 1**.
- The condition in Lemma G.2 has requirement on the gradient norm, while this requirement is temporarily ignored in the color-ball method of the 2nd kind.
- The result in Lemma G.2 has additional error terms other than $\mathcal{O}(1/\sqrt{k})$. This is slightly different from the setting in Lemma A.2.

It requires some technical lemmas to handle these gaps. We fill in these gaps in Lemma G.4. The technical details can be seen Appendix G.4.

Bounding $\mathbb{E}\left[\sum_{l \text{ large}}(b_1)\right]$: Step 3. Now we shift gear to tackle (iii): handling the random variable " l large". We rewrite " l large" into the indicator function as follows:

$$\mathbb{E}\left[\sum_{l \text{ large}}(b_1)\right] = \mathbb{E}\left[\sum_{l \text{ large}} \frac{\partial_l f(x_{k,0})}{\sqrt{v_{l,k,0}}} \sum_{i=0}^{n-1}\left(m_{l,k,i}-\partial_l f_i(x_{k,0})\right)\right] = \mathbb{E}\left[\sum_{l=1}^{d} \mathbb{I}_k \frac{\partial_l f(x_{k,0})}{\sqrt{v_{l,k,0}}} \sum_{i=0}^{n-1}\left(m_{l,k,i}-\partial_l f_i(x_{k,0})\right)\right],$$

where $\mathbb{I}_k := \mathbb{I}\left(\max_i |\partial_l f_i(x_{k,0})| \geq Q_k := \triangle_1 \frac{n\sqrt{n}}{\sqrt{k}} \frac{32\sqrt{2}}{(1-\beta_2)^n \beta_2^n}\right)$ is the indicator function ($\mathbb{I}(A) = 1$ when event A holds and $\mathbb{I}(A) = 0$ otherwise.) Similarly as before, when taking $\mathbb{E}_k(\cdot)$, " $\mathbb{I}_k$" can be regarded as a constant index. Therefore, $\mathbb{E}_k\left[\sum_{l=1}^{d} \mathbb{I}_k \frac{\partial_l f(x_{k,0})}{\sqrt{v_{l,k,0}}} \sum_{i=0}^{n-1}\left(m_{l,k,i}-\partial_l f_i(x_{k,0})\right)\right]$ can be calculated following the same idea as color-ball model of the 1st kind. However, when taking $\mathbb{E}_{k-1}(\cdot)$, $\mathbb{I}_k$ will become a random variable which changes with different trajectories. In this case, the color-ball method *cannot* be applied. Similarly as in **Step 2**, we introduce the following lemma to change $\mathbb{I}_k$ into $\mathbb{I}_{k-1}$ (defined later), which can again be regarded as a fixed when taking $\mathbb{E}_{k-1}(\cdot)$.

Lemma G.3. *Suppose Assumption 2.1 holds and $\beta_1 < \sqrt{\beta_2}$. For $0 \leq j \leq k$, we define $\mathbb{I}_{k-j} := \mathbb{I}\left(\max_i |\partial_l f_i(x_{k-j,0})| \geq \sum_{p=k-j}^{k} Q_p\right)$, where $Q_k := \triangle_1 \frac{n\sqrt{n}}{\sqrt{k}} \frac{32\sqrt{2}}{(1-\beta_2)^n \beta_2^n}$, then we have the following results.*

$$\mathbb{I}_k = \mathbb{I}\left(\max_i |\partial_l f_i(x_{k,0})| \geq Q_k \textit{ and } \max_i |\partial_l f_i(x_{k-j,0})| \geq \sum_{p=k-j}^{k} Q_p\right) + \mathbb{I}\left(\max_i |\partial_l f_i(x_{k,0})| \geq Q_k \textit{ and } \max_i |\partial_l f_i(x_{k-j,0})| \leq \sum_{p=k-j}^{k} Q_p\right), \tag{32}$$

$$\mathbb{I}\left(\max_i |\partial_l f_i(x_{k,0})| \geq Q_k \textit{ and } \max_i |\partial_l f_i(x_{k-j,0})| \geq \sum_{p=k-j}^{k} Q_p\right) = \mathbb{I}\left(\max_i |\partial_l f_i(x_{k-j,0})| \geq \sum_{p=k-j}^{k} Q_p\right) = \mathbb{I}_{k-j}. \tag{33}$$

Proof. Equation (32) is straightforward, we only prove (33) here. Under Assumption 2.1, we have $|\partial_l f_i(x_{k,0}) - \partial_l f_i(x_{k-j,0})| \leq n\triangle_{n(k-1)} + \cdots + n\triangle_{n(k-j)} \leq Q_{k-1} + \cdots + Q_{k-j}$. To show the second inequality, it requires comparing the value between Q_k and $n\triangle_{n(k)}$, which are both problem-dependent constants. Here, the inequality holds when $n\triangle_{n(k)} \leq Q_k$. If otherwise, we can always define $\tilde{Q}_k := \max\{Q_k, n\triangle_{n(k)}\}$ and the inequality still holds by changing all the Q_k into $\tilde{Q}_k$. We temporarily omit this step for now.

Since $|\partial_l f_i(x_{k,0}) - \partial_l f_i(x_{k-j,0})| \leq Q_{k-1} + \cdots + Q_{k-j}$, the event $\left\{\max_i |\partial_l f_i(x_{k-j,0})| \geq \sum_{p=k-j}^{k} Q_p\right\}$ implies the event $\{\max_i |\partial_l f_i(x_{k,0})| \geq Q_k\}$, so the proof is completed. □

Now we are ready to bound $\mathbb{E}\left[\sum_{l \text{ large}}(b_1)\right]$. Combining **Step 1, 2 and 3** together, we prove the following Lemma G.4.

Lemma G.4. *Under Assumption 2.1, consider $\beta_1 < \sqrt{\beta_2}$, when k is large such that: $k \geq 4$; $\beta_1^{(k-1)n} \leq \frac{\beta_1^n}{\sqrt{k-1}}$, we have the following result:*

$$\mathbb{E}\left[\sum_{l \textit{ large}}(b_1)\right] \geq -\mathcal{O}\left(\frac{1}{\sqrt{k}}\right) - \mathcal{O}\left(\delta_1 \mathbb{E}\left[\sum_{l=1}^{d}\sum_{i=0}^{n-1} |\partial_l f_i(x_{k,0})|\right]\right),$$

where $\delta_1 = \frac{(1-\beta_2)4n\rho_2}{\beta_2^n} + \left(\frac{1}{\sqrt{\beta_2^n}} - 1\right)$, which goes to 0 when β_2 goes to 1.

Proof can be seen in Appendix G.4. Now we bound the error terms: $\mathbb{E}\left[\sum_{l \text{ large}}\{(a_2) + (b_2)\}\right]$. Since they are multiplied by δ_1, these two terms vanish when $\beta_2 \to 1$.

Bounding $\mathbb{E}\left[\sum_{l \textbf{ large}}\{(a_2) + (b_2)\}\right]$. We bound these two terms in the following Lemma G.5.

Lemma G.5. *Given all the history up to $x_{k,0}$, we denote α as the index of the coordinate with the greatest gradient: $\alpha = \arg\max_{l=1,2,\cdots,d} |\partial_l f(x_{k,0})|$. Under Assumption 2.1 and 2.2, consider $\beta_1 < \sqrt{\beta_2}$, when k is large such that: $k \geq 4$; $\beta_1^{(k-1)n} \leq \frac{\beta_1^n}{\sqrt{k-1}}$, we have the following results:*

$$\mathbb{E}\left[\sum_{l \textit{ large}}(a_2)\right] := \mathbb{E}\left[\sum_{l \textit{ large}} \delta_1 \sqrt{\frac{2\rho_3^2}{\beta_2^n}} \sum_{i=0}^{n-1} |\partial_l f_i(x_{k,0})|\right] \overset{(24)}{\leq} \mathcal{O}\left(\delta_1 \mathbb{E}|\partial_\alpha f(x_{k,0})|\right) + \mathcal{O}\left(\delta_1\sqrt{D_0}\right),$$

$$\mathbb{E}\left[\sum_{l \textit{ large}}(b_2)\right] := \mathbb{E}\left[\sum_{l \textit{ large}} \delta_1 \sqrt{\frac{2\rho_3^2}{\beta_2^n}} \sum_{i=0}^{n-1} |m_{l,k,i} - \partial_l f_i(x_{k,0})|\right] \leq \mathcal{O}\left(\delta_1 \mathbb{E}|\partial_\alpha f(x_{k,0})|\right) + \mathcal{O}\left(\delta_1\sqrt{D_0}\right) + \mathcal{O}\left(\frac{1}{\sqrt{k}}\right),$$

where δ_1 is defined in (17)*, D_0 is defined in Assumption 2.2.*

Detailed proof of Lemma G.5 is shown in Appendix G.8.

Bounding $\mathbb{E}\left\{\sum_{l \text{ large}}(a_1) + \sum_{l \text{ large}}(b_1) - \sum_{l \text{ large}}\{(a_2) + (b_2)\}\right\}$. With the help of Lemma G.4 and G.5, we can bound $\mathbb{E}\left\{\sum_{l \text{ large}}(a_1) + \sum_{l \text{ large}}(b_1) - \sum_{l \text{ large}}\{(a_2) + (b_2)\}\right\}$. The intuition is as follows:

- (a_1) is in the order of $|\partial_l f(x_{k,0})|$, multiplied by some positive constant;
- $\sum_{l \text{ large}}\{(a_2) + (b_2)\}$ vanishes when $\beta_2 \to 1$.
- $\mathbb{E}\left\{\sum_{l \text{ large}}(b_1)\right\}$ vanishes when $\beta_2 \to 1$ and k goes to infinity.

Therefore, $\mathbb{E}\left\{\sum_{l \text{ large}}(a_1) + \sum_{l \text{ large}}(b_1) - \sum_{l \text{ large}}\{(a_2) + (b_2)\}\right\}$ is still in the order of $|\partial_l f(x_{k,0})|$ (multiplied by a positive constant when β_2 is large). More formal results are shown in Lemma G.6.

Lemma G.6. *Under Assumption 2.1 and 2.2, when the hyperparameters satisfy: i) $\beta_1 < \sqrt{\beta_2} < 1$, ii) β_2 is large enough such that $A(\beta_2)$ is small enough to satisfy* (34)*, where $A(\beta_2)$ is a non-negative constant that approaches 0 when β_2 approaches* 1*. More Specifically, $A(\beta_2)$ needs to satisfy (ρ_1, ρ_2 and ρ_3 are defined in Appendix F.1).*

$$
\begin{aligned}
A(\beta_2) \quad &:= \quad \left\{\frac{(1-\beta_2)4n\rho_2}{\beta_2^n} + \left(\frac{1}{\sqrt{\beta_2^n}} - 1\right)\right\}\left(\sqrt{\frac{2\rho_3^2}{\beta_2^n}}4n + \left(\sqrt{\frac{2\rho_3^2}{\beta_2^n}}\frac{3n}{\left(1 - \frac{(1-\beta_2)4n\rho_2}{\beta_2^n}\right)}\right)\frac{1}{(1-\beta_1^n)}\right)\sqrt{D_1}\rho_1 d \\
&\leq \quad \frac{1}{\sqrt{10D_1 d}},
\end{aligned} \tag{34}
$$

Then, we have the following result when k is large enough such that $\beta_1^{(k-1)n} \leq \frac{\beta_1^n}{\sqrt{k-1}}$ and $k \geq 4$:

$$
\begin{aligned}
& \mathbb{E}\left\{\sum_{l \text{ large}}(a_1) + \sum_{l \text{ large}}(b_1) - \sum_{l \text{ large}}\{(a_2) + (b_2)\}\right\} \\
:= \quad & \mathbb{E}\left[\sum_{l \text{ large}}\frac{\partial_l f\left(x_{k,0}\right)^2}{\sqrt{v_{l,k,0}}}\right] + \mathbb{E}\left[\sum_{l \text{ large}}\frac{\partial_l f(x_{k,0})}{\sqrt{v_{l,k,0}}}\sum_{i=0}^{n-1}\left(m_{l,k,i} - \partial_l f_i(x_{k,0})\right)\right] \\
& -d\delta_1\sqrt{\frac{2\rho_3^2}{\beta_2^n}}\mathbb{E}\left[\sum_{i=0}^{n-1}\left|\partial_l f_i\left(x_{k,0}\right)\right|\right] - d\delta_1\sqrt{\frac{2\rho_3^2}{\beta_2^n}}\mathbb{E}\left[\sum_{i=0}^{n-1}\left|m_{l,k,i} - \partial_l f_i(x_{k,0})\right|\right] \\
\geq \quad & \frac{1}{d\sqrt{10D_1 d}}\mathbb{E}\min\left\{\sqrt{\frac{2D_1 d}{D_0}}\|\nabla f(x_{k,0})\|_2^2, \|\nabla f(x_{k,0})\|_1\right\} \\
& -\mathcal{O}(\frac{1}{\sqrt{k}}) - \mathcal{O}(\sqrt{D_0}).
\end{aligned}
$$

Proof of Lemma G.6 can be seen in Appendix G.9.

Remark G.7. Condition (34) specifies the smallest threshold of β_2 to ensure the convergence. This condition can be translated into the threshold funtion $\gamma_1(n)$ mentioned in Theorem 3.1. As a rough estimate, Lemma G.6 requires $\beta_2 \geq \gamma_1(n) = 1 - \mathcal{O}\left((1-\beta_1^n)/(n^2\rho)\right)$, where $\rho = \rho_1\rho_2\rho_3$. As discussed in Appendix F.1, we have $0 \leq \rho_3 \leq \sqrt{n}\rho_1 \leq n$. When ρ_1, ρ_2, ρ_3 achieve their upper bound at the same time, we get the worst case bound $\beta_2 \geq \gamma_1(n) = 1 - \mathcal{O}\left((1-\beta_1^n)/n^{4.5}\right)$. However, ρ is highly dependent on the problem instance $f(x)$ and training process. Our experiments in Appendix B shows that ρ is often much smaller than its worst case bound, making the threshold of β_2 lower than it appears to be.

We further remark that $\gamma_1(n) \propto (1-\beta_1^n)$. That is to say, as β_1 increases, the threshold of β_2 also slowly increases (to ensure the convergence). However, such phenomenon is not observed in our experiments. We conjecture $\gamma_1(n)$ should be independent of β_1, removing the dependence $(1-\beta_1^n)$ is considered as an interesting future direction.

Remark G.8. We emphasize that the constant term $\mathcal{O}(\sqrt{D_0})$ will vanish to 0 as β_2 goes to 1. This can be seen in the proof in Appendix G.9 (the definition of F_4) and Remark G.14.

Based on Lemma G.6, we can further rewrite (31) as follows.

$$\begin{aligned}
\mathbb{E}\left[\sum_{l=1}^{d}\sum_{i=0}^{n-1}\partial_l f(x_{k,0})\frac{m_{l,k,i}}{\sqrt{v_{l,k,i}}}\right] &\overset{(31)}{\geq} \mathbb{E}\left\{\sum_{l \text{ large}}(a_1)+\sum_{l \text{ large}}(b_1)-\sum_{l \text{ large}}\{(a_2)+(b_2)\}\right\}-dF_1\frac{1}{\sqrt{k}}, \\
&\overset{\text{Lemma G.6}}{\geq} \frac{1}{d\sqrt{10D_1 d}}\mathbb{E}\min\left\{\sqrt{\frac{2D_1 d}{D_0}}\|\nabla f(x_{k,0})\|_2^2, \|\nabla f(x_{k,0})\|_1\right\} \\
&\quad -\mathcal{O}(\frac{1}{\sqrt{k}})-\mathcal{O}(\sqrt{D_0})-d\frac{F_1}{\sqrt{k}} \qquad (35)
\end{aligned}$$

The proof of Theorem 3.1 is concluded by plugging (35) into Descent Lemma (25) and then taking telescope some from $k=t_0$ to $k=T$. These steps are quite standard in non-convex optimization. We finish these calculation in Lemma G.9

Lemma G.9. *When inequality* (35) *holds, we have the following results based on Descent Lemma* (25)*:*

$$\begin{aligned}
&\min_{k\in[1,T]}\mathbb{E}\left[\min\left\{\sqrt{\frac{2D_1 d}{D_0}}\|\nabla f(x_{k,0})\|_2^2, \|\nabla f(x_{k,0})\|_1\right\}\right] \\
&= \mathcal{O}\left(\frac{\log T}{\sqrt{T}}\right)+\mathcal{O}(\sqrt{D_0}).
\end{aligned}$$

Proof of Lemma G.9 can be seen in Appendix G.10. Now, the whole proof of Theorem 3.1 is completed.

G.2 Proof of Lemma G.1

To prove Lemma G.1, we only prove (28). The proof for (27) can be analogized from the proof of (28). We discuss the following two cases:

Case 1: When $\partial_l f\left(x_{k,0}\right)\left(m_{l,k,i}-\partial_l f_i(x_{k,0})\right)\leq 0$, we have

$$\frac{\partial_l f\left(x_{k,0}\right)\left(m_{l,k,i}-\partial_l f_i(x_{k,0})\right)}{\sqrt{v_{l,k,i}}} \overset{(a)}{\geq} \frac{\partial_l f(x_{k,0})(m_{l,k,i}-\partial_l f_i(x_{k,0}))}{\sqrt{v_{l,k,0}}}\frac{1}{\sqrt{\beta_2^i}},$$

where (a) is because of $\sqrt{v_{l,k,i}}\geq\sqrt{\beta_2^i}\sqrt{v_{l,k,0}}$.

Case 2: When $\partial_l f\left(x_{k,0}\right)\left(m_{l,k,i}-\partial_l f_i(x_{k,0})\right)\geq 0$, we have

$$\begin{aligned}
\frac{\partial_l f\left(x_{k,0}\right)\left(m_{l,k,i}-\partial_l f_i(x_{k,0})\right)}{\sqrt{v_{l,k,i}}} &= \frac{\partial_l f\left(x_{k,0}\right)\left(m_{l,k,i}-\partial_l f_i(x_{k,0})\right)}{\sqrt{v_{l,k,0}}}\frac{1}{\sqrt{(1+(v_{l,k,i}-v_{l,k,0})/v_{l,k,0})}} \\
&\overset{(*)}{\geq} \frac{\partial_l f\left(x_{k,0}\right)\left(m_{l,k,i}-\partial_l f_i(x_{k,0})\right)}{\sqrt{v_{l,k,0}}}\left(1-\frac{|v_{l,k,i}-v_{l,k,0}|}{2v_{l,k,0}}\right) \qquad (36)
\end{aligned}$$

where $(*)$ is due to $\frac{1}{\sqrt{1+x}}\geq 1-\frac{x}{2}$. We further have

$$
\begin{aligned}
|v_{l,k,i} - v_{l,k,0}| &= (1-\beta_2)(\partial_l f_{\tau_{k,i}}(x_{\tau_{k,i}})^2 + \beta_2 \partial_l f_{\tau_{k,i-1}}(x_{\tau_{k,i-1}})^2 + \cdots + \beta_2^{i-1}\partial_l f_{\tau_{k,1}}(x_{\tau_{k,1}})^2 \\
&\quad +(\beta_2^i - 1)\partial_l f_{\tau_{k,0}}(x_{\tau_{k,0}})^2 + (\beta_2^{i+1}-1)\partial_l f_{\tau_{k-1,n-1}}(x_{\tau_{k-1,n-1}})^2 + \cdots) \\
&\overset{\text{since } \beta_2^i - 1 < 0}{\leq} (1-\beta_2)\sum_{j=0}^{i-1}\beta_2^j \partial_l f_{\tau_{k,i-j}}(x_{\tau_{k,i-j}})^2 \\
&\leq (1-\beta_2)\sum_{j=0}^{i-1}\beta_2^j \left(\partial_l f_{\tau_{k,i-j}}(x_{\tau_{k,0}})^2 + 2(i-j)\triangle_{nk}|\partial_l f_{\tau_{k,i-j}}(x_{\tau_{k,0}})| + (i-j)^2\triangle_{nk}^2\right) \\
&\leq (1-\beta_2)\sum_{j=0}^{i-1}\beta_2^j \left(\max_i |\partial_l f_i(x_{\tau_{k,0}})|^2 + 2(i-j)\triangle_{nk}\max_i|\partial_l f_i(x_{\tau_{k,0}})| + (i-j)^2\triangle_{nk}^2\right) \\
&\overset{(**)}{\leq} (1-\beta_2)\sum_{j=0}^{i-1}\beta_2^j \left(\max_i |\partial_l f_i(x_{\tau_{k,0}})|^2 + 2\max_i|\partial_l f_i(x_{\tau_{k,0}})|^2 + \max_i|\partial_l f_i(x_{\tau_{k,0}})|^2\right) \\
&\leq (1-\beta_2)4n\max_i|\partial_l f_i(x_{\tau_{k,0}})|^2
\end{aligned}
$$

where $(**)$ is due to the condition in the Lemma $\max_i |\partial_l f_i(x_{\tau_{k,0}})| \geq Q_k \geq n\triangle_{nk}$. Plug the above result into (36) we have

$$
\begin{aligned}
\frac{\partial_l f\left(x_{k,0}\right)\left(m_{l,k,i} - \partial_l f_i(x_{k,0})\right)}{\sqrt{v_{l,k,i}}} &\geq \frac{\partial_l f\left(x_{k,0}\right)\left(m_{l,k,i} - \partial_l f_i(x_{k,0})\right)}{\sqrt{v_{l,k,0}}}\left(1 - \frac{(1-\beta_2)4n\max_i|\partial_l f_i(x_{\tau_{k,0}})|^2}{2v_{l,k,0}}\right) \\
&\geq \frac{\partial_l f\left(x_{k,0}\right)\left(m_{l,k,i} - \partial_l f_i(x_{k,0})\right)}{\sqrt{v_{l,k,0}}}\left(1 - \frac{(1-\beta_2)4n\rho_2\sum_{i=0}^{n-1}|\partial_l f_i(x_{\tau_{k,0}})|^2/n}{2v_{l,k,0}}\right) \\
&\overset{(***)}{\geq} \frac{\partial_l f\left(x_{k,0}\right)\left(m_{l,k,i} - \partial_l f_i(x_{k,0})\right)}{\sqrt{v_{l,k,0}}}\left(1 - \frac{(1-\beta_2)4n\rho_2}{\beta_2^n}\right) \qquad (37)
\end{aligned}
$$

In the last step $(***)$, we use the following Lemma G.10.

Lemma G.10. *Under Assumption 2.1, if the l-th component of $\nabla f_i(x_{k,0})$ satisfies $\max_i |\partial_l f_i(x_{k,0})| \geq Q_k := \triangle_1 \frac{n\sqrt{n}}{\sqrt{k}}\frac{32\sqrt{2}}{(1-\beta_2)^n\beta_2^n}$, we have*

$$
\frac{v_{l,k,0}}{\frac{1}{n}\sum_i \partial_l f_{\tau_{k,i}}(x_{k,0})^2} \geq \frac{\beta_2^n}{2},
$$

$$
\frac{v_{l,k,0}}{\left(\partial_l f\left(x_{k,0}\right)\right)^2} \geq \frac{\beta_2^n}{2\rho_3^2}.
$$

Proof. The proof idea of Lemma G.10 is similar as Lemma F.1 in (Shi et al., 2020), but with the following differences:

1. The condition of Lemma F.1 in (Shi et al., 2020) both require the full batch gradient $|\partial_l f(x_{k,0})| \geq nQ_k$, which is different from our condition. Here, we choose the condition of Lemma G.10 because it meets the need of our decomposition strategy in (31) .
2. The constant Q_k is different. The difference is due to the different update formula of RMSProp and general Adam.

Anyhow, Lemma G.10 can be easily proved following most of the steps in Lemma F.1 in (Shi et al., 2020). We omit the proof for brevity. □

Combining the above **Case 1** and **Case 2**, we have

$$
\begin{aligned}
\sum \frac{\partial_l f\left(x_{k,0}\right)\left(m_{l,k,i}-\partial_l f_i(x_{k,0})\right)}{\sqrt{v_{l,k,i}}} &\geq \sum_{i-} \frac{\partial_l f\left(x_{k,0}\right)\left(m_{l,k,i}-\partial_l f_i(x_{k,0})\right)}{\sqrt{v_{l,k,0}}} \frac{1}{\sqrt{\beta_2^i}} \\
&\quad + \sum_{i+} \frac{\partial_l f\left(x_{k,0}\right)\left(m_{l,k,i}-\partial_l f_i(x_{k,0})\right)}{\sqrt{v_{l,k,0}}} \left(1-\frac{(1-\beta_2)4n\rho_2}{\beta_2^n}\right) \\
&= \sum_{i=0}^{n-1} \frac{\partial_l f\left(x_{k,0}\right)\left(m_{l,k,i}-\partial_l f_i(x_{k,0})\right)}{\sqrt{v_{l,k,0}}} \\
&\quad + \sum_{i-} \frac{\partial_l f\left(x_{k,0}\right)\left(m_{l,k,i}-\partial_l f_i(x_{k,0})\right)}{\sqrt{v_{l,k,0}}} \left(\frac{1}{\sqrt{\beta_2^i}}-1\right) \\
&\quad + \sum_{i+} \frac{\partial_l f\left(x_{k,0}\right)\left(m_{l,k,i}-\partial_l f_i(x_{k,0})\right)}{\sqrt{v_{l,k,0}}} \left(-\frac{(1-\beta_2)4n\rho_2}{\beta_2^n}\right) \\
&\geq \sum_{i=0}^{n-1} \frac{\partial_l f\left(x_{k,0}\right)\left(m_{l,k,i}-\partial_l f_i(x_{k,0})\right)}{\sqrt{v_{l,k,0}}} \\
&\quad -\delta_1 \left|\frac{\partial_l f\left(x_{k,0}\right)}{\sqrt{v_{l,k,0}}}\right| \sum_{i=0}^{n-1} \left|m_{l,k,i}-\partial_l f_i\left(x_{k,0}\right)\right|,
\end{aligned}
$$

where $\delta_1 = \frac{(1-\beta_2)4n\rho_2}{\beta_2^n} + \left(\frac{1}{\sqrt{\beta_2^n}}-1\right)$. Proof is completed.

G.3 Proof of Lemma G.2

We first prove the result for $j=1$. We discuss the following two cases.

Case 1: when $\frac{\partial_l f(x_{k,0})}{\sqrt{v_{l,k,0}}} \geq \frac{\partial_l f(x_{k-1,0})}{\sqrt{v_{l,k-1,0}}}$: when $\partial_l f(x_{k,0}) \leq 0$, we have

$$
\frac{\partial_l f(x_{k,0})}{\sqrt{v_{l,k,0}}} \overset{(37)}{\leq} \frac{\partial_l f(x_{k,0})}{\sqrt{v_{l,k-1,0}}} \left(1-\frac{(1-\beta_2)4n\rho_2}{\beta_2^n}\right).
$$

When $\partial_l f(x_{k,0}) > 0$, we have

$$
\frac{\partial_l f(x_{k,0})}{\sqrt{v_{l,k,0}}} \leq \frac{\partial_l f(x_{k,0})}{\sqrt{v_{l,k-1,0}}} \frac{1}{\sqrt{\beta_2^n}}
$$

.

In conclusion, we have:

$$
\begin{aligned}
\frac{\partial_l f(x_{k,0})}{\sqrt{v_{l,k,0}}} &\leq \max\left\{\frac{\partial_l f(x_{k,0})}{\sqrt{v_{l,k-1,0}}}\left(1-\frac{(1-\beta_2)4n\rho_2}{\beta_2^n}\right), \frac{\partial_l f(x_{k,0})}{\sqrt{v_{l,k-1,0}}}\frac{1}{\sqrt{\beta_2^n}}\right\} \\
&\leq \frac{\partial_l f(x_{k,0})}{\sqrt{v_{l,k-1,0}}} + \max\left\{\frac{\partial_l f(x_{k,0})}{\sqrt{v_{l,k-1,0}}}\left(-\frac{(1-\beta_2)4n\rho_2}{\beta_2^n}\right), \frac{\partial_l f(x_{k,0})}{\sqrt{v_{l,k-1,0}}}\left(\frac{1}{\sqrt{\beta_2^n}}-1\right)\right\} \\
&\leq \frac{\partial_l f(x_{k,0})}{\sqrt{v_{l,k-1,0}}} + \frac{|\partial_l f(x_{k,0})|}{\sqrt{v_{l,k-1,0}}}\left(\frac{1}{\sqrt{\beta_2^n}}-1+\frac{(1-\beta_2)4n\rho_2}{\beta_2^n}\right) \\
&\overset{(37)}{\leq} \frac{\partial_l f(x_{k,0})}{\sqrt{v_{l,k-1,0}}} + \frac{|\partial_l f(x_{k,0})|}{\sqrt{v_{l,k,0}}}\left(\frac{1}{\sqrt{\beta_2^n}}-1+\frac{(1-\beta_2)4n\rho_2}{\beta_2^n}\right)\frac{1}{\left(1-\frac{(1-\beta_2)4n\rho_2}{\beta_2^n}\right)}
\end{aligned}
$$

$$\overset{\text{Lemma G.10}}{\leq} \quad \frac{\partial_l f(x_{k,0})}{\sqrt{v_{l,k-1,0}}} + \sqrt{\frac{2\rho_3^2}{\beta_2^n}} \left(\frac{1}{\sqrt{\beta_2^n}} - 1 + \frac{(1-\beta_2)4n\rho_2}{\beta_2^n} \right) \frac{1}{\left(1 - \frac{(1-\beta_2)4n\rho_2}{\beta_2^n}\right)}$$

$$= \quad \frac{\partial_l f(x_{k,0})}{\sqrt{v_{l,k-1,0}}} + \sqrt{\frac{2\rho_3^2}{\beta_2^n}} \frac{\delta_1}{\left(1 - \frac{(1-\beta_2)4n\rho_2}{\beta_2^n}\right)},$$

where $\delta_1 = \left(\frac{1}{\sqrt{\beta_2^n}} - 1 + \frac{(1-\beta_2)4n\rho_2}{\beta_2^n} \right)$ is a constant that goes to 0 when β_2 goes to 1. Therefore, we have

$$\frac{\partial_l f(x_{k,0})}{\sqrt{v_{l,k,0}}} - \frac{\partial_l f(x_{k-1,0})}{\sqrt{v_{l,k-1,0}}} \quad \leq \quad \frac{\partial_l f(x_{k,0}) - \partial_l f(x_{k-1,0})}{\sqrt{v_{l,k-1,0}}} + \sqrt{\frac{2\rho_3^2}{\beta_2^n}} \frac{1}{\left(1 - \frac{(1-\beta_2)4n\rho_2}{\beta_2^n}\right)} \delta_1$$

$$\overset{\text{Lemma F.2}}{\leq} \quad \frac{n^2 \triangle_{n(k-1)}}{\sqrt{v_{l,k-1,0}}} + \sqrt{\frac{2\rho_3^2}{\beta_2^n}} \frac{1}{\left(1 - \frac{(1-\beta_2)4n\rho_2}{\beta_2^n}\right)} \delta_1.$$

Note that

Case 2: when $\frac{\partial_l f(x_{k,0})}{\sqrt{v_{l,k,0}}} \leq \frac{\partial_l f(x_{k-1,0})}{\sqrt{v_{l,k-1,0}}}$: when $\partial_l f(x_{k,0}) \geq 0$, we have

$$\frac{\partial_l f(x_{k,0})}{\sqrt{v_{l,k,0}}} \overset{(37)}{\geq} \frac{\partial_l f(x_{k,0})}{\sqrt{v_{l,k-1,0}}} \left(1 - \frac{(1-\beta_2)4n\rho_2}{\beta_2^n}\right).$$

When $\partial_l f(x_{k,0}) < 0$, we have

$$\frac{\partial_l f(x_{k,0})}{\sqrt{v_{l,k,0}}} \geq \frac{\partial_l f(x_{k,0})}{\sqrt{v_{l,k-1,0}}} \frac{1}{\sqrt{\beta_2^n}}$$

.

Following the same strategy as in Case 1, we can show that

$$\frac{\partial_l f(x_{k,0})}{\sqrt{v_{l,k,0}}} \quad \geq \quad \frac{\partial_l f(x_{k,0})}{\sqrt{v_{l,k-1,0}}} - \sqrt{\frac{2\rho_3^2}{\beta_2^n}} \frac{1}{\left(1 - \frac{(1-\beta_2)4n\rho_2}{\beta_2^n}\right)} \delta_1,$$

which further implies

$$\frac{\partial_l f(x_{k,0})}{\sqrt{v_{l,k,0}}} - \frac{\partial_l f(x_{k-1,0})}{\sqrt{v_{l,k-1,0}}} \quad \geq \quad \frac{\partial_l f(x_{k,0}) - \partial_l f(x_{k-1,0})}{\sqrt{v_{l,k-1,0}}} - \sqrt{\frac{2\rho_3^2}{\beta_2^n}} \frac{1}{\left(1 - \frac{(1-\beta_2)4n\rho_2}{\beta_2^n}\right)} \delta_1$$

$$\overset{\text{Lemma F.2}}{\geq} \quad -\frac{n^2 \triangle_{n(k-1)}}{\sqrt{v_{l,k-1,0}}} - \sqrt{\frac{2\rho_3^2}{\beta_2^n}} \frac{1}{\left(1 - \frac{(1-\beta_2)4n\rho_2}{\beta_2^n}\right)} \delta_1.$$

Case 1 and Case 2 together, we have

$$\left| \frac{\partial_l f(x_{k,0})}{\sqrt{v_{l,k,0}}} - \frac{\partial_l f(x_{k-1,0})}{\sqrt{v_{l,k-1,0}}} \right| \leq \frac{n^2 \triangle_{n(k-1)}}{\sqrt{v_{l,k-1,0}}} + \sqrt{\frac{2\rho_3^2}{\beta_2^n}} \frac{1}{\left(1 - \frac{(1-\beta_2)4n\rho_2}{\beta_2^n}\right)} \delta_1.$$

Now we consider the case when $j > 1$. Based on the above inequality, we have

$$
\begin{aligned}
\left|\frac{\partial_l f(x_{k,0})}{\sqrt{v_{l,k,0}}} - \frac{\partial_l f(x_{k-j,0})}{\sqrt{v_{l,k-j,0}}}\right| &\leq \left(\frac{n^2\triangle_{n(k-1)}}{\sqrt{v_{l,k-1,0}}} + \frac{n^2\triangle_{n(k-2)}}{\sqrt{v_{l,k-2,0}}} + \cdots + \frac{n^2\triangle_{n(k-j)}}{\sqrt{v_{l,k-j,0}}}\right) + j\sqrt{\frac{2\rho_3^2}{\beta_2^n}}\frac{1}{\left(1-\frac{(1-\beta_2)4n\rho_2}{\beta_2^n}\right)}\delta_1 \\
&\leq \left(\frac{1}{\sqrt{\beta_2^{jn}}} + \frac{1}{\sqrt{\beta_2^{(j-1)n}}} + \cdots + 1\right)\frac{n^2\triangle_{n(k-j)}}{\sqrt{v_{k-j,0}}} + j\sqrt{\frac{2\rho_3^2}{\beta_2^n}}\frac{1}{\left(1-\frac{(1-\beta_2)4n\rho_2}{\beta_2^n}\right)}\delta_1 \\
&\leq \frac{1}{1-\frac{1}{\sqrt{\beta_2^n}}}\frac{n^2\triangle_{n(k-j)}}{\sqrt{v_{l,k-j,0}}} + j\sqrt{\frac{2\rho_3^2}{\beta_2^n}}\frac{1}{\left(1-\frac{(1-\beta_2)4n\rho_2}{\beta_2^n}\right)}\delta_1.
\end{aligned}
$$

The proof is completed.

G.4 Proof of Lemma G.4

To prove Lemma G.4, we need to further decompose $\mathbb{E}[\sum_{l \text{ large}}(b_1)]$. First and foremost, we write $\sum_{i=0}^{n-1} m_{l,k,i}$ in an explicit form.

$$
\begin{aligned}
m_{l,k,i} = \; & (1-\beta_1)\{\partial_l f_{\tau_{k,i}}(x_{k,i}) + \cdots + \beta_1^i \partial_l f_{\tau_{k,0}}(x_{k,0}) \\
& +\beta_1^{i+1} f_{\tau_{k-1,n-1}}(x_{k-1,n-1}) + \cdots + \beta_1^{i+n} f_{\tau_{k-1,0}}(x_{k-1,0}) \\
& + \\
& \vdots \\
& + \\
& +\beta_1^{(k-2)n+i+1}\partial_l f_{\tau_{1,n-1}}(x_{1,n-1}) + \cdots + \beta_1^{(k-1)n+i}\partial_l f_{\tau_{1,0}}(x_{1,0})\} \\
& +\beta_1^{(k-1)n+i+1}\partial_l f(x_{1,0})
\end{aligned} \tag{38}
$$

Since $\partial_l f(x_{1,0}) = \partial_l f(x_{1,0})(1-\beta_1)(1+\beta_1+\cdots+\beta_1^\infty)$ and $\partial_l f(x_{1,0}) = \sum_{i=0}^{n-1}\partial_l f_i(x_{1,0})$, we have

$$
\begin{aligned}
\beta_1^{(k-1)n+i+1}\partial_l f(x_{1,0}) = \; & (1-\beta_1)\{\beta_1^{(k-1)n+i+1}\partial_l f_0(x_{1,0}) + \cdots + \beta_1^{(k-1)n+i+1}\partial_l f_{n-1}(x_{1,0}) \\
& +\beta_1^{(k-1)n+i+2}\partial_l f_0(x_{1,0}) + \cdots + \beta_1^{(k-1)n+i+2}\partial_l f_{n-1}(x_{1,0}) \\
& + \\
& \vdots \\
& + \\
& +\beta_1^{\infty}\partial_l f_0(x_{1,0}) + \cdots + \beta_1^{\infty}\partial_l f_{n-1}(x_{1,0})\}
\end{aligned} \tag{39}
$$

Plugging (39) into (38), we have

$$
\begin{aligned}
m_{l,k,i} = \; & (1-\beta_1)\{\partial_l f_{\tau_{k,i}}(x_{k,i}) + \cdots + \beta_1^i \partial_l f_{\tau_{k,0}}(x_{k,0}) \\
& +\beta_1^{i+1} f_{\tau_{k-1,n-1}}(x_{k-1,n-1}) + \cdots + \beta_1^{i+n} f_{\tau_{k-1,0}}(x_{k-1,0}) \\
& + \cdots \\
& +\beta_1^{(k-2)n+i+1}\partial_l f_{\tau_{1,n-1}}(x_{1,n-1}) + \cdots + \beta_1^{(k-1)n+i}\partial_l f_{\tau_{1,0}}(x_{1,0}) \\
& +\beta_1^{(k-1)n+i+1}\partial_l f_0(x_{1,0}) + \cdots + \beta_1^{(k-1)n+i+1}\partial_l f_{n-1}(x_{1,0}) \\
& +\beta_1^{(k-1)n+i+2}\partial_l f_0(x_{1,0}) + \cdots + \beta_1^{(k-1)n+i+2}\partial_l f_{n-1}(x_{1,0}) \\
& + \cdots \\
& +\beta_1^{\infty}\partial_l f_0(x_{1,0}) + \cdots + \beta_1^{\infty}\partial_l f_{n-1}(x_{1,0})\}
\end{aligned} \tag{40}
$$

Using (40), we have (For each 'epoch', we suggest readers to read from bottom to the top.)

$$
\begin{aligned}
M_{l,k} := \sum_{i=0}^{n-1} m_{l,k,i} &= m_{l,k,n-1} + \cdots + m_{l,k,0} \\
&= (1-\beta_1)\{ \\
&\quad \underbrace{\begin{aligned}
&\partial_l f_{\tau_{k,n-1}}(x_{k,n-1}) + \cdots + \beta_1^{n-1}\partial_l f_{\tau_{k,0}}(x_{k,0}) \\
&+\partial_l f_{\tau_{k,n-2}}(x_{k,n-2}) + \cdots + \beta_1^{n-2}\partial_l f_{\tau_{k,0}}(x_{k,0}) \\
&+\cdots \\
&+\partial_l f_{\tau_{k,0}}(x_{k,0})
\end{aligned}}_{k\text{-th epoch}} \\
&\quad \underbrace{\begin{aligned}
&+\beta_1^{n}\partial_l f_{\tau_{k-1,n-1}}(x_{k-1,n-1}) + \cdots + \beta_1^{n+n-1}\partial_l f_{\tau_{k-1,0}}(x_{k-1,0}) \\
&+\beta_1^{n-1}\partial_l f_{\tau_{k-1,n-1}}(x_{k-1,n-1}) + \cdots + \beta_1^{n+n-2}\partial_l f_{\tau_{k-1,0}}(x_{k-1,0}) \\
&+\cdots \\
&+\beta_1\partial_l f_{\tau_{k-1,n-1}}(x_{k-1,n-1}) + \cdots + \beta_1^{n}\partial_l f_{\tau_{k-1,0}}(x_{k-1,0})
\end{aligned}}_{k-1\text{-th epoch}} \\
&\quad + \\
&\quad \vdots \\
&\quad + \\
&\quad \underbrace{\begin{aligned}
&+\beta_1^{(k-1)n}\partial_l f_{\tau_{1,n-1}}(x_{1,n-1}) + \cdots + \beta_1^{(k-1)n+n-1}\partial_l f_{\tau_{1,0}}(x_{1,0}) \\
&+\beta_1^{(k-2)n+n-1}\partial_l f_{\tau_{1,n-1}}(x_{1,n-1}) + \cdots + \beta_1^{(k-1)n+n-2}\partial_l f_{\tau_{1,0}}(x_{1,0}) \\
&+\cdots \\
&+\beta_1^{(k-2)n+1}\partial_l f_{\tau_{1,n-1}}(x_{1,n-1}) + \cdots + \beta_1^{(k-1)n}\partial_l f_{\tau_{1,0}}(x_{1,0})
\end{aligned}}_{1\text{-th epoch}} \\
&\quad \underbrace{\begin{aligned}
&+\beta_1^{(k-1)n+n}\partial_l f_0(x_{1,0}) + \cdots + \beta_1^{(k-1)n+n}\partial_l f_{n-1}(x_{1,0}) \\
&+\beta_1^{(k-1)n+n-1}\partial_l f_0(x_{1,0}) + \cdots + \beta_1^{(k-1)n+n-1}\partial_l f_{n-1}(x_{1,0}) \\
&+\cdots \\
&+\beta_1^{(k-1)n+1}\partial_l f_0(x_{1,0}) + \cdots + \beta_1^{(k-1)n+1}\partial_l f_{n-1}(x_{1,0}) +
\end{aligned}}_{0\text{-th epoch}} \\
&\quad \vdots \} \qquad (41)
\end{aligned}
$$

Note that in (41), the power of β_1 grows slower in the blue part (when $k = 0$), such a transition will cause trouble in bounding the $\sum_{i=0}^{n-1}(m_{l,k,i} - \partial_l f_i(x_{k,0}))$. Therefore, we need to define an auxillary sequence $M'_{l,k}$ which does not involve such a phase transition. We define $M'_{l,k}$ as follows. (For each 'epoch', we suggest readers to read from bottom to the top.)

$$
\begin{aligned}
M'_{l,k} &:= (1-\beta_1)\{ \\
&\quad \underbrace{\begin{aligned}
&\partial_l f_{\tau_{k,n-1}}(x_{k,n-1}) + \cdots + \beta_1^{n-1}\partial_l f_{\tau_{k,0}}(x_{k,0}) \\
&+\partial_l f_{\tau_{k,n-2}}(x_{k,n-2}) + \cdots + \beta_1^{n-2}\partial_l f_{\tau_{k,0}}(x_{k,0}) \\
&+\cdots \\
&+\partial_l f_{\tau_{k,0}}(x_{k,0})
\end{aligned}}_{k\text{-th epoch}}
\end{aligned}
$$

$$
\begin{aligned}
&+\beta_1^n \partial_l f_{\tau_{k-1,n-1}}(x_{k-1,n-1}) + \cdots + \beta_1^{n+n-1} \partial_l f_{\tau_{k-1,0}}(x_{k-1,0}) \\
&+\beta_1^{n-1} \partial_l f_{\tau_{k-1,n-1}}(x_{k-1,n-1}) + \cdots + \beta_1^{n+n-2} \partial_l f_{\tau_{k-1,0}}(x_{k-1,0}) \\
&+\cdots \\
&\underbrace{+\beta_1 \partial_l f_{\tau_{k-1,n-1}}(x_{k-1,n-1}) + \cdots + \beta_1^{n} \partial_l f_{\tau_{k-1,0}}(x_{k-1,0})}_{k-1\text{-th epoch}} \\
&+ \\
&\vdots \\
&+ \\
&+\beta_1^{(k-1)n} \partial_l f_{\tau_{1,n-1}}(x_{1,n-1}) + \cdots + \beta_1^{(k-1)n+n-1} \partial_l f_{\tau_{1,0}}(x_{1,0}) \\
&+\beta_1^{(k-2)n+n-1} \partial_l f_{\tau_{1,n-1}}(x_{1,n-1}) + \cdots + \beta_1^{(k-1)n+n-2} \partial_l f_{\tau_{1,0}}(x_{1,0}) \\
&+\cdots \\
&\underbrace{+\beta_1^{(k-2)n+1} \partial_l f_{\tau_{1,n-1}}(x_{1,n-1}) + \cdots + \beta_1^{(k-1)n} \partial_l f_{\tau_{1,0}}(x_{1,0})}_{1\text{-th epoch}} \\
&+\beta_1^{(k-1)n+n} \partial_l f_0(x_{1,0}) + \cdots + \beta_1^{(k-1)n+n+n-1} \partial_l f_{n-1}(x_{1,0}) \\
&+\beta_1^{(k-1)n+n-1} \partial_l f_0(x_{1,0}) + \cdots + \beta_1^{(k-1)n+2(n-1)} \partial_l f_{n-1}(x_{1,0}) \\
&+\cdots \\
&\underbrace{+\beta_1^{(k-1)n+1} \partial_l f_0(x_{1,0}) + \cdots + \beta_1^{(k-1)n+n} \partial_l f_{n-1}(x_{1,0}) +}_{0\text{-th epoch}} \\
&\vdots\}
\end{aligned}
\tag{42}
$$

Now we bound $\sum_{i=0}^{n-1}(m_{l,k,i} - \partial_l f_i(x_{k,0}))$ with the help of $M'_{l,k}$. Denoting $F_{l,k} := \sum_{i=0}^{n-1} \partial_l f_i(x_{k,0})$, we have:

$$
\begin{aligned}
\sum_{i=0}^{n-1}(m_{l,k,i} - \partial_l f_i(x_{k,0})) &= \sum_{i=0}^{n-1} m_{l,k,i} - \sum_{i=0}^{n-1} \partial_l f_i(x_{k,0}) \\
&:= M_{l,k} - F_{l,k} \\
&\geq -|M_{l,k} - M'_{l,k}| + M'_{l,k} - F_{l,k}
\end{aligned}
\tag{43}
$$

To proceed, we use the relation $1 = (1-\beta_1)(1+\beta_1+\beta_1^2+\cdots)$ to rewrite $F_{l,k}$.

$$
\begin{aligned}
F_{l,k} := \sum_{i=0}^{n-1} \partial_l f_i(x_{k,0}) &= (1-\beta_1)\{ \\
&\partial_l f_{n-1}(x_{k,0}) + \cdots + \beta_1^{n-1} \partial_l f_{n-1}(x_{k,0}) \\
&+\partial_l f_{n-2}(x_{k,0}) + \cdots + \beta_1^{n-1} \partial_l f_{n-2}(x_{k,0}) \\
&+\cdots \\
&\underbrace{+\partial_l f_0(x_{k,0}) + \cdots + \beta_1^{n-1} \partial_l f_0(x_{k,0})}_{k\text{-th epoch}} \\
&+ \\
&\vdots \\
&+
\end{aligned}
$$

$$
\begin{aligned}
&+\beta_1^{(k-1)n}\partial_l f_{n-1}(x_{k,0}) + \cdots + \beta_1^{(k-1)n+n-1}\partial_l f_{n-1}(x_{k,0}) \\
&+\beta_1^{(k-1)n}\partial_l f_{n-2}(x_{k,0}) + \cdots + \beta_1^{(k-1)n+n-1}\partial_l f_{n-2}(x_{k,0}) \\
&+\cdots \\
&\underbrace{+\beta_1^{(k-1)n}\partial_l f_0(x_{k,0}) + \cdots + \beta_1^{(k-1)n+n-1}\partial_l f_0(x_{k,0})}_{\text{1-th epoch}}
\end{aligned}
$$

$$
\begin{aligned}
&+\beta_1^{kn}\partial_l f_{n-1}(x_{k,0}) + \cdots + \beta_1^{kn+n-1}\partial_l f_{n-1}(x_{k,0}) \\
&+\beta_1^{kn}\partial_l f_{n-2}(x_{k,0}) + \cdots + \beta_1^{kn+n-1}\partial_l f_{n-2}(x_{k,0}) \\
&+\cdots \\
&\underbrace{+\beta_1^{kn}\partial_l f_0(x_{k,0}) + \cdots + \beta_1^{kn+n-1}\partial_l f_0(x_{k,0})}_{\text{0-th epoch}} \\
&\vdots\}
\end{aligned} \tag{44}
$$

For the sake of better presentation, we rewrite $F_{l,k}$ and $M'_{l,k}$ as follows:

$$
F_{l,k} := (F_{l,k})_k + \cdots + (F_{l,k})_1 + (F_{l,k})_0 + (F_{l,k})_{-1} + \cdots ,
$$

$$
M'_{l,k} := \left(M'_{l,k}\right)_k + \cdots + \left(M'_{l,k}\right)_1 + \left(M'_{l,k}\right)_0 + \left(M'_{l,k}\right)_{-1} + \cdots ,
$$

where $(F_{l,k})_j$ contains the summand of $F_{l,k}$ in the j-th epoch, $j = k, k-1, \cdots - \infty$. Similarly for $M'_{l,k}$. Now, we separate $M'_{l,k} - F_{l,k}$ into two parts.

$$
\begin{aligned}
M'_{l,k} - F_{l,k} \quad = \quad & \left[\left(M'_{l,k}\right)_k - (F_{l,k})_k + \cdots \left(M'_{l,k}\right)_1 - (F_{l,k})_1\right] \\
& + \left[\left(M'_{l,k}\right)_0 - (F_{l,k})_0 + \cdots \left(M'_{l,k}\right)_{-\infty} - (F_{l,k})_{-\infty}\right]
\end{aligned}
$$

Now, we rewrite $\mathbb{E}[\sum_{l \text{ large}}(b_1)]$:

$$
\begin{aligned}
& \mathbb{E}\left[\sum_{l \text{ large}} \frac{\partial_l f(x_{k,0})}{\sqrt{v_{k,0}}} \sum_{i=0}^{n-1}(m_{l,k,i} - \partial_l f_i(x_{k,0}))\right] \\
= \quad & \mathbb{E}\left[\sum_{l \text{ large}} \frac{\partial_l f(x_{k,0})}{\sqrt{v_{k,0}}} \left(M_{l,k} - F_{l,k}\right)\right] \\
\geq \quad & -\mathbb{E}\left[\sum_{l \text{ large}} \frac{|\partial_l f(x_{k,0})|}{\sqrt{v_{k,0}}} |M_{l,k} - M'_{l,k}|\right] + \mathbb{E}\left[\sum_{l \text{ large}} \frac{\partial_l f(x_{k,0})}{\sqrt{v_{k,0}}} (M'_{l,k} - F_{l,k})\right] \\
\geq \quad & \underbrace{-\mathbb{E}\left[\sum_{l \text{ large}} \frac{|\partial_l f(x_{k,0})|}{\sqrt{v_{k,0}}} |M_{l,k} - M'_{l,k}|\right]}_{(1)}
\end{aligned}
$$

$$
\underbrace{+\mathbb{E}\left[\sum_{l \text{ large}} \frac{\partial_l f(x_{k,0})}{\sqrt{v_{k,0}}}\left(\left(M'_{l,k}\right)_k - \left(F_{l,k}\right)_k + \cdots + \left(M'_{l,k}\right)_1 - \left(F_{l,k}\right)_1\right)\right]}_{(2)}
$$

$$
\underbrace{-\mathbb{E}\left[\sum_{l \text{ large}} \frac{|\partial_l f(x_{k,0})|}{\sqrt{v_{k,0}}}\left|\left(M'_{l,k}\right)_0 - \left(F_{l,k}\right)_0 + \cdots \left(M'_{l,k}\right)_{-\infty} - \left(F_{l,k}\right)_{-\infty}\right|\right]}_{(3)} \tag{45}
$$

We bound (1), (2) and (3) respectively. We bound (1) and (3) in the following Lemma G.11 and Lemma G.12. Since the difference of $M_{l,k} - M'_{l,k}$ only occurs in the high order terms of the infinite sum sequence, (1) is expected to vanish as k grows. Similarly for (3).

Lemma G.11. *When k is large enough such that: $\beta_1^{(k-1)n} \leq \frac{\beta_1^n}{\sqrt{k-1}}$ and $k \geq 4$, then we have*

$$
\mathbb{E}\left[\sum_{l \text{ large}} \frac{|\partial_l f(x_{k,0})|}{\sqrt{v_{k,0}}}\left|M_{l,k} - M'_{l,k}\right|\right] \leq G_4 \frac{1}{\sqrt{k}}, \tag{46}
$$

where $G_4 = d\sqrt{\frac{2\rho_3^2}{\beta_2^n}}\beta_1^n\sqrt{2}n(n-1)\sum_{i=0}^{n-1}\mathbb{E}\left(|\partial_\alpha f_i(x_{1,0})|\right)$.

Lemma G.12. *When k is large enough such that: $\beta_1^{(k-1)n} \leq \frac{\beta_1^n}{\sqrt{k-1}}$ and $k \geq 4$, then we have*

$$
\mathbb{E}\left[\sum_{l \text{ large}} \frac{|\partial_l f(x_{k,0})|}{\sqrt{v_{k,0}}}\left|\left(M'_{l,k}\right)_0 - \left(F_{l,k}\right)_0 + \cdots \left(M'_{l,k}\right)_{-\infty} - \left(F_{l,k}\right)_{-\infty}\right|\right] \leq G_5 \frac{1}{\sqrt{k}}, \tag{47}
$$

where $G_5 = d\sqrt{\frac{2\rho_3^2}{\beta_2^n}}\left(\frac{\beta_1^{2n}2n^3\triangle_1\sqrt{2}}{\sqrt{n}}\frac{1-\beta_1}{(1-\beta_1^n)^2} + n\left(1-\beta_1^{n-1}\right)\sum_{i=0}^{n-1}\mathbb{E}|\partial_\alpha f_i(x_{1,0})|\frac{(1-\beta_1)\beta_1^n\sqrt{2}}{1-\beta_1^n}\right)$.

We relegate the proof of Lemma G.11 and G.12 to Appendix G.5 and G.6.

Now we bound (2). This part involves the difficulties (i), (ii) and (iii) mentioned in Appendix G.1. We bound (2) in Lemma G.13.

Lemma G.13. *When k is large enough such that: $\beta_1^{(k-1)n} \leq \frac{\beta_1^n}{\sqrt{k-1}}$ and $k \geq 2$, then we have*

$$
\begin{aligned}
&\mathbb{E}\left[\sum_{l \text{ large}} \frac{\partial_l f(x_{k,0})}{\sqrt{v_{k,0}}}\left(\left(M'_{l,k}\right)_k - \left(F_{l,k}\right)_k + \cdots + \left(M'_{l,k}\right)_1 - \left(F_{l,k}\right)_1\right)\right] \\
\geq\ & -\frac{G_6}{\sqrt{k}} - G_7\delta_1\mathbb{E}\left(\sum_{l=1}^{d}\sum_{i=0}^{n-1}|\partial_l f_i(x_{k,0})|\right).
\end{aligned}
$$

The constant terms G_6 and G_7 are specified in Appendix G.7.

Proof is shown in Appendix G.7.

Combining Lemma G.11, G.12 and G.13 together, we conclude the proof.

$$
\mathbb{E}[\sum_{l \text{ large}}(b_1)] \geq -\frac{1}{\sqrt{k}}\left(G_4 + G_5 + G_6\right) - G_7\delta_1\mathbb{E}\left(\sum_{l=1}^{d}\sum_{i=0}^{n-1}|\partial_l f_i(x_{k,0})|\right).
$$

G.5 Proof of Lemma G.11

By definition of $M_{l,k}$ and $M'_{l,k}$ (see (41) and (42)), they only differ when $k \leq 0$. More specifically, We have (For each 'epoch', we suggest readers to read from bottom to the top.)

$$
\begin{aligned}
\frac{M_{l,k} - M'_{l,k}}{1-\beta_1} \quad = \quad & \left(\beta_1^{(k-1)n+n} - \beta_1^{(k-1)n+n+1}\right) \partial_l f_1(x_{1,0}) + \cdots + \left(\beta_1^{(k-1)n+n} - \beta_1^{(k-1)n+n+n-1}\right) \partial_l f_{n-1}(x_{1,0}) \\
& + \cdots \\
& \underbrace{\begin{aligned}
& + \left(\beta_1^{(k-1)n+2} - \beta_1^{(k-1)n+3}\right) \partial_l f_1(x_{1,0}) + \cdots + \left(\beta_1^{(k-1)n+2} - \beta_1^{(k-1)n+n+1}\right) \partial_l f_{n-1}(x_{1,0}) \\
& + \left(\beta_1^{(k-1)n+1} - \beta_1^{(k-1)n+2}\right) \partial_l f_1(x_{1,0}) + \cdots + \left(\beta_1^{(k-1)n+1} - \beta_1^{(k-1)n+n}\right) \partial_l f_{n-1}(x_{1,0})
\end{aligned}}_{\text{0-th epoch}} \\
& + \left(\beta_1^{(k-1)n+n+1} - \beta_1^{kn+n}\right) \partial_l f_0(x_{1,0}) + \cdots + \left(\beta_1^{(k-1)n+n+1} - \beta_1^{kn+n+n-1}\right) \partial_l f_{n-1}(x_{1,0}) \\
& + \cdots \\
& \underbrace{\begin{aligned}
& + \left(\beta_1^{(k-1)n+3} - \beta_1^{kn+2}\right) \partial_l f_0(x_{1,0}) + \cdots + \left(\beta_1^{(k-1)n+3} - \beta_1^{kn+n+1}\right) \partial_l f_{n-1}(x_{1,0}) \\
& + \left(\beta_1^{(k-1)n+2} - \beta_1^{kn+1}\right) \partial_l f_0(x_{1,0}) + \cdots + \left(\beta_1^{(k-1)n+2} - \beta_1^{kn+n}\right) \partial_l f_{n-1}(x_{1,0})
\end{aligned}}_{\text{-1-th epoch}} \\
& + \left(\beta_1^{(k-1)n+n+2} - \beta_1^{(k+1)n+n}\right) \partial_l f_0(x_{1,0}) + \cdots + \left(\beta_1^{(k-1)n+n+2} - \beta_1^{(k+1)n+n+n-1}\right) \partial_l f_{n-1}(x_{1,0}) \\
& + \cdots \\
& \underbrace{\begin{aligned}
& + \left(\beta_1^{(k-1)n+4} - \beta_1^{(k+1)n+2}\right) \partial_l f_0(x_{1,0}) + \cdots + \left(\beta_1^{(k-1)n+4} - \beta_1^{(k+1)n+n+1}\right) \partial_l f_{n-1}(x_{1,0}) \\
& + \left(\beta_1^{(k-1)n+3} - \beta_1^{(k+1)n+1}\right) \partial_l f_0(x_{1,0}) + \cdots + \left(\beta_1^{(k-1)n+3} - \beta_1^{(k+1)n+n}\right) \partial_l f_{n-1}(x_{1,0})
\end{aligned}}_{\text{-2-th epoch}} \\
& + \cdots
\end{aligned} \tag{48}
$$

We start with the 1st column in the '0-th epoch' (from the bottom to the top).

$$
\begin{aligned}
\text{The 1st column in the '0-th epoch'} \quad = \quad & \beta_1^{(k-1)n+1}(1-\beta_1)|\partial_l f_1(x_{1,0})| \\
& + \beta_1^{(k-1)n+2}(1-\beta_1)|\partial_l f_1(x_{1,0})| \\
& + \cdots \\
& + \beta_1^{(k-1)n+n}(1-\beta_1)|\partial_l f_1(x_{1,0})| \\
\leq \quad & \beta_1^{(k-1)n+1} n(1-\beta_1)|\partial_l f_1(x_{1,0})|
\end{aligned} \tag{49}
$$

Similarly, we can bound every column in the in the '0-th epoch', e.g. last ($n-1$-th) column can be bounded as follows.

$$
\begin{aligned}
\text{The last column in the '0-th epoch'} \quad = \quad & \beta_1^{(k-1)n+1}(1-\beta_1^{n-1})|\partial_l f_{n-1}(x_{1,0})| \\
& + \beta_1^{(k-1)n+2}(1-\beta_1^{n-1})|\partial_l f_{n-1}(x_{1,0})| \\
& + \cdots \\
& + \beta_1^{(k-1)n+n}(1-\beta_1^{n-1})|\partial_l f_{n-1}(x_{1,0})| \\
\leq \quad & \beta_1^{(k-1)n+1} n(n-1)(1-\beta_1)|\partial_l f_{n-1}(x_{1,0})|
\end{aligned} \tag{50}
$$

Summing up all the columns, we have

$$
\begin{aligned}
\text{The '0-th epoch'} &\leq \beta_1^{(k-1)n+1} n(n-1)(1-\beta_1) \sum_{i=1}^{n-1} |\partial_l f_i(x_{1,0})| \\
&\leq \beta_1^{(k-1)n+1} n(n-1)(1-\beta_1) \sum_{i=0}^{n-1} |\partial_l f_i(x_{1,0})| \qquad (51)
\end{aligned}
$$

Using the same technique, it can be shown that

$$
\text{The '-1-th epoch'} \leq \beta_1^{(k-1)n+2} 2n(n-1)(1-\beta_1) \sum_{i=0}^{n-1} |\partial_l f_i(x_{1,0})|, \qquad (52)
$$

$$
\text{The '-2-th epoch'} \leq \beta_1^{(k-1)n+3} 3n(n-1)(1-\beta_1) \sum_{i=0}^{n-1} |\partial_l f_i(x_{1,0})| \qquad (53)
$$

$$
\cdots
$$

Plugging all these results in (48), we have

$$
\begin{aligned}
\frac{\left|M_{l,k} - M'_{l,k}\right|}{1-\beta_1} &\leq \beta_1^{(k-1)n+1} n(n-1)(1-\beta_1) \sum_{i=0}^{n-1} |\partial_l f_i(x_{1,0})| \left(1 + 2\beta_1 + 3\beta_1^2 + \cdots\right) \\
&= \beta_1^{(k-1)n+1} n(n-1) \sum_{i=0}^{n-1} |\partial_l f_i(x_{1,0})| \frac{1}{1-\beta_1}. \\
&\leq \beta_1^{(k-1)n} n(n-1) \sum_{i=0}^{n-1} |\partial_l f_i(x_{1,0})| \frac{1}{1-\beta_1}.
\end{aligned}
$$

That is to say, when k is large enough such that $\beta_1^{(k-1)n} \leq \frac{\beta_1^n}{\sqrt{k-1}}$ we have

$$
\begin{aligned}
\left|M_{l,k} - M'_{l,k}\right| &\leq \frac{\beta_1^n}{\sqrt{k-1}} n(n-1) \sum_{i=0}^{n-1} |\partial_l f_i(x_{1,0})| \qquad (54) \\
&\overset{\text{When } k \geq 2}{\leq} \frac{\beta_1^n \sqrt{2}}{\sqrt{k}} n(n-1) \sum_{i=0}^{n-1} |\partial_l f_i(x_{1,0})|. \qquad (55)
\end{aligned}
$$

Combining with Lemma G.10, the proof is completed.

G.6 Proof of Lemma G.12

We start with $\left(M'_{l,k}\right)_0 - (F_{l,k})_0$.

$$
\begin{aligned}
\frac{\left(M'_{l,k}\right)_0 - (F_{l,k})_0}{1-\beta_1} = \; & \beta_1^{(k-1)n+n} \partial_l f_0(x_{1,0}) + \cdots + \beta_1^{(k-1)n+n+n-1} \partial_l f_{n-1}(x_{1,0}) \\
& + \beta_1^{(k-1)n+n-1} \partial_l f_0(x_{1,0}) + \cdots + \beta_1^{(k-1)n+2(n-1)} \partial_l f_{n-1}(x_{1,0}) \\
& + \cdots \\
& \underbrace{+ \beta_1^{(k-1)n+1} \partial_l f_0(x_{1,0}) + \cdots + \beta_1^{(k-1)n+n} \partial_l f_{n-1}(x_{1,0})}_{\left(M'_{l,k}\right)_0}
\end{aligned}
$$

$$
\begin{aligned}
& - \Big\{ \beta_1^{kn} \partial_l f_{n-1}(x_{k,0}) + \cdots + \beta_1^{kn+n-1} \partial_l f_{n-1}(x_{k,0}) \\
& + \beta_1^{kn} \partial_l f_{n-2}(x_{k,0}) + \cdots + \beta_1^{kn+n-1} \partial_l f_{n-2}(x_{k,0}) \\
& + \cdots \\
& \underbrace{+ \beta_1^{kn} \partial_l f_0(x_{k,0}) + \cdots + \beta_1^{kn+n-1} \partial_l f_0(x_{k,0})}_{\left(F_{l,k}\right)_0} \Big\} \\
:= \quad & \sum_{i=0}^{n-1} \delta_i,
\end{aligned}
$$

where

$$
\begin{aligned}
\delta_i &= \sum_{j=1}^{n} \left(\beta_1^{(k-1)n+j} \partial_l f_i(x_{1,0}) - \beta_1^{kn+j-1} \partial_l f_i(x_{k,0}) \right) \\
&= \underbrace{\sum_{j=1}^{n} \left(\beta_1^{(k-1)n+j} - \beta_1^{kn+j-1} \right) \partial_l f_i(x_{1,0})}_{\delta_i^a} + \underbrace{\sum_{j=1}^{n} \beta_1^{kn+j-1} \left(\partial_l f_i(x_{1,0}) - \partial_l f_i(x_{k,0}) \right)}_{\delta_i^b}.
\end{aligned}
$$

We further have

$$
\begin{aligned}
\delta_i^a &= \sum_{j=1}^{n} \beta_1^{(k-1)n+j} \left(1 - \beta_1^{n-1} \right) \partial_l f_i(x_{1,0}) \\
&\leq n \beta_1^{(k-1)n+1} \left(1 - \beta_1^{n-1} \right) \left| \partial_l f_i(x_{1,0}) \right|
\end{aligned} \tag{56}
$$

$$
\begin{aligned}
\delta_i^b &\leq \sum_{j=1}^{n} \beta_1^{kn+j-1} \frac{\triangle_1 (k-1) 2n}{\sqrt{n(k-1)-1}} \\
&\leq \beta_1^{kn} \frac{\triangle_1 (k-1) 2n^2}{\sqrt{n(k-1)-1}}.
\end{aligned} \tag{57}
$$

Therefore,

$$
\begin{aligned}
\frac{\left| \left(M'_{l,k}\right)_0 - \left(F_{l,k}\right)_0 \right|}{1-\beta_1} &= \left| \sum_{i=0}^{n-1} \delta_i \right| \\
&\leq \sum_{i=0}^{n-1} \left(n \beta_1^{(k-1)n+1} \left(1 - \beta_1^{n-1} \right) \left| \partial_l f_i(x_{1,0}) \right| + \beta_1^{kn} \frac{\triangle_1 (k-1) 2n^2}{\sqrt{n(k-1)-1}} \right) \\
&= \beta_1^{kn} \frac{\triangle_1 (k-1) 2n^3}{\sqrt{n(k-1)-1}} + n \beta_1^{(k-1)n+1} \left(1 - \beta_1^{n-1} \right) \sum_{i=0}^{n-1} \left| \partial_l f_i(x_{1,0}) \right|
\end{aligned} \tag{58}
$$

Using the same calculation, we can get the following result:

$$
\frac{\left| \left(M'_{l,k}\right)_{-1} - \left(F_{l,k}\right)_{-1} \right|}{1-\beta_1} \leq \beta_1^{(k+1)n} \frac{\triangle_1 k 2n^3}{\sqrt{n(k-1)-1}} + n \beta_1^{kn+1} \left(1 - \beta_1^{n-1} \right) \sum_{i=0}^{n-1} \left| \partial_l f_i(x_{1,0}) \right|.
$$

Repeat this calculation, we have

$$
\begin{aligned}
& \frac{1}{1-\beta_1}\left[\left(M'_{l,k}\right)_0-\left(F_{l,k}\right)_0+\cdots\left(M'_{l,k}\right)_{-\infty}-\left(F_{l,k}\right)_{-\infty}\right] \\
\leq\quad & \frac{\beta_1^{2n}2n^3\triangle_1}{\sqrt{n(k-1)-1}}\left(\beta_1^{(k-2)n}(k-1)+\beta_1^{(k-1)n}k+\cdots\right) \\
& +n\left(1-\beta_1^{n-1}\right)\sum_{i=0}^{n-1}\left|\partial_l f_i(x_{1,0})\right|\left(\beta_1^{(k-1)n+1}+\beta_1^{kn+1}+\cdots\right) \\
\leq\quad & \frac{\beta_1^{2n}2n^3\triangle_1}{\sqrt{n(k-1)-1}}\left(1+\beta_1^n 2+\cdots\right) \\
& +n\left(1-\beta_1^{n-1}\right)\sum_{i=0}^{n-1}\left|\partial_l f_i(x_{1,0})\right|\left(\beta_1^{(k-1)n+1}+\beta_1^{kn+1}+\cdots\right) \\
\overset{\text{Lemma F.1}}{\leq}\quad & \frac{\beta_1^{2n}2n^3\triangle_1}{\sqrt{n(k-1)-1}}\frac{1}{(1-\beta_1^n)^2} \\
& +n\left(1-\beta_1^{n-1}\right)\sum_{i=0}^{n-1}\left|\partial_l f_i(x_{1,0})\right|\frac{\beta_1^{(k-1)n}}{1-\beta_1^n}
\end{aligned}
$$

When $\beta_1^{(k-1)n}\leq\frac{\beta_1^n}{\sqrt{k-1}}$, we further have:

$$
\begin{aligned}
& \frac{1}{1-\beta_1}\left[\left(M'_{l,k}\right)_0-\left(F_{l,k}\right)_0+\cdots\left(M'_{l,k}\right)_{-\infty}-\left(F_{l,k}\right)_{-\infty}\right] \\
\leq\quad & \frac{\beta_1^{2n}2n^3\triangle_1}{\sqrt{n(k-1)-1}}\frac{1}{(1-\beta_1^n)^2} \\
& +n\left(1-\beta_1^{n-1}\right)\sum_{i=0}^{n-1}\left|\partial_l f_i(x_{1,0})\right|\frac{\beta_1^n}{1-\beta_1^n}\frac{1}{\sqrt{k-1}} \\
\overset{\frac{1}{\sqrt{k-1}}\leq\sqrt{\frac{2}{k}}}{\leq}\quad & \frac{\beta_1^{2n}2n^3\triangle_1}{\sqrt{n(k-1)-1}}\frac{1}{(1-\beta_1^n)^2} \\
& +n\left(1-\beta_1^{n-1}\right)\sum_{i=0}^{n-1}\left|\partial_l f_i(x_{1,0})\right|\frac{\beta_1^n}{1-\beta_1^n}\sqrt{\frac{2}{k}} \\
\overset{(*)}{\leq}\quad & \frac{\beta_1^{2n}2n^3\triangle_1\sqrt{2}}{\sqrt{nk}}\frac{1}{(1-\beta_1^n)^2} \\
& +n\left(1-\beta_1^{n-1}\right)\sum_{i=0}^{n-1}\left|\partial_l f_i(x_{1,0})\right|\frac{\beta_1^n}{1-\beta_1^n}\sqrt{\frac{2}{k}},
\end{aligned}
$$

where $(*):\frac{1}{\sqrt{n(k-1)-1}}\leq\sqrt{\frac{2}{nk}}$ when $k\geq 4$. Therefore, we have

$$
\left|\left(M'_{l,k}\right)_0-\left(F_{l,k}\right)_0+\cdots\left(M'_{l,k}\right)_{-\infty}-\left(F_{l,k}\right)_{-\infty}\right|\leq\frac{1}{\sqrt{k}}\tilde{G}_5
$$

,

$\tilde{G}_5=\frac{\beta_1^{2n}2n^3\triangle_1\sqrt{2}}{\sqrt{n}}\frac{1-\beta_1}{(1-\beta_1^n)^2}+n\left(1-\beta_1^{n-1}\right)\sum_{i=0}^{n-1}\left|\partial_l f_i(x_{1,0})\right|\frac{(1-\beta_1)\beta_1^n\sqrt{2}}{1-\beta_1^n}$.

Combining with Lemma G.10, the proof is completed with constant G_5 defined in Lemma G.12.

G.7 Proof of Lemma G.13

In this section, we derive a lower bound for $\mathbb{E}\left[\sum_{l\text{ large}}\frac{\partial_l f(x_{k,0})}{\sqrt{v_{k,0}}}\left(\left(M'_{l,k}\right)_k-\left(F_{l,k}\right)_k+\cdots+\left(M'_{l,k}\right)_1-\left(F_{l,k}\right)_1\right)\right]$. We will use the ideas mentioned in Appendix G.1 (i.e., Step 1,2 and 3). We first rewrite "l large" into indicator function as follows:

$$\mathbb{E}\left[\sum_{l \text{ large}} \frac{\partial_l f(x_{k,0})}{\sqrt{v_{k,0}}}\left(\left(M'_{l,k}\right)_k - (F_{l,k})_k + \cdots + \left(M'_{l,k}\right)_1 - (F_{l,k})_1\right)\right] = \mathbb{E}\left[\sum_{l=1}^{d} \mathbb{I}_k \frac{\partial_l f(x_{k,0})}{\sqrt{v_{k,0}}}\left(\left(M'_{l,k}\right)_k - (F_{l,k})_k + \cdots + \left(M'_{l,k}\right)_1 - (F_{l,k})_1\right)\right],$$

where $\mathbb{I}_k := \mathbb{I}\left(\max_i |\partial_l f_i(x_{k,0})| \geq Q_k := \triangle_1 \frac{n\sqrt{n}}{\sqrt{k}} \frac{32\sqrt{2}}{(1-\beta_2)^n \beta_2^n}\right)$. We also define $\mathbb{I}_{k-j} := \mathbb{I}\left(\max_i |\partial_l f_i(x_{k-j,0})| \geq \sum_{p=k-j}^{k} Q_p\right)$, it will be used later.

We take the conditional expectation over the history before $x_{k,0}$. We first focus on $\mathbb{E}_k\left[\sum_{l=1}^{d} \mathbb{I}_k \frac{\partial_l f(x_{k,0})}{\sqrt{v_{k,0}}}\left(\left(M'_{l,k}\right)_k - (F_{l,k})_k\right)\right]$ and we delegate the history part for later analysis.

For each possible $\left(M'_{l,k}\right)_k - (F_{l,k})_k$, we first convert all $x_{k,i}$ into $x_{k,0}$ using Lemma F.2. Since $\left(M'_{l,k}\right)_k$ contains $(n-1) + \cdots + 1 = \frac{n(n-1)}{2}$ terms of $x_{k,i}$ (with $i \neq 0$), we have

$$\begin{aligned}
\left(M'_{l,k}\right)_k &\overset{\text{Lemma F.2}}{\geq} -\frac{(1-\beta_1)n^2(n-1)\triangle_{nk}}{2} + (1-\beta_1)\{ \\
&\quad \underbrace{\begin{aligned}&\partial_l f_{\tau_{k,n-1}}(x_{k,0}) + \cdots + \beta_1^{n-1}\partial_l f_{\tau_{k,0}}(x_{k,0}) \\ &+\partial_l f_{\tau_{k,n-2}}(x_{k,0}) + \cdots + \beta_1^{n-2}\partial_l f_{\tau_{k,0}}(x_{k,0}) \\ &+\cdots \\ &+\partial_l f_{\tau_{k,0}}(x_{k,0})\end{aligned}}_{k\text{-th epoch}}\} \\
&:= -\frac{(1-\beta_1)n^2(n-1)\triangle_{nk}}{2} + \mathscr{M}_{l,k}.
\end{aligned}$$

Using the same strategy for analyzing the color-ball toy example, we have

$$\begin{aligned}
\frac{\mathbb{E}_k\left[\mathscr{M}_{l,k} - (F_{l,k})_k\right]}{1-\beta_1} &= \frac{1}{n!}\left(-(n-1)!\beta_1 - 2(n-1)!\beta_1^2 - \cdots - (n-1)(n-1)!\beta_1^{n-1}\right)\sum_{i=0}^{n-1}\partial_l f_i(x_{k,0}) \\
&= \left(-\frac{1}{n}\beta_1 - \frac{2}{n}\beta_1^2 - \cdots - \frac{n-1}{n}\beta_1^{n-1}\right)\sum_{i=0}^{n-1}\partial_l f_i(x_{k,0})
\end{aligned}$$

$$\begin{aligned}
\mathbb{E}_k\left[\sum_{l=1}^{d} \mathbb{I}_k \frac{\partial_l f(x_{k,0})}{\sqrt{v_{k,0}}}\left(\left(M'_{l,k}\right)_k - (F_{l,k})_k\right)\right] &\geq -d\sqrt{\frac{2\rho_3^2}{\beta_2^n}}\frac{(1-\beta_1)n^2(n-1)\triangle_{nk}}{2} + \mathbb{E}_k\left[\sum_{l=1}^{d} \mathbb{I}_k \frac{\partial_l f(x_{k,0})}{\sqrt{v_{k,0}}}\left(\mathscr{M}_{l,k} - (F_{l,k})_k\right)\right] \\
&= -d\sqrt{\frac{2\rho_3^2}{\beta_2^n}}\frac{(1-\beta_1)n^2(n-1)\triangle_{nk}}{2} \\
&\quad + \sum_{l=1}^{d} \mathbb{I}_k(1-\beta_1)\left(-\frac{1}{n}\beta_1 - \frac{2}{n}\beta_1^2 - \cdots - \frac{n-1}{n}\beta_1^{n-1}\right)\sum_{i=0}^{n-1}\partial_l f_i(x_{k,0}) \\
&:= -d\sqrt{\frac{2\rho_3^2}{\beta_2^n}}\frac{(1-\beta_1)n^2(n-1)\triangle_{nk}}{2} + \sum_{l=1}^{d} \mathbb{I}_k \frac{\partial_l f(x_{k,0})}{\sqrt{v_{k,0}}}(1-\beta_1)J_1\sum_{i=0}^{n-1}\partial_l f_i(x_{k,0})
\end{aligned}$$

We denote $J_1 := \left(-\frac{1}{n}\beta_1 - \frac{2}{n}\beta_1^2 - \cdots - \frac{n-1}{n}\beta_1^{n-1}\right)$, it will be used repeatedly in the following derivation.

Now we move one step further exert $\mathbb{E}_{k-1}(\cdot)$. In particular, we need to calculate

$$
\begin{aligned}
& \mathbb{E}_{k-1}\left\{\mathbb{E}_k\left[\sum_{l=1}^{d}\mathbb{I}_k\frac{\partial_l f(x_{k,0})}{\sqrt{v_{k,0}}}\left(\left(M'_{l,k}\right)_k-\left(F_{l,k}\right)_k\right)+\sum_{l=1}^{d}\mathbb{I}_k\frac{\partial_l f(x_{k,0})}{\sqrt{v_{k,0}}}\left(\left(M'_{l,k}\right)_{k-1}-\left(F_{l,k}\right)_{k-1}\right)\right]\right\} \\
\geq\ & \mathbb{E}_{k-1}\left\{\underbrace{\sum_{l=1}^{d}\mathbb{I}_k\frac{\partial_l f(x_{k,0})}{\sqrt{v_{k,0}}}(1-\beta_1)J_1\sum_{i=0}^{n-1}\partial_l f_i(x_{k,0})}_{(a)}+\underbrace{\sum_{l=1}^{d}\mathbb{I}_k\frac{\partial_l f(x_{k,0})}{\sqrt{v_{k,0}}}\left(\left(M'_{l,k}\right)_{k-1}-\left(F_{l,k}\right)_{k-1}\right)}_{(b)}\right\} \\
& -d\sqrt{\frac{2\rho_3^2}{\beta_2^n}}\frac{(1-\beta_1)n^2(n-1)\triangle_{nk}}{2}. \qquad (59)
\end{aligned}
$$

The blue term is the residue from the k-th epoch. The red term is the main component in the $(k-1)$-th epoch. Before calculating $\mathbb{E}_{k-1}(\cdot)$, we need to convert all the variable x into $x_{k-1,0}$ using Lipschitz property. First of all, we work on (a).

$$
\begin{aligned}
(a) \quad &= \sum_{l=1}^{d}\mathbb{I}_k\frac{\partial_l f(x_{k,0})}{\sqrt{v_{k,0}}}(1-\beta_1)J_1\sum_{i=0}^{n-1}\partial_l f_i(x_{k,0}) \\
&\overset{\text{Lemma G.3}}{=} \sum_{l=1}^{d}\mathbb{I}_{k,k-1}\frac{\partial_l f(x_{k,0})}{\sqrt{v_{k,0}}}(1-\beta_1)J_1\sum_{i=0}^{n-1}\partial_l f_i(x_{k,0}) \\
&\quad +\sum_{l=1}^{d}\tilde{\mathbb{I}}_{k,k-1}\frac{\partial_l f(x_{k,0})}{\sqrt{v_{k,0}}}(1-\beta_1)J_1\sum_{i=0}^{n-1}\partial_l f_i(x_{k,0}) \\
&\overset{\text{Lemma G.10}}{\geq} \sum_{l=1}^{d}\mathbb{I}_{k,k-1}\frac{\partial_l f(x_{k,0})}{\sqrt{v_{k,0}}}(1-\beta_1)J_1\sum_{i=0}^{n-1}\partial_l f_i(x_{k,0})-\sum_{l=1}^{d}\tilde{\mathbb{I}}_{k,k-1}\sqrt{\frac{2\rho_3^2}{\beta_2^n}}(1-\beta_1)|J_1||\sum_{i=0}^{n-1}\partial_l f_i(x_{k,0})| \\
&\geq \sum_{l=1}^{d}\mathbb{I}_{k,k-1}\frac{\partial_l f(x_{k,0})}{\sqrt{v_{k,0}}}(1-\beta_1)J_1\sum_{i=0}^{n-1}\partial_l f_i(x_{k,0})-\sum_{l=1}^{d}\tilde{\mathbb{I}}_{k,k-1}\sqrt{\frac{2\rho_3^2}{\beta_2^n}}(1-\beta_1)|J_1|\left(\sum_{i=0}^{n-1}|\partial_l f_i(x_{k-1,0})|+n^2\triangle_{n(k-1)}\right) \\
&\geq \sum_{l=1}^{d}\mathbb{I}_{k,k-1}\frac{\partial_l f(x_{k,0})}{\sqrt{v_{k,0}}}(1-\beta_1)J_1\sum_{i=0}^{n-1}\partial_l f_i(x_{k,0}) \\
&\quad -\sum_{l=1}^{d}\tilde{\mathbb{I}}_{k,k-1}\sqrt{\frac{2\rho_3^2}{\beta_2^n}}(1-\beta_1)|J_1|\sum_{i=0}^{n-1}|\partial_l f_i(x_{k-1,0})|-d\sqrt{\frac{2\rho_3^2}{\beta_2^n}}(1-\beta_1)|J_1|n^2\triangle_{n(k-1)}
\end{aligned}
$$

$$
\begin{aligned}
&\overset{\text{Lemma G.10 and F.2}}{\geq} \sum_{l=1}^{d}\mathbb{I}_{k,k-1}\frac{\partial_l f(x_{k,0})}{\sqrt{v_{k,0}}}(1-\beta_1)J_1\sum_{i=0}^{n-1}\partial_l f_i(x_{k-1,0}) \\
&\quad -(1-\beta_1)d\sqrt{\frac{2\rho_3^2}{\beta_2^n}}|J_1|n^2\triangle_{n(k-1)}-(1-\beta_1)d\sqrt{\frac{2\rho_3^2}{\beta_2^n}}|J_1|n(Q_k+Q_{k-1})-(1-\beta_1)d\sqrt{\frac{2\rho_3^2}{\beta_2^n}}|J_1|n^2\triangle_{n(k-1)} \\
&\geq \sum_{l=1}^{d}\mathbb{I}_{k,k-1}\frac{\partial_l f(x_{k-1,0})}{\sqrt{v_{k-1,0}}}(1-\beta_1)J_1\sum_{i=0}^{n-1}\partial_l f_i(x_{k-1,0}) \\
&\quad -\sum_{l=1}^{d}\mathbb{I}_{k,k-1}\left|\frac{\partial_l f(x_{k-1,0})}{\sqrt{v_{k-1,0}}}-\frac{\partial_l f(x_{k,0})}{\sqrt{v_{k,0}}}\right|(1-\beta_1)|J_1|\left|\sum_{i=0}^{n-1}\partial_l f_i(x_{k-1,0})\right| \\
&\quad -2(1-\beta_1)d\sqrt{\frac{2\rho_3^2}{\beta_2^n}}|J_1|n^2\triangle_{n(k-1)}-(1-\beta_1)d\sqrt{\frac{2\rho_3^2}{\beta_2^n}}|J_1|n(Q_k+Q_{k-1})
\end{aligned}
$$

$$
\begin{aligned}
\overset{\text{Lemma G.2}}{\geq} \quad & \sum_{l=1}^{d} \mathbb{I}_{k,k-1} \frac{\partial_l f(x_{k-1,0})}{\sqrt{v_{k-1,0}}} (1-\beta_1) J_1 \sum_{i=0}^{n-1} \partial_l f_i(x_{k-1,0}) \\
& - \sum_{l=1}^{d} \mathbb{I}_{k,k-1} (1-\beta_1) |J_1| \left| \sum_{i=0}^{n-1} \partial_l f_i(x_{k-1,0}) \right| \left(\frac{1}{1-\frac{1}{\sqrt{\beta_2^n}}} \frac{n^2 \triangle_{n(k-1)}}{\sqrt{v_{k-1,0}}} + \sqrt{\frac{2\rho_3^2}{\beta_2^n}} \frac{1}{\left(1-\frac{(1-\beta_2)4n\rho_2}{\beta_2^n}\right)} \delta_1 \right) \\
& - 2(1-\beta_1) d \sqrt{\frac{2\rho_3^2}{\beta_2^n}} |J_1| n^2 \triangle_{n(k-1)} - (1-\beta_1) d \sqrt{\frac{2\rho_3^2}{\beta_2^n}} |J_1| n (Q_k + Q_{k-1})
\end{aligned}
$$

where $\mathbb{I}_{k,k-j} := \mathbb{I}\left(\max_i |\partial_l f_i(x_{k,0})| \geq Q_k \text{ and } \max_i |\partial_l f_i(x_{k-j,0})| \geq \sum_{p=k-j}^{k} Q_p\right)$ and $\tilde{\mathbb{I}}_{k,k-j} := \mathbb{I}\left(\max_i |\partial_l f_i(x_{k,0})| \geq Q_k \text{ and } \max_i |\partial_l f_i(x_{k-j,0})| \leq \sum_{p=k-j}^{k} Q_p\right)$. By Lemma G.3, we know $\mathbb{I}_{k,k-1} = \mathbb{I}_{k-1}$, so we have:

$$
\begin{aligned}
(a) \quad \overset{\text{Lemma G.10}}{\geq} \quad & \sum_{l=1}^{d} \mathbb{I}_{k-1} \frac{\partial_l f(x_{k-1,0})}{\sqrt{v_{k-1,0}}} (1-\beta_1) J_1 \sum_{i=0}^{n-1} \partial_l f_i(x_{k-1,0}) \\
& - d(1-\beta_1) |J_1| \frac{1}{1-\frac{1}{\sqrt{\beta_2^n}}} n^2 \triangle_{n(k-1)} \sqrt{\frac{2}{n\beta_2^n}} \\
& - \sum_{l=1}^{d} (1-\beta_1) |J_1| \left| \sum_{i=0}^{n-1} \partial_l f_i(x_{k-1,0}) \right| \left(\sqrt{\frac{2\rho_3^2}{\beta_2^n}} \frac{1}{\left(1-\frac{(1-\beta_2)4n\rho_2}{\beta_2^n}\right)} \delta_1 \right) \\
& - 2(1-\beta_1) d \sqrt{\frac{2\rho_3^2}{\beta_2^n}} |J_1| n^2 \triangle_{n(k-1)} - (1-\beta_1) d \sqrt{\frac{2\rho_3^2}{\beta_2^n}} |J_1| n (Q_k + Q_{k-1})
\end{aligned}
$$

$$
\begin{aligned}
\overset{\text{Lemma F.2}}{\geq} \quad & \sum_{l=1}^{d} \mathbb{I}_{k-1} \frac{\partial_l f(x_{k-1,0})}{\sqrt{v_{k-1,0}}} (1-\beta_1) J_1 \sum_{i=0}^{n-1} \partial_l f_i(x_{k-1,0}) \\
& - d(1-\beta_1) |J_1| \frac{1}{1-\frac{1}{\sqrt{\beta_2^n}}} n^2 \triangle_{n(k-1)} \sqrt{\frac{2}{n\beta_2^n}} \\
& - \sum_{l=1}^{d} (1-\beta_1) |J_1| \left(\left| \sum_{i=0}^{n-1} \partial_l f_i(x_{k,0}) \right| + n^2 \triangle_{n(k-1)} \right) \left(\sqrt{\frac{2\rho_3^2}{\beta_2^n}} \frac{1}{\left(1-\frac{(1-\beta_2)4n\rho_2}{\beta_2^n}\right)} \delta_1 \right) \\
& - 2(1-\beta_1) d \sqrt{\frac{2\rho_3^2}{\beta_2^n}} |J_1| n^2 \triangle_{n(k-1)} - (1-\beta_1) d \sqrt{\frac{2\rho_3^2}{\beta_2^n}} |J_1| n (Q_k + Q_{k-1}).
\end{aligned}
$$

The blue term will be handled using color-ball method when taking conditional expectation $\mathbb{E}_{k-1}(\cdot)$. Now we derive a lower bound for (b). Similarly as before, we rewrite $\left(M'_{l,k}\right)_{k-1}$ and $(F_{l,k})_{k-1}$ as follows.

$$
\left(M'_{l,k}\right)_{k-1} \overset{\text{Lemma F.2}}{\geq} \mathscr{M}_{l,k-1} - (1-\beta_1)\beta_1 n^3 \triangle_{n(k-1)};
$$

$$
(F_{l,k})_{k-1} \overset{\text{Lemma F.2}}{\geq} (F_{l,k-1})_{k-1} - (1-\beta_1)\beta_1^n n^3 \triangle_{n(k-1)};
$$

where

$$
\begin{aligned}
\mathscr{M}_{l,k-1} \quad := \quad & (1-\beta_1)\{ \\
& +\beta_1^n \partial_l f_{\tau_{k-1,n-1}}(x_{k-1,0}) + \cdots + \beta_1^{n+n-1} \partial_l f_{\tau_{k-1,0}}(x_{k-1,0}) \\
& +\beta_1^{n-1} \partial_l f_{\tau_{k-1,n-1}}(x_{k-1,0}) + \cdots + \beta_1^{n+n-2} \partial_l f_{\tau_{k-1,0}}(x_{k-1,0}) \\
& + \cdots \\
& \underbrace{+\beta_1 \partial_l f_{\tau_{k-1,n-1}}(x_{k-1,0}) + \cdots + \beta_1^n \partial_l f_{\tau_{k-1,0}}(x_{k-1,0})}_{k-1\text{-th epoch}}\}
\end{aligned}
$$

$$
\begin{aligned}
(F_{l,k-1})_{k-1} := \sum_{i=0}^{n-1} \partial_l f_i(x_{k-1,0}) \quad = \quad & (1-\beta_1)\beta_1^n\{ \\
& \partial_l f_{n-1}(x_{k-1,0}) + \cdots + \beta_1^{n-1} \partial_l f_{n-1}(x_{k-1,0}) \\
& +\partial_l f_{n-2}(x_{k-1,0}) + \cdots + \beta_1^{n-1} \partial_l f_{n-2}(x_{k-1,0}) \\
& + \cdots \\
& \underbrace{+\partial_l f_0(x_{k-1,0}) + \cdots + \beta_1^{n-1} \partial_l f_0(x_{k-1,0})}_{(k-1)\text{-th epoch}}\}
\end{aligned}
$$

We now calculate (b). Using the same idea as in (a), we have

$$
\begin{aligned}
(b) \quad = \quad & \sum_{l=1}^{d} \mathbb{I}_k \frac{\partial_l f(x_{k,0})}{\sqrt{v_{k,0}}} \left(\left(M'_{l,k}\right)_{k-1} - (F_{l,k})_{k-1} \right) \\
\overset{\text{Lemma G.10 and F.2}}{\geq} \quad & \sum_{l=1}^{d} \mathbb{I}_k \frac{\partial_l f(x_{k,0})}{\sqrt{v_{k,0}}} \left(\mathscr{M}_{l,k-1} - (F_{l,k-1})_{k-1} \right) - d\sqrt{\frac{2\rho_3^2}{\beta_2^n}} (1-\beta_1)\left(\beta_1 + \beta_1^n\right) n^3 \triangle_{n(k-1)} \\
\overset{\text{Lemma G.3}}{=} \quad & \sum_{l=1}^{d} \mathbb{I}_{k,k-1} \frac{\partial_l f(x_{k,0})}{\sqrt{v_{k,0}}} \left(\mathscr{M}_{l,k-1} - (F_{l,k-1})_{k-1} \right) + \sum_{l=1}^{d} \tilde{\mathbb{I}}_{k,k-1} \frac{\partial_l f(x_{k,0})}{\sqrt{v_{k,0}}} \left(\mathscr{M}_{l,k-1} - (F_{l,k-1})_{k-1} \right) \\
& -d\sqrt{\frac{2\rho_3^2}{\beta_2^n}} (1-\beta_1)\left(\beta_1 + \beta_1^n\right) n^3 \triangle_{n(k-1)} \\
\overset{\text{Lemma G.10}}{\geq} \quad & \sum_{l=1}^{d} \mathbb{I}_{k,k-1} \frac{\partial_l f(x_{k,0})}{\sqrt{v_{k,0}}} \left(\mathscr{M}_{l,k-1} - (F_{l,k-1})_{k-1} \right) - \sum_{l=1}^{d} \tilde{\mathbb{I}}_{k,k-1} \sqrt{\frac{2\rho_3^2}{\beta_2^n}} \left| \mathscr{M}_{l,k-1} - (F_{l,k-1})_{k-1} \right| \\
& -d\sqrt{\frac{2\rho_3^2}{\beta_2^n}} (1-\beta_1)\left(\beta_1 + \beta_1^n\right) n^3 \triangle_{n(k-1)} \\
\overset{\text{Def of } \tilde{\mathbb{I}}_{k,k-1}}{\geq} \quad & \sum_{l=1}^{d} \mathbb{I}_{k,k-1} \frac{\partial_l f(x_{k,0})}{\sqrt{v_{k,0}}} \left(\mathscr{M}_{l,k-1} - (F_{l,k-1})_{k-1} \right) - d\sqrt{\frac{2\rho_3^2}{\beta_2^n}} (1-\beta_1)(\beta_1 + \beta_1^n) n^2 \left(Q_k + Q_{k-1}\right) \\
& -d\sqrt{\frac{2\rho_3^2}{\beta_2^n}} (1-\beta_1)\left(\beta_1 + \beta_1^n\right) n^3 \triangle_{n(k-1)} \\
\overset{\text{Lemma G.2}}{\geq} \quad & \sum_{l=1}^{d} \mathbb{I}_{k,k-1} \frac{\partial_l f(x_{k-1,0})}{\sqrt{v_{k-1,0}}} \left(\mathscr{M}_{l,k-1} - (F_{l,k-1})_{k-1} \right) \\
& -\sum_{l=1}^{d} \left(\frac{1}{1 - \frac{1}{\sqrt{\beta_2^n}}} \frac{n^2 \triangle_{n(k-1)}}{\sqrt{v_{k-1,0}}} + \sqrt{\frac{2\rho_3^2}{\beta_2^n}} \frac{1}{\left(1 - \frac{(1-\beta_2)4n\rho_2}{\beta_2^n}\right)} \delta_1 \right) \left| \mathscr{M}_{l,k-1} - (F_{l,k-1})_{k-1} \right| \\
& -d\sqrt{\frac{2\rho_3^2}{\beta_2^n}} (1-\beta_1)(\beta_1 + \beta_1^n) n^2 \left(Q_k + Q_{k-1}\right) - d\sqrt{\frac{2\rho_3^2}{\beta_2^n}} (1-\beta_1)\left(\beta_1 + \beta_1^n\right) n^3 \triangle_{n(k-1)}
\end{aligned}
$$

To proceed, we derive an upper bound for $\left|\mathscr{M}_{l,k-1} - (F_{l,k-1})_{k-1}\right|$.

$$\begin{aligned}
\left|\mathscr{M}_{l,k-1} - (F_{l,k-1})_{k-1}\right| &\leq |\mathscr{M}_{l,k-1}| + \left|(F_{l,k-1})_{k-1}\right| \\
&\leq (1-\beta_1)\beta_1 n \sum_{i=0}^{n-1} |\partial_l f_i(x_{k-1,0})| + (1-\beta_1)\beta_1^n n \sum_{i=0}^{n-1} |\partial_l f_i(x_{k-1,0})|
\end{aligned}$$

Therefore, we have:

$$\begin{aligned}
(b) \quad \geq \quad & \sum_{l=1}^{d} \mathbb{I}_{k,k-1} \frac{\partial_l f(x_{k-1,0})}{\sqrt{v_{k-1,0}}} \left(\mathscr{M}_{l,k-1} - (F_{l,k-1})_{k-1}\right) \\
& - \sum_{l=1}^{d} \left(\frac{1}{1 - \frac{1}{\sqrt{\beta_2^n}}} \frac{n^2 \triangle_{n(k-1)}}{\sqrt{v_{k-1,0}}} + \sqrt{\frac{2\rho_3^2}{\beta_2^n}} \frac{1}{\left(1 - \frac{(1-\beta_2)4n\rho_2}{\beta_2^n}\right)} \delta_1 \right) (1-\beta_1)(\beta_1 + \beta_1^n) n \sum_{i=0}^{n-1} |\partial_l f_i(x_{k-1,0})| \\
& - d\sqrt{\frac{2\rho_3^2}{\beta_2^n}} (1-\beta_1)(\beta_1 + \beta_1^n) n^2 \left(Q_k + Q_{k-1}\right) - d\sqrt{\frac{2\rho_3^2}{\beta_2^n}} (1-\beta_1)\left(\beta_1 + \beta_1^n\right) n^3 \triangle_{n(k-1)}
\end{aligned}$$

$$\begin{aligned}
\overset{\text{Lemma G.10 and G.3}}{\geq} \quad & \sum_{l=1}^{d} \mathbb{I}_{k-1} \frac{\partial_l f(x_{k-1,0})}{\sqrt{v_{k-1,0}}} \left(\mathscr{M}_{l,k-1} - (F_{l,k-1})_{k-1}\right) \\
& - d \left(\frac{1}{1 - \frac{1}{\sqrt{\beta_2^n}}} \sqrt{\frac{2}{n\beta_2^n}} \right) (1-\beta_1)(\beta_1 + \beta_1^n) n^3 \triangle_{n(k-1)} \\
& - \sum_{l=1}^{d} \sqrt{\frac{2\rho_3^2}{\beta_2^n}} \frac{1}{\left(1 - \frac{(1-\beta_2)4n\rho_2}{\beta_2^n}\right)} \delta_1 (1-\beta_1)(\beta_1 + \beta_1^n) n \sum_{i=0}^{n-1} \left(|\partial_l f_i(x_{k-1,0})|\right) \\
& - d\sqrt{\frac{2\rho_3^2}{\beta_2^n}} (1-\beta_1)(\beta_1 + \beta_1^n) n^2 \left(Q_k + Q_{k-1}\right) - d\sqrt{\frac{2\rho_3^2}{\beta_2^n}} (1-\beta_1)\left(\beta_1 + \beta_1^n\right) n^3 \triangle_{n(k-1)}
\end{aligned}$$

The red term will be handled using color-ball method when taking conditional expectation $Ex_{k-1}(\cdot)$. Now we have derived lower bounds for both (a) and (b). Combining together, we have:

$$
\begin{aligned}
& \mathbb{E}_{k-1}\left\{\mathbb{E}_k\left[\sum_{l=1}^{d}\mathbb{I}_k\frac{\partial_l f(x_{k,0})}{\sqrt{v_{k,0}}}\left(\left(M'_{l,k}\right)_k-\left(F_{l,k}\right)_k\right)+\sum_{l=1}^{d}\mathbb{I}_k\frac{\partial_l f(x_{k,0})}{\sqrt{v_{k,0}}}\left(\left(M'_{l,k}\right)_{k-1}-\left(F_{l,k}\right)_{k-1}\right)\right]\right\} \\
\overset{(59)}{\geq}\ & \mathbb{E}_{k-1}\left\{\underbrace{\sum_{l=1}^{d}\mathbb{I}_k\frac{\partial_l f(x_{k,0})}{\sqrt{v_{k,0}}}(1-\beta_1)J_1\sum_{i=0}^{n-1}\partial_l f_i(x_{k,0})}_{(a)}+\underbrace{\sum_{l=1}^{d}\mathbb{I}_k\frac{\partial_l f(x_{k,0})}{\sqrt{v_{k,0}}}\left(\left(M'_{l,k}\right)_{k-1}-\left(F_{l,k}\right)_{k-1}\right)}_{(b)}\right\} \\
& -d\sqrt{\frac{2\rho_3^2}{\beta_2^n}}\frac{(1-\beta_1)n^2(n-1)\triangle_{nk}}{2} \\
\geq\ & \mathbb{E}_{k-1}\left\{\sum_{l=1}^{d}\mathbb{I}_{k-1}\frac{\partial_l f(x_{k-1,0})}{\sqrt{v_{k-1,0}}}(1-\beta_1)J_1\sum_{i=0}^{n-1}\partial_l f_i(x_{k-1,0})+\sum_{l=1}^{d}\mathbb{I}_{k-1}\frac{\partial_l f(x_{k-1,0})}{\sqrt{v_{k-1,0}}}\left(\mathscr{M}_{l,k-1}-\left(F_{l,k-1}\right)_{k-1}\right)\right\} \\
& -d(1-\beta_1)|J_1|\frac{1}{1-\frac{1}{\sqrt{\beta_2^n}}}n^2\triangle_{n(k-1)}\sqrt{\frac{2}{n\beta_2^n}} \\
& -\sum_{l=1}^{d}(1-\beta_1)|J_1|\left(\left|\sum_{i=0}^{n-1}\partial_l f_i(x_{k,0})\right|+n^2\triangle_{n(k-1)}\right)\left(\sqrt{\frac{2\rho_3^2}{\beta_2^n}}\frac{1}{\left(1-\frac{(1-\beta_2)4n\rho_2}{\beta_2^n}\right)}\delta_1\right) \\
& -2(1-\beta_1)d\sqrt{\frac{2\rho_3^2}{\beta_2^n}}|J_1|n^2\triangle_{n(k-1)}-(1-\beta_1)d\sqrt{\frac{2\rho_3^2}{\beta_2^n}}|J_1|n(Q_k+Q_{k-1}) \\
& -d\left(\frac{1}{1-\frac{1}{\sqrt{\beta_2^n}}}\sqrt{\frac{2}{n\beta_2^n}}\right)(1-\beta_1)(\beta_1+\beta_1^n)n^2\triangle_{n(k-1)} \\
& -\sum_{l=1}^{d}\sqrt{\frac{2\rho_3^2}{\beta_2^n}}\frac{1}{\left(1-\frac{(1-\beta_2)4n\rho_2}{\beta_2^n}\right)}\delta_1(1-\beta_1)(\beta_1+\beta_1^n)n\left(\sum_{i=0}^{n-1}|\partial_l f_i(x_{k,0})|+n^3\triangle_{n(k-1)}\right) \\
& -d\sqrt{\frac{2\rho_3^2}{\beta_2^n}}(1-\beta_1)(\beta_1+\beta_1^n)n^2\left(Q_k+Q_{k-1}\right)-d\sqrt{\frac{2\rho_3^2}{\beta_2^n}}(1-\beta_1)\left(\beta_1+\beta_1^n\right)n^3\triangle_{n(k-1)} \\
& -d\sqrt{\frac{2\rho_3^2}{\beta_2^n}}\frac{(1-\beta_1)n^2(n-1)\triangle_{nk}}{2}
\end{aligned}
$$

For the first term in the above inequality, we can calculate it using the idea in the color-ball toy example:

$$
\begin{aligned}
& \mathbb{E}_{k-1}\left\{\sum_{l=1}^{d}\mathbb{I}_{k-1}\frac{\partial_l f(x_{k-1,0})}{\sqrt{v_{k-1,0}}}(1-\beta_1)J_1\sum_{i=0}^{n-1}\partial_l f_i(x_{k-1,0})+\sum_{l=1}^{d}\mathbb{I}_{k-1}\frac{\partial_l f(x_{k-1,0})}{\sqrt{v_{k-1,0}}}\left(\mathscr{M}_{l,k-1}-\left(F_{l,k-1}\right)_{k-1}\right)\right\} \\
= \quad & \sum_{l=1}^{d}\mathbb{I}_{k-1}\frac{\partial_l f(x_{k-1,0})}{\sqrt{v_{k-1,0}}}(1-\beta_1)\beta_1^n J_1\sum_{i=0}^{n-1}\partial_l f_i(x_{k-1,0}).
\end{aligned}
$$

To proceed, we further take $\mathbb{E}_{k-2}(\cdot)$ and bound

$$
\mathbb{E}_{k-2}\left\{\underbrace{\sum_{l=1}^{d}\mathbb{I}_{k-1}\frac{\partial_l f(x_{k-1,0})}{\sqrt{v_{k-1,0}}}(1-\beta_1)\beta_1^n J_1\sum_{i=0}^{n-1}\partial_l f_i(x_{k-1,0})}_{(a)}+\underbrace{\sum_{l=1}^{d}\mathbb{I}_k\frac{\partial_l f(x_{k,0})}{\sqrt{v_{k,0}}}\left(\left(M'_{l,k}\right)_{k-2}-\left(F_{l,k}\right)_{k-2}\right)}_{(b)}\right\}.
$$

Repeat this process until $k=1$, we have:

$$
\begin{aligned}
& \mathbb{E}\left[\sum_{l \text{ large}} \frac{\partial_l f(x_{k,0})}{\sqrt{v_{k,0}}}\left(\left(M'_{l,k}\right)_k - \left(F_{l,k}\right)_k + \cdots + \left(M'_{l,k}\right)_1 - \left(F_{l,k}\right)_1\right)\right] \\
\geq \quad & (1-\beta_1)\beta_1^{kn} J_1 \mathbb{E}\left[\sum_{l=1}^{d} \mathbb{I}_1 \frac{\partial_l f(x_{1,0})}{\sqrt{v_{1,0}}} \sum_{i=0}^{n-1} \partial_l f_i(x_{1,0})\right] \\
& + \text{Error}_1 + \text{Error}_2 + \text{Error}_3 \\
\overset{(*)}{\geq} \quad & -\frac{\beta_1^n}{\sqrt{k-1}}(1-\beta_1)\left|J_1 \mathbb{E}\left[\sum_{l=1}^{d} \mathbb{I}_1 \frac{\partial_l f(x_{1,0})}{\sqrt{v_{1,0}}} \sum_{i=0}^{n-1} \partial_l f_i(x_{1,0})\right]\right| \\
& + \text{Error}_1 + \text{Error}_2 + \text{Error}_3
\end{aligned}
$$

where $(*)$ holds for large k such that $\beta^{(k-1)n} \leq \frac{\beta_1^n}{\sqrt{k-1}}$. We specify $\text{Error}_1, \text{Error}_2, \text{Error}_3$ as follows.

$$
\begin{aligned}
\text{Error}_1 \quad = \quad & -d(1-\beta_1)|J_1| \frac{1}{1-\frac{1}{\sqrt{\beta_2^n}}} n^2 \sqrt{\frac{2}{n\beta_2^n}} \left(\sum_{j=0}^{\infty} \beta_1^{jn} \triangle_{n(k-j)}\right) \\
& -\sum_{l=1}^{d}(1-\beta_1)|J_1| \left(\left|\sum_{i=0}^{n-1} \partial_l f_i(x_{k,0})\right|\right) \left(\sqrt{\frac{2\rho_3^2}{\beta_2^n}} \frac{1}{\left(1-\frac{(1-\beta_2)4n\rho_2}{\beta_2^n}\right)} \delta_1\right) \left(\sum_{j=0}^{\infty} \beta_1^{jn}(j+1)\right) \\
& -d(1-\beta_1)\triangle_{n(k-1)}|J_1| n^2 \left(\sqrt{\frac{2\rho_3^2}{\beta_2^n}} \frac{1}{\left(1-\frac{(1-\beta_2)4n\rho_2}{\beta_2^n}\right)} \delta_1\right) \left(\sum_{j=0}^{\infty} \beta_1^{jn}(j+1)^2\right) \\
& -2(1-\beta_1)d\sqrt{\frac{2\rho_3^2}{\beta_2^n}}|J_1| n^2 \left(\sum_{j=0}^{\infty} \beta_1^{jn} \triangle_{n(k-1-j)}\right) \\
& -(1-\beta_1)d\sqrt{\frac{2\rho_3^2}{\beta_2^n}}|J_1| n \left[Q_k + Q_{k-1} + \beta_1^n(Q_k + Q_{k-1} + Q_{k-2}) + \cdots\right]
\end{aligned}
$$

Since $\delta_2 = \lim_{k\to\infty} \sum_{j=1}^{k-1} (\beta_1^n)^j \sqrt{\frac{k}{k-j}}$ is a finite constant, we have $\sum_{j=0}^{\infty} \beta_1^{jn} \triangle_{n(k-j)} = \frac{\triangle_1 \delta_2}{\sqrt{nk}}$. In addition, we have

$$
\begin{aligned}
& \left[Q_k + Q_{k-1} + \beta_1^n(Q_k + Q_{k-1} + Q_{k-2}) + \cdots\right] \\
\overset{(*)}{\leq} \quad & Q_k(1 + \beta_1^n + \cdots) \\
& + Q_{k-1} + \beta_1^n(Q_{k-1} + Q_{k-2}) + \beta_1^{2n}(Q_{k-1} + Q_{k-2} + Q_{k-3}) + \cdots \\
\overset{(*)}{\leq} \quad & Q_k(1 + \beta_1^n + \cdots) + 2Q_{k-1} + 2\left(\beta_1^n 2Q_{k-1} + \beta_1^{2n} 3Q_{k-1} + \cdots\right) \\
\overset{\text{Lemma F.1}}{\leq} \quad & Q_k \frac{1}{(1-\beta_1^n)} + 2Q_{k-1} \frac{1}{(1-\beta_1^n)^2} \\
\leq \quad & 5Q_k \frac{1}{(1-\beta_1^n)^2}
\end{aligned}
$$

where $(*)$ uses the following fact: consider integers $k > J > 0$, we have $\sum_{j=1}^{J} \frac{1}{\sqrt{k-j}} \leq 2\frac{J}{\sqrt{k-1}}$. This inequality can be simply proved by taking the integral over $\frac{1}{\sqrt{k}}$. The final inequality is due to $Q_{k-1} < 2Q_k$. Now, we have

$$
\begin{aligned}
\text{Error}_1 \quad \geq \quad & -d(1-\beta_1)|J_1|\frac{1}{1-\frac{1}{\sqrt{\beta_2^n}}}n^2\sqrt{\frac{2}{n\beta_2^n}}\frac{\triangle_1\delta_2}{\sqrt{nk}} \\
& -\sum_{l=1}^{d}(1-\beta_1)|J_1|\left(\left|\sum_{i=0}^{n-1}\partial_l f_i(x_{k,0})\right|\right)\left(\sqrt{\frac{2\rho_3^2}{\beta_2^n}}\frac{1}{\left(1-\frac{(1-\beta_2)4n\rho_2}{\beta_2^n}\right)}\delta_1\right)\frac{1}{(1-\beta_1^n)^2} \\
& -2d(1-\beta_1)|J_1|n^2\left(\sqrt{\frac{2\rho_3^2}{\beta_2^n}}\frac{1}{\left(1-\frac{(1-\beta_2)4n\rho_2}{\beta_2^n}\right)}\delta_1\right)\frac{1+\beta_1^n}{(1-\beta_1^n)^3}\frac{\triangle_1}{\sqrt{n(k-1)}} \\
& -(1-\beta_1)d\sqrt{\frac{2\rho_3^2}{\beta_2^n}}|J_1|n^2\frac{\triangle_1\delta_2}{\sqrt{n(k-1)}}-(1-\beta_1)d\sqrt{\frac{2\rho_3^2}{\beta_2^n}}|J_1|n5Q_k\frac{1}{(1-\beta_1^n)^2}
\end{aligned}
$$

$$
\begin{aligned}
\text{Error}_2 \quad = \quad & -d\left(\frac{1}{1-\frac{1}{\sqrt{\beta_2^n}}}\sqrt{\frac{2}{n\beta_2^n}}\right)(1-\beta_1)(\beta_1+\beta_1^n)n^3\left(\sum_{j=0}^{\infty}\beta_1^{jn}\triangle_{n(k-1-j)}\right) \\
& -\sum_{l=1}^{d}\sqrt{\frac{2\rho_3^2}{\beta_2^n}}\frac{1}{\left(1-\frac{(1-\beta_2)4n\rho_2}{\beta_2^n}\right)}\delta_1(1-\beta_1)(\beta_1+\beta_1^n)n\left(\sum_{i=0}^{n-1}|\partial_l f_i(x_{k,0})|\right)\left(\sum_{j=0}^{\infty}(j+1)\beta_1^{nj}\right) \\
& -d\sqrt{\frac{2\rho_3^2}{\beta_2^n}}\frac{1}{\left(1-\frac{(1-\beta_2)4n\rho_2}{\beta_2^n}\right)}\delta_1(1-\beta_1)(\beta_1+\beta_1^n)n^3\triangle_{n(k-1)}\left(\sum_{j=0}^{\infty}(j+1)^2\beta_1^{nj}\right) \\
& -d\sqrt{\frac{2\rho_3^2}{\beta_2^n}}(1-\beta_1)(\beta_1+\beta_1^n)n^2\left((Q_k+Q_{k-1})+\beta_1^n(Q_k+Q_{k-1}+Q_{k-2})+\cdots\right) \\
& -d\sqrt{\frac{2\rho_3^2}{\beta_2^n}}(1-\beta_1)\left(\beta_1+\beta_1^n\right)n^3\left(\sum_{j=0}^{\infty}\beta_1^{jn}\triangle_{n(k-1-j)}\right)
\end{aligned}
$$

Based on the calculation in Lemma F.1, we have

$$
\begin{aligned}
\text{Error}_2 \quad \geq \quad & -d\left(\frac{1}{1-\frac{1}{\sqrt{\beta_2^n}}}\sqrt{\frac{2}{n\beta_2^n}}\right)(1-\beta_1)(\beta_1+\beta_1^n)n^3\frac{\triangle_1}{\sqrt{n}}\frac{\delta_2}{\sqrt{k}} \\
& -\sum_{l=1}^{d}\sqrt{\frac{2\rho_3^2}{\beta_2^n}}\frac{1}{\left(1-\frac{(1-\beta_2)4n\rho_2}{\beta_2^n}\right)}\delta_1(1-\beta_1)(\beta_1+\beta_1^n)n\left(\sum_{i=0}^{n-1}|\partial_l f_i(x_{k,0})|\right)\frac{1}{(1-\beta_1^n)^2} \\
& -d\sqrt{\frac{2\rho_3^2}{\beta_2^n}}\frac{1}{\left(1-\frac{(1-\beta_2)4n\rho_2}{\beta_2^n}\right)}\delta_1(1-\beta_1)(\beta_1+\beta_1^n)n^3\frac{1+\beta_1^n}{(1-\beta_1^n)^3}\frac{\triangle_1\delta_2}{\sqrt{n(k-1)}} \\
& -d\sqrt{\frac{2\rho_3^2}{\beta_2^n}}(1-\beta_1)(\beta_1+\beta_1^n)n^2 2Q_k\frac{1}{\beta_1^n(1-\beta_1^n)^2} \\
& -d\sqrt{\frac{2\rho_3^2}{\beta_2^n}}(1-\beta_1)\left(\beta_1+\beta_1^n\right)n^3\frac{\triangle_1}{\sqrt{n}}\frac{\delta_2}{\sqrt{k}}.
\end{aligned}
$$

$$
\text{Error}_3 = -d\sqrt{\frac{2\rho_3^2}{\beta_2^n}}(1-\beta_1)n^3\left(\sum_{j=0}^{\infty}\beta_1^{jn}\triangle_{n(k-j)}\right) = -\frac{d\sqrt{\frac{2\rho_3^2}{\beta_2^n}}(1-\beta_1)n^3}{\sqrt{k}}\frac{\triangle_1}{\sqrt{n}}\delta_2,
$$

Since $\frac{1-\beta_1}{1-\beta_1^n} \leq 1$ and $|J_1| \leq n$, we have

$$
\begin{aligned}
& |J_1| \left(\sqrt{\frac{2\rho_3^2}{\beta_2^n}} \frac{1}{\left(1 - \frac{(1-\beta_2)4n\rho_2}{\beta_2^n}\right)} \right) \frac{1-\beta_1}{(1-\beta_1^n)^2} + \sqrt{\frac{2\rho_3^2}{\beta_2^n}} \frac{1}{\left(1 - \frac{(1-\beta_2)4n\rho_2}{\beta_2^n}\right)} \frac{2n(1-\beta_1)}{(1-\beta_1^n)^2} \\
\leq \quad & \left(\sqrt{\frac{2\rho_3^2}{\beta_2^n}} \frac{3n}{\left(1 - \frac{1-\beta_2}{2}\left(-1 + \frac{4\rho_2 n}{\beta_2^n}\right)\right)} \right) \frac{1}{(1-\beta_1^n)}.
\end{aligned}
$$

Using the fact that $\frac{1}{\sqrt{k-1}} \leq \frac{\sqrt{2}}{\sqrt{k}}$ (for $k \geq 2$), we have:

$$
\begin{aligned}
& \mathbb{E}\left[\sum_{l \text{ large}} \frac{\partial_l f(x_{k,0})}{\sqrt{v_{k,0}}} \left(\left(M'_{l,k}\right)_k - \left(F_{l,k}\right)_k + \cdots + \left(M'_{l,k}\right)_1 - \left(F_{l,k}\right)_1 \right) \right] \\
\geq \quad & -\frac{\beta_1^n}{\sqrt{k-1}}(1-\beta_1) \left| J_1 \mathbb{E}\left[\sum_{l=1}^{d} \mathbb{I}_1 \frac{\partial_l f(x_{1,0})}{\sqrt{v_{1,0}}} \sum_{i=0}^{n-1} \partial_l f_i(x_{1,0}) \right] \right| \\
& + \text{Error}_1 + \text{Error}_2 + \text{Error}_3 \\
\geq \quad & -\frac{G_6}{\sqrt{k}} - G_7 \delta_1 \mathbb{E}\left(\sum_{l=1}^{d} \sum_{i=0}^{n-1} |\partial_l f_i(x_{k,0})| \right),
\end{aligned}
$$

where

$$
\begin{aligned}
G_6 \quad := \quad & \beta_1^n (1-\beta_1)\sqrt{2}\,|J_1| \sqrt{\frac{2\rho_3^2}{\beta_2^n}} \mathbb{E}\left[\sum_{l=1}^{d} \left| \mathbb{I}_1 \sum_{i=0}^{n-1} \partial_l f_i(x_{1,0}) \right| \right] + \frac{\triangle_1}{\sqrt{n}} \delta_2 d \sqrt{\frac{2\rho_3^2}{\beta_2^n}} (1-\beta_1) n^3 \\
& + d(1-\beta_1)|J_1| \frac{1}{1 - \frac{1}{\sqrt{\beta_2^n}}} n^2 \sqrt{\frac{2}{n\beta_2^n}} \frac{\triangle_1 \delta_2}{\sqrt{n}} \\
& + d(1-\beta_1)|J_1| n^2 \left(\sqrt{\frac{2\rho_3^2}{\beta_2^n}} \frac{1}{\left(1 - \frac{(1-\beta_2)4n\rho_2}{\beta_2^n}\right)} \delta_1 \right) \frac{1+\beta_1^n}{(1-\beta_1^n)^3} \frac{\triangle_1 \sqrt{2}}{\sqrt{n}} \\
& + 2(1-\beta_1) d \sqrt{\frac{2\rho_3^2}{\beta_2^n}} |J_1| n^2 \frac{\triangle_1 \delta_2 \sqrt{2}}{\sqrt{n}} - 5(1-\beta_1) d \sqrt{\frac{2\rho_3^2}{\beta_2^n}} |J_1| n \frac{1}{(1-\beta_1^n)^2} \Delta_1 n \sqrt{n} \frac{32\sqrt{2}}{(1-\beta_2)^n \beta_2^n} \\
& + d \left(\frac{1}{1 - \frac{1}{\sqrt{\beta_2^n}}} \sqrt{\frac{2}{n\beta_2^n}} \right) (1-\beta_1)(\beta_1 + \beta_1^n) n^3 \frac{\triangle_1}{\sqrt{n}} \delta_2 \\
& + d \sqrt{\frac{2\rho_3^2}{\beta_2^n}} \frac{1}{\left(1 - \frac{(1-\beta_2)4n\rho_2}{\beta_2^n}\right)} \delta_1 (1-\beta_1)(\beta_1 + \beta_1^n) n^3 \frac{1+\beta_1^n}{(1-\beta_1^n)^3} \frac{\triangle_1 \delta_2 \sqrt{2}}{\sqrt{n}} \\
& + 2d \sqrt{\frac{2\rho_3^2}{\beta_2^n}} (1-\beta_1)(\beta_1 + \beta_1^n) n^2 \frac{1}{\beta_1^n (1-\beta_1^n)^2} \Delta_1 n \sqrt{n} \frac{32\sqrt{2}}{(1-\beta_2)^n \beta_2^n} \\
& + d \sqrt{\frac{2\rho_3^2}{\beta_2^n}} (1-\beta_1)\left(\beta_1 + \beta_1^n\right) n^3 \frac{\triangle_1}{\sqrt{n}} \delta_2,
\end{aligned}
$$

$$
G_7 \quad := \quad \left(\sqrt{\frac{2\rho_3^2}{\beta_2^n}} \frac{3n}{\left(1 - \frac{1-\beta_2}{2}\left(-1 + \frac{4\rho_2 n}{\beta_2^n}\right)\right)} \right) \frac{1}{(1-\beta_1^n)}
$$

where $J_1 = \left(-\frac{1}{n}\beta_1 - \frac{2}{n}\beta_1^2 - \cdots - \frac{n-1}{n}\beta_1^{n-1}\right)$, $\delta_2 = \lim_{k\to\infty}\sum_{j=1}^{k-1}(\beta_1^n)^j\sqrt{\frac{k}{k-j}}$ (if needed, we can further bound J_1 by n for simplicity). This conclude the proof.

G.8 Proof of Lemma G.5

We now derive upper bounds for $\sum_{l \text{ large}}(a_2)$ and $\sum_{l \text{ large}}(b_2)$. The upper bound for $\sum_{l \text{ large}}(a_2)$ is very straightforward using inequality (24).

$$\sum_{l \text{ large}}(a_2) = \delta_1\sqrt{\frac{2\rho_3^2}{\beta_2^n}}\sum_{l \text{ large}}\sum_{i=0}^{n-1}|\partial_l f_i(x_{k,0})| \overset{(24)}{\leq} \delta_1\sqrt{\frac{2\rho_3^2}{\beta_2^n}}\sqrt{D_1}\rho_1 d\left(|\partial_\alpha f(x_{k,0})| + \sqrt{\frac{D_0}{D_1 d}}\right).$$

Now we shift gear to $\sum_{l \text{ large}}(b_2) := \delta_1\sqrt{\frac{2\rho_3^2}{\beta_2^n}}\sum_{l \text{ large}}\sum_{i=0}^{n-1}|m_{l,k,i} - \partial_l f_i(x_{k,0})|$. To proceed, we need an upper bound for $\sum_{l \text{ large}}\sum_{i=0}^{n-1}|m_{l,k,i} - \partial_l f_i(x_{k,0})|$. For each i, we perform the following decomposition.

$$\begin{aligned}\sum_{l \text{ large}}|m_{l,k,i} - \partial_l f_i(x_{k,0})| \quad \leq \quad & \underbrace{\sum_{l=1}^{d}|(1-\beta_1)\left[\beta_1^i\partial_l f_{\tau_{k,0}}(x_{k,0}) + \cdots + \partial_l f_{\tau_{k,i}}(x_{k,i})\right] - \partial_l f_i(x_{k,0})|}_{(d_1)} \\ & + \underbrace{\sum_{l=1}^{d}\left|\beta_1^{i+1}m_{l,k-1,n-1}\right|}_{(d_2)}. \end{aligned} \tag{60}$$

To start, we bound (d_1).

$$\begin{aligned}(d_1) \quad &\leq \quad \sum_{l=1}^{d}\left\{|\partial_l f_{\tau_{k,0}}(x_{k,0})| + |\partial_l f_{\tau_{k,1}}(x_{k,1})| + \cdots + |\partial_l f_{\tau_{k,i}}(x_{k,i})| + |\partial_l f_i(x_{k,0})|\right\} \\ &\leq \quad \sum_{l=1}^{d}\left\{|\partial_l f_{\tau_{k,0}}(x_{k,0})| + |\partial_l f_{\tau_{k,1}}(x_{k,1})| + \cdots + |\partial_l f_{\tau_{k,n-1}}(x_{k,n-1})| + |\partial_l f_i(x_{k,0})|\right\} \\ &\leq \quad \sum_{l=1}^{d}\sum_{i=0}^{n-1}\left\{\ |\partial_l f_i(x_{k,0})|\ \right\} + \sum_{l=1}^{d}|\partial_l f_i(x_{k,0})| + d\triangle_{nk} + \cdots + nd\triangle_{nk} \\ &\overset{(24)}{\leq} \quad 2\sqrt{D_1}\rho_1 d\left(|\partial_\alpha f(x_{k,0})| + \sqrt{\frac{D_0}{D_1 d}}\right) + \frac{n(n+1)d}{2}\triangle_{nk} \\ &= \quad 2\sqrt{D_1}\rho_1 d\left(|\partial_\alpha f(x_{k,0})| + \sqrt{\frac{D_0}{D_1 d}}\right) + \frac{(n+1)\sqrt{n}d}{2\sqrt{k}}\triangle_1. \end{aligned} \tag{61}$$

Now, we bound (d_2). Recall $\sum_{i=0}^{n-1}\partial_l f_i(x_{1,0}) = \partial_l f(x_{1,0})$, we have

$$\begin{aligned}|m_{l,k-1,n-1}| \quad \leq \quad & (1-\beta_1)\left[|\partial_l f_{\tau_{k-1,n-1}}(x_{k-1,n-1})| + \beta_1|\partial_l f_{\tau_{k-1,n-2}}(x_{k-1,n-2})| + \cdots\right] \\ & + \beta_1^{(k-1)n}\sum_{i=0}^{n-1}|\partial_l f_i(x_{1,0})| \end{aligned} \tag{62}$$

Note that for any $i \in [0, n-1]$, $j \in [0, n-1]$, $t \in [1, k-1]$, we have the following result.

$$
\begin{aligned}
|\partial_l f_i(x_{k-t,j})| &\leq |\partial_l f_i(x_{k,0})| + |\partial_l f_i(x_{k,0}) - \partial_l f_i(x_{k-t,j})| \\
&\overset{\text{Lemma } F.2}{\leq} |\partial_l f_i(x_{k,0})| + (n-j)\triangle_{(k-t)n} + n\triangle_{(k-t+1)n} + \cdots + n\triangle_{(k-1)n} \\
&\leq |\partial_l f_i(x_{k,0})| + \triangle_{(k-1)n} + \triangle_{(k-1)n-1} + \cdots + \triangle_{(k-1)n-[(n-j)+(t-1)n-1]} \\
&\leq |\partial_l f_i(x_{k,0})| + \triangle_{(k-1)n-1} + \triangle_{(k-1)n-2} + \cdots + \triangle_{(k-1)n-[(n-j)+(t-1)n]} \\
&\overset{(*)}{\leq} |\partial_l f_i(x_{k,0})| + \frac{2[(n-j)+(t-1)n]\triangle_1}{\sqrt{n(k-1)-1}}, \qquad (63)
\end{aligned}
$$

where $(*)$ uses the following fact: consider integers $k > J > 0$, we have $\sum_{j=1}^{J} \frac{1}{\sqrt{k-j}} \leq 2\frac{J}{\sqrt{k-1}}$.

Plugging (63) into (62) and re-arranging the index, we have

$$
\begin{aligned}
\sum_{l=1}^{d} |m_{l,k-1,n-1}| &\overset{(62)}{\leq} (1-\beta_1)\sum_{l=1}^{d}\left[|\partial_l f_{\tau_{k-1,n-1}}(x_{k-1,n-1})| + \beta_1|\partial_l f_{\tau_{k-1,n-2}}(x_{k-1,n-2})| + \cdots\right] \\
&\quad + \beta_1^{(k-1)n}\sum_{l=1}^{d}\sum_{i=0}^{n-1}|\partial_l f_i(x_{1,0})| \\
&\overset{(24),(63)}{\leq} (1-\beta_1)\sum_{q=1}^{(k-1)n}\beta_1^{q-1}\left[\sqrt{D_1}\rho_1 d\left(|\partial_\alpha f(x_{k,0})| + \sqrt{\frac{D_0}{D_1 d}}\right) + \frac{2qd\triangle_1}{\sqrt{n(k-1)-1}}\right] \\
&\quad + \beta_1^{(k-1)n}\sum_{l=1}^{d}\sum_{i=0}^{n-1}|\partial_l f_i(x_{1,0})| \\
&\leq (1-\beta_1)\sum_{q=1}^{\infty}\beta_1^{q-1}\left[\sqrt{D_1}\rho_1 d\left(|\partial_\alpha f(x_{k,0})| + \sqrt{\frac{D_0}{D_1 d}}\right) + \frac{2qd\triangle_1}{\sqrt{n(k-1)-1}}\right] \\
&\quad + \beta_1^{(k-1)n}\sum_{l=1}^{d}\sum_{i=0}^{n-1}|\partial_l f_i(x_{1,0})| \\
&\overset{\text{Lemma } F.1}{\leq} \sqrt{D_1}\rho_1 d\left(|\partial_\alpha f(x_{k,0})| + \sqrt{\frac{D_0}{D_1 d}}\right) + \frac{1}{1-\beta_1}\frac{2d\triangle_1}{\sqrt{n(k-1)-1}} \\
&\quad + \beta_1^{(k-1)n}\sum_{l=1}^{d}\sum_{i=0}^{n-1}|\partial_l f_i(x_{1,0})| \\
&\overset{\text{When } k\geq 4}{\leq} \sqrt{D_1}\rho_1 d\left(|\partial_\alpha f(x_{k,0})| + \sqrt{\frac{D_0}{D_1 d}}\right) + \frac{1}{1-\beta_1}\frac{2\sqrt{2}d\triangle_1}{\sqrt{nk}} \\
&\quad + \beta_1^{(k-1)n}\sum_{l=1}^{d}\sum_{i=0}^{n-1}|\partial_l f_i(x_{1,0})| \\
&\overset{(i)}{\leq} \sqrt{D_1}\rho_1 d\left(|\partial_\alpha f(x_{k,0})| + \sqrt{\frac{D_0}{D_1 d}}\right) + \frac{1}{1-\beta_1}\frac{2\sqrt{2}d\triangle_1}{\sqrt{nk}} \\
&\quad + \frac{\sqrt{2}\beta_1^n}{\sqrt{k}}\sum_{l=1}^{d}\sum_{i=0}^{n-1}|\partial_l f_i(x_{1,0})| \qquad (64)
\end{aligned}
$$

where the second last inequality holds because: when $k \geq 4$, $\frac{1}{\sqrt{n(k-1)-1}} \leq \frac{\sqrt{2}}{\sqrt{nk}}$. (i) holds when k is large enough such that $\beta_1^{(k-1)n} \leq \frac{\beta_1^n}{\sqrt{k-1}}$. Further, $\frac{\beta_1^n}{\sqrt{k-1}} \leq \frac{\sqrt{2}\beta_1^n}{\sqrt{k}}$ when $k \geq 2$.

Now, we have derived upper bounds for (d_1) and (d_2). Plugging (64) and (61) into (60), we conclude the proof.

$$
\begin{aligned}
\sum_{l=1}^{d}\sum_{i=0}^{n-1}\left|m_{l,k,i}-\partial_l f_{\tau_{k,i}}(x_{k,0})\right| &\overset{(61),(64)}{\leq} 3n\sqrt{D_1}\rho_1 d\left(\left|\partial_\alpha f\left(x_{k,0}\right)\right|+\sqrt{\frac{D_0}{D_1 d}}\right)+\frac{(n+1)nd\sqrt{n}}{2\sqrt{k}}\Delta_1 \\
&\quad +\frac{nd}{1-\beta_1}\frac{2\sqrt{2}\triangle_1}{\sqrt{nk}}+\frac{\sqrt{2}n\beta_1^n}{\sqrt{k}}\sum_{l=1}^{d}\sum_{i=0}^{n-1}\left|\partial_l f_i(x_{1,0})\right| \\
&= \frac{1}{\sqrt{k}}\left[\frac{d(n+1)n^{\frac{3}{2}}}{2}\Delta_1+\frac{d2\sqrt{2}\sqrt{n}\triangle_1}{1-\beta_1}+\sqrt{2}n\beta_1^n\sum_{i=0}^{n-1}\|\nabla f_i(x_{1,0})\|_1\right] \\
&\quad +3n\sqrt{D_1}\rho_1 d\left(\left|\partial_\alpha f\left(x_{k,0}\right)\right|+\sqrt{\frac{D_0}{D_1 d}}\right). \qquad (65)
\end{aligned}
$$

$$
\begin{aligned}
\sum_{l \text{ large}}(b_2) &= \delta_1\sqrt{\frac{2\rho_3^2}{\beta_2^n}}\sum_{l \text{ large}}\sum_{i=0}^{n-1}\left|m_{l,k,i}-\partial_l f_i(x_{k,0})\right| \\
&\leq \delta_1\sqrt{\frac{2\rho_3^2}{\beta_2^n}}\left\{\frac{1}{\sqrt{k}}\left[\frac{d(n+1)n^{\frac{3}{2}}}{2}\Delta_1+\frac{d2\sqrt{2}\sqrt{n}\triangle_1}{1-\beta_1}+\sqrt{2}n\beta_1^n\sum_{i=0}^{n-1}\|\nabla f_i(x_{1,0})\|_1\right]\right. \\
&\quad \left.+3n\sqrt{D_1}\rho_1 d\left(\left|\partial_\alpha f\left(x_{k,0}\right)\right|+\sqrt{\frac{D_0}{D_1 d}}\right)\right\}.
\end{aligned}
$$

The proof is concluded by adding expectation on both sides of the inequality.

G.9 Proof of Lemma G.6

$$
\begin{aligned}
&\mathbb{E}\left\{\sum_{l \text{ large}}(a_1)+\sum_{l \text{ large}}(b_1)-\sum_{l \text{ large}}\{(a_2)+(b_2)\}\right\} \\
= &\mathbb{E}\left[\sum_{l \text{ large}}\frac{\partial_l f\left(x_{k,0}\right)^2}{\sqrt{v_{l,k,0}}}\right]+\mathbb{E}\left[\sum_{l \text{ large}}\frac{\partial_l f(x_{k,0})}{\sqrt{v_{l,k,0}}}\sum_{i=0}^{n-1}\left(m_{l,k,i}-\partial_l f_i(x_{k,0})\right)\right] \\
&-d\delta_1\sqrt{\frac{2\rho_3^2}{\beta_2^n}}\mathbb{E}\left[\sum_{i=0}^{n-1}\left|\partial_l f_i\left(x_{k,0}\right)\right|\right]-d\delta_1\sqrt{\frac{2\rho_3^2}{\beta_2^n}}\mathbb{E}\left[\sum_{i=0}^{n-1}\left|m_{l,k,i}-\partial_l f_i(x_{k,0})\right|\right] \\
\overset{\text{Lemma G.4 and G.5 and F.3}}{\geq} &\mathbb{E}\left[\sum_{l \text{ large}}\frac{\partial_l f\left(x_{k,0}\right)^2}{\sqrt{v_{l,k,0}}}\right]-\frac{1}{\sqrt{k}}\left(G_4+G_5+G_6\right)-G_7\delta_1\sqrt{D_1}\rho_1 d\left(\mathbb{E}\left|\partial_\alpha f\left(x_{k,0}\right)\right|+\sqrt{\frac{D_0}{D_1 d}}\right) \\
&-\delta_1\sqrt{\frac{2\rho_3^2}{\beta_2^n}}\sqrt{D_1}\rho_1 d\left(\mathbb{E}\left|\partial_\alpha f\left(x_{k,0}\right)\right|+\sqrt{\frac{D_0}{D_1 d}}\right) \\
&-\delta_1\sqrt{\frac{2\rho_3^2}{\beta_2^n}}\left[\frac{d(n+1)n^{\frac{3}{2}}}{2}\Delta_1+\frac{d2\sqrt{2}\sqrt{n}\triangle_1}{1-\beta_1}+\sqrt{2}n\beta_1^n\sum_{i=0}^{n-1}\mathbb{E}\|\nabla f_i(x_{1,0})\|_1\right]\frac{1}{\sqrt{k}} \\
&-\delta_1\sqrt{\frac{2\rho_3^2}{\beta_2^n}}3n\sqrt{D_1}\rho_1 d\left(\mathbb{E}\left|\partial_\alpha f\left(x_{k,0}\right)\right|+\sqrt{\frac{D_0}{D_1 d}}\right),
\end{aligned}
$$

where constant terms G_4, G_5, G_6, G_7 can be seen at the end of Appendix G.7.

Since $\alpha=\arg\max_{l=1,2,\cdots,d}\left|\partial_l f\left(x_{k,0}\right)\right|$ and $\sum_{l \text{ large}}\frac{\partial_l f(x_{k,0})^2}{\sqrt{v_{l,k,0}}}\geq\frac{\partial_\alpha f(x_{k,0})^2}{\sqrt{v_{\alpha,k,0}}}$, we have

$$
\begin{aligned}
& \mathbb{E}\left\{\sum_{l \text{ large}}(a_1)+\sum_{l \text{ large}}(b_1)-\sum_{l \text{ large}}\{(a_2)+(b_2)\}\right\} \\
\geq\ & \mathbb{E}\left\{\frac{\partial_\alpha f\left(x_{k,0}\right)^2}{\sqrt{v_{\alpha,k,0}}}\right\} \\
& -\left[G_4+G_5+G_6+\delta_1\sqrt{\frac{2\rho_3^2}{\beta_2^n}}\left(\frac{d(n+1)n^{\frac{3}{2}}}{2}\Delta_1+\frac{d2\sqrt{2}\sqrt{n}\triangle_1}{1-\beta_1}+\sqrt{2}n\beta_1^n\sum_{i=0}^{n-1}\mathbb{E}\|\nabla f_i(x_{1,0})\|_1\right)\right]\frac{1}{\sqrt{k}} \\
& -\delta_1\left(\sqrt{\frac{2\rho_3^2}{\beta_2^n}}4n+G_7\right)\sqrt{D_1}\rho_1 d\left(\mathbb{E}\left|\partial_\alpha f\left(x_{k,0}\right)\right|+\sqrt{\frac{D_0}{D_1 d}}\right) \\
=\ & \mathbb{E}\left\{\frac{\partial_\alpha f\left(x_{k,0}\right)^2}{\sqrt{v_{\alpha,k,0}}}\right\}-F_2\frac{1}{\sqrt{k}}-F_3\mathbb{E}\left|\partial_\alpha f\left(x_{k,0}\right)\right|-F_4, \qquad (66)
\end{aligned}
$$

where $F_2 := \delta_1\sqrt{\frac{2\rho_3^2}{\beta_2^n}}\left[\frac{d(n+1)n^{\frac{3}{2}}}{2}\Delta_1+\frac{d2\sqrt{2}\sqrt{n}\triangle_1}{1-\beta_1}+\sqrt{2}n\beta_1^n\sum_{i=0}^{n-1}\|\nabla f_i(x_{1,0})\|_1\right]+G_4+G_5+G_6$;

$F_3 := \delta_1\left(\sqrt{\frac{2\rho_3^2}{\beta_2^n}}4n+G_7\right)\sqrt{D_1}\rho_1 d$;

$F_4 := \delta_1\left(\sqrt{\frac{2\rho_3^2}{\beta_2^n}}4n+G_7\right)\sqrt{D_1}\rho_1 d\sqrt{\frac{D_0}{D_1 d}}$.

Now, we discuss two cases.

Case (a): when $|\partial_\alpha f\left(x_{k,0}\right)| \geq 4\sqrt{2}\frac{\Delta_1}{(1-\beta_2)\sqrt{D_1 nkd}}$. In this case, we have the following result.

$$
\begin{aligned}
\frac{\partial_\alpha f(x_{k,0})^2}{\sqrt{v_{\alpha,k,0}}} &\geq \frac{\partial_\alpha f(x_{k,0})^2}{\sqrt{(1-\beta_2)\left(|\partial_\alpha f_{\tau_{k,0}}(x_{k,0})|^2+\beta_2|\partial_\alpha f_{\tau_{k-1,n-1}}(x_{k-1,n-1})|^2+\cdots\right)}} \\
&\geq \frac{\partial_\alpha f(x_{k,0})^2}{\sqrt{(1-\beta_2)\left(|\partial_\alpha f_{\tau_{k,0}}(x_{k,0})|^2+\beta_2|\partial_\alpha f_{\tau_{k-1,n-1}}(x_{k,0})+\triangle_{n(k-1)}|^2\cdots\right)}} \\
&\overset{\text{Lemma F.3}}{\geq} \frac{\partial_\alpha f(x_{k,0})^2}{\sqrt{(1-\beta_2)\left(\sum_{j=0}^{\infty}\left(\sqrt{|\partial_\alpha f\left(x_{k,0}\right)|^2+\frac{D_0}{D_1 d}}\sqrt{D_1 d}+\sum_{t=1}^{j}\Delta_{n(k-1)-t}\right)^2\beta_2^j\right)}} \\
&\geq \frac{\partial_\alpha f(x_{k,0})^2}{\sqrt{(1-\beta_2)\left(\sum_{j=0}^{\infty}\beta_2^j\left(\left(|\partial_\alpha f\left(x_{k,0}\right)|^2+\frac{D_0}{D_1 d}\right)D_1 d+4\sqrt{2}j\triangle_{nk}\sqrt{|\partial_\alpha f\left(x_{k,0}\right)|^2+\frac{D_0}{D_1 d}}\sqrt{D_1 d}+8j^2\triangle_{nk}^2\right)\right)}} \\
&\overset{\text{Lemma F.1}}{\geq} \frac{\partial_\alpha f(x_{k,0})^2}{\sqrt{D_1 d\left(\left(|\partial_\alpha f\left(x_{k,0}\right)|^2+\frac{D_0}{D_1 d}\right)+\sqrt{|\partial_\alpha f\left(x_{k,0}\right)|^2+\frac{D_0}{D_1 d}}\frac{4\sqrt{2}\triangle_{nk}}{(1-\beta_2)\sqrt{D_1 d}}+\frac{16\triangle_{nk}^2}{D_1 d(1-\beta_2)^2}\right)}} \\
&\overset{\text{Case (a)}}{\geq} \frac{\partial_\alpha f(x_{k,0})^2}{\sqrt{\frac{5}{2}D_1 d\left(|\partial_\alpha f\left(x_{k,0}\right)|^2+\frac{D_0}{D_1 d}\right)}},
\end{aligned}
$$

Now we consider the following two sub-cases.

- When $\partial_\alpha f(x_{k,0})^2 \leq \frac{D_0}{D_1 d}$:

$$
\begin{aligned}
& \frac{\partial_\alpha f\left(x_{k,0}\right)^2}{\sqrt{v_{\alpha,k,0}}}-F_2\frac{1}{\sqrt{k}}-F_3\left|\partial_\alpha f\left(x_{k,0}\right)\right|-F_4 \\
\geq\ & \frac{\partial_\alpha f\left(x_{k,0}\right)^2}{\sqrt{5D_0}}-F_2\frac{1}{\sqrt{k}}-F_3\sqrt{\frac{D_0}{D_1 d}}-F_4
\end{aligned}
$$

- When $\partial_\alpha f(x_{k,0})^2 \geq \frac{D_0}{D_1 d}$:

$$\begin{aligned}
&\frac{\partial_\alpha f\left(x_{k,0}\right)^2}{\sqrt{v_{\alpha,k,0}}} - F_2\frac{1}{\sqrt{k}} - F_3\left|\partial_\alpha f\left(x_{k,0}\right)\right| - F_4 \\
&\geq \frac{\left|\partial_\alpha f(x_{k,0})\right|}{\sqrt{5D_1 d}} - F_2\frac{1}{\sqrt{k}} - F_3\left|\partial_\alpha f\left(x_{k,0}\right)\right| - F_4 \\
&= \left|\partial_\alpha f\left(x_{k,0}\right)\right|\left(\frac{1}{\sqrt{5D_1 d}} - F_3\right) - F_2\frac{1}{\sqrt{k}} - F_4 \\
&\geq \left|\partial_\alpha f\left(x_{k,0}\right)\right|\left(\frac{1}{\sqrt{5D_1 d}} - F_3\right) - F_2\frac{1}{\sqrt{k}} - F_3\sqrt{\frac{D_0}{D_1 d}} - F_4
\end{aligned}$$

Combining together, we have the following results for **Case (a)**.

$$\left\{\frac{\partial_\alpha f\left(x_{k,0}\right)^2}{\sqrt{v_{\alpha,k,0}}}\right\} - F_2\frac{1}{\sqrt{k}} - F_3\left|\partial_\alpha f\left(x_{k,0}\right)\right| - F_4 \geq \min\left\{\frac{\partial_\alpha f(x_{k,0})^2}{\sqrt{5D_0}}, \left|\partial_\alpha f\left(x_{k,0}\right)\right|\left(\frac{1}{\sqrt{5D_1 d}} - F_3\right)\right\} - F_2\frac{1}{\sqrt{k}} - F_3\sqrt{\frac{D_0}{D_1 d}} - F_4.$$

Case (b): When $\left|\partial_\alpha f\left(x_{k,0}\right)\right| < 4\sqrt{2}\frac{\Delta_1}{(1-\beta_2)\sqrt{D_1 nkd}}$, we have

$$\begin{aligned}
\left\{\frac{\partial_\alpha f\left(x_{k,0}\right)^2}{\sqrt{v_{\alpha,k,0}}}\right\} - F_2\frac{1}{\sqrt{k}} - F_3\left|\partial_\alpha f\left(x_{k,0}\right)\right| - F_4 &\geq -F_2\frac{1}{\sqrt{k}} - F_3\left|\partial_\alpha f\left(x_{k,0}\right)\right| - F_4 \\
&\geq -F_2\frac{1}{\sqrt{k}} - F_3 4\sqrt{2}\frac{\Delta_1}{(1-\beta_2)\sqrt{D_1 nkd}} - F_4 \\
&= -\frac{1}{\sqrt{k}}G_1 - F_4, \qquad (67)
\end{aligned}$$

where $G_1 := F_2 + F_3 4\sqrt{2}\frac{\Delta_1}{(1-\beta_2)\sqrt{D_1 nd}}$. Now, the following two claims are both true.

- Claim 1:

$$(67) \quad \geq \quad \frac{\partial_\alpha f\left(x_{k,0}\right)^2}{\sqrt{5D_0}} - \frac{1}{k}\frac{\left(4\sqrt{2}\frac{\Delta_1}{(1-\beta_2)\sqrt{D_1 nd}}\right)^2}{\sqrt{5D_0}} - \frac{1}{\sqrt{k}}G_1 - F_4.$$

- Claim 2:

$$\begin{aligned}
(67) \quad \geq \quad & \left|\partial_\alpha f\left(x_{k,0}\right)\right|\left(\frac{1}{\sqrt{5D_1 d}} - F_3\right) - \frac{1}{\sqrt{k}}4\sqrt{2}\frac{\Delta_1}{(1-\beta_2)\sqrt{D_1 nd}}\left(\frac{1}{\sqrt{5D_1 d}} - F_3\right) \\
& -\frac{1}{\sqrt{k}}G_1 - F_4.
\end{aligned}$$

Combining Claim 1 and Claim 2, we have

$$\begin{aligned}
(67) \quad \geq \quad & \min\left\{\frac{\partial_\alpha f\left(x_{k,0}\right)^2}{\sqrt{5D_0}}, \left|\partial_\alpha f\left(x_{k,0}\right)\right|\left(\frac{1}{\sqrt{5D_1 d}} - F_3\right)\right\} - F_4 \\
& -\frac{1}{\sqrt{k}}\left[\max\left\{\frac{\left(4\sqrt{2}\frac{\Delta_1}{(1-\beta_2)\sqrt{D_1 nd}}\right)^2}{\sqrt{5D_0}}, \frac{4\sqrt{2}\Delta_1}{(1-\beta_2)\sqrt{D_1 nd}}\left(\frac{1}{\sqrt{5D_1 d}} - F_3\right)\right\} + G_1\right] \\
:= \quad & \min\left\{\frac{\partial_\alpha f\left(x_{k,0}\right)^2}{\sqrt{5D_0}}, \left|\partial_\alpha f\left(x_{k,0}\right)\right|\left(\frac{1}{\sqrt{5D_1 d}} - F_3\right)\right\} - \frac{1}{\sqrt{k}}G_2 - F_4, \qquad (68)
\end{aligned}$$

where $G_2 := \max\left\{ \frac{\left(4\sqrt{2}\frac{\Delta_1}{(1-\beta_2)\sqrt{D_1 nd}}\right)^2}{\sqrt{5D_0}}, \frac{4\sqrt{2}\Delta_1}{(1-\beta_2)\sqrt{D_1 nd}}\left(\frac{1}{\sqrt{5D_1 d}} - F_3\right)\right\} + G_1.$

Combining **Case (a)** and **Case (b)** together, we have

$$\begin{aligned}
\mathbb{E}\left\{\sum_{l \text{ large}}(a_1) + \sum_{l \text{ large}}(b_1) - \sum_{l \text{ large}}\{(a_2)+(b_2)\}\right\} &\geq \mathbb{E}\min\left\{\frac{\partial_\alpha f\left(x_{k,0}\right)^2}{\sqrt{5D_0}}, \left|\partial_\alpha f\left(x_{k,0}\right)\right|\left(\frac{1}{\sqrt{5D_1 d}} - F_3\right)\right\} \\
&\quad -\frac{1}{\sqrt{k}}G_2 - F_4 \\
&\geq \mathbb{E}\min\left\{\frac{\|\nabla f(x_{k,0})\|_2^2}{d\sqrt{5D_0}}, \|\nabla f(x_{k,0})\|_1\left(\frac{1}{d\sqrt{5D_1 d}} - \frac{F_3}{d}\right)\right\} \\
&\quad -\frac{1}{\sqrt{k}}G_2 - F_4,
\end{aligned}$$

where the last inequality is because of $\|\nabla f(x_{k,0})\|_2^2 \leq d\partial_\alpha f\left(x_{k,0}\right)^2$, $\|\nabla f(x_{k,0})\|_1 \leq d|\partial_\alpha f\left(x_{k,0}\right)|$. Recall $F_3 \to 0$ when $\beta_2 \to 1$, so there exists an interval $(1-\epsilon, 1]$, such that $\frac{1}{\sqrt{5D_1 d}} - F_3 \geq \frac{1}{\sqrt{10D_1 d}}$, or equivalently $F_3 \leq \frac{1}{\sqrt{10D_1 d}}$ (note that F_3 is the same as "$A(\beta_2)$" stated in the condition of Lemma G.6). With such a choice of β_2, we have the following results by changing all the F_3 into $\frac{1}{\sqrt{10D_1 d}}$:

$$\begin{aligned}
\mathbb{E}\left\{\sum_{l \text{ large}}(a_1) + \sum_{l \text{ large}}(b_1) - \sum_{l \text{ large}}\{(a_2)+(b_2)\}\right\} &\geq \mathbb{E}\min\left\{\frac{\|\nabla f(x_{k,0})\|_2^2}{d\sqrt{5D_0}}, \|\nabla f(x_{k,0})\|_1\frac{1}{d\sqrt{10D_1 d}}\right\} \\
&\quad -\frac{1}{\sqrt{k}}G_2 - F_4. \\
&\overset{(*)}{\geq} \frac{1}{d\sqrt{10D_1 d}}\mathbb{E}\min\left\{\sqrt{\frac{2D_1 d}{D_0}}\|\nabla f(x_{k,0})\|_2^2, \|\nabla f(x_{k,0})\|_1\right\} \\
&\quad -\frac{1}{\sqrt{k}}G_2 - F_5.
\end{aligned}$$

In inequality $(*)$, we change F_4 into $F_5 := \sqrt{\frac{D_0}{D_1 d}}\frac{1}{\sqrt{10D_1 d}}$. This is because: first, $F_4 = F_3\sqrt{\frac{D_0}{D_1 d}}$; second, $F_3 \leq \frac{1}{\sqrt{10D_1 d}}$.

The proof of Lemma G.6 is completed.

We restate all the constants as follows (G_4, G_5, G_6 are specified in Appendix G.7):

$G_2 := \max\left\{\frac{\left(4\sqrt{2}\frac{\Delta_1}{(1-\beta_2)\sqrt{D_1 nd}}\right)^2}{\sqrt{5D_0}}, \frac{4\sqrt{2}\Delta_1}{(1-\beta_2)\sqrt{D_1 nd}\sqrt{10D_1 d}}\right\} + G_1;$

$G_1 := F_2 + 4\sqrt{2}\frac{\Delta_1}{(1-\beta_2)\sqrt{D_1 nd}\sqrt{10D_1 d}};$

$F_2 := \delta_1\sqrt{\frac{2\rho_3^2}{\beta_2^n}}\left[\frac{d(n+1)n^{\frac{3}{2}}}{2}\Delta_1 + \frac{d2\sqrt{2}\sqrt{n}\triangle_1}{1-\beta_1} + \sqrt{2}n\beta_1^n\sum_{i=0}^{n-1}\|\nabla f_i(x_{1,0})\|_1\right] + G_4 + G_5 + G_6;$

$F_5 := \sqrt{\frac{D_0}{D_1 d}}\frac{1}{\sqrt{10D_1 d}}.$

Remark G.14. We comment that we can always replace F_5 in the final result by F_4, i.e., we can choose not to apply the last inequality $(*)$ in the proof. The benefit of using F_4 is that F_4 monotonously decrease to 0 when increasing β_2 to 1. This monotone property is not shown in the notation of F_5. Nevertheless, we choose to use F_5 since it is a much cleaner constant.

G.10 Proof of Lemma G.9

Based on Descent Lemma, we have

$$\begin{aligned}
\sum_{k=t_0}^{T} \frac{\eta_0}{\sqrt{nk}}(\text{r.h.s. of (35)}) &\leq \sum_{k=t_0}^{T} \mathbb{E}\left\langle \nabla f\left(x_{k,0}\right), x_{k,0}-x_{k+1,0}\right\rangle \\
&\leq \mathbb{E} f\left(x_{t_0,0}\right)-\mathbb{E} f\left(x_{T+1,0}\right)+\sum_{k=t_0}^{T} \frac{L}{2} \mathbb{E}\left\|x_{k+1,0}-x_{k,0}\right\|_2^2 \\
&\overset{(21)}{\leq} \mathbb{E} f\left(x_{t_0,0}\right)-f^*+\sum_{k=t_0}^{T} \frac{L d}{2}\left(\frac{n \eta_0}{\sqrt{n k}} \frac{(1-\beta_1)}{\sqrt{1-\beta_2}} \frac{1}{1-\frac{\beta_1}{\sqrt{\beta_2}}}\right)^2 \\
&= \mathbb{E} f\left(x_{t_0,0}\right)-f^*+\sum_{k=t_0}^{T} \frac{L d n}{2 k}\left(\eta_0 \frac{(1-\beta_1)}{\sqrt{1-\beta_2}} \frac{1}{1-\frac{\beta_1}{\sqrt{\beta_2}}}\right)^2
\end{aligned}$$

Plugging in the r.h.s. of (35), we have the following relation after rearranging.

$$\begin{aligned}
&\sum_{k=t_0}^{T} \frac{\eta_0}{\sqrt{nk}}\left[\frac{1}{d\sqrt{10 D_1 d}} \mathbb{E} \min\left\{\sqrt{\frac{2 D_1 d}{D_0}}\|\nabla f(x_{k,0})\|_2^2, \|\nabla f(x_{k,0})\|_1\right\}-\mathbb{E}\left[\mathcal{O}(\frac{1}{\sqrt{k}})\right]-\mathcal{O}(\sqrt{D_0})\right] \\
&\leq \mathbb{E} f\left(x_{t_0,0}\right)-f^*+\sum_{k=t_0}^{T} \frac{1}{k}\left[\frac{L d n}{2}\left(\eta_0 \frac{(1-\beta_1)}{\sqrt{1-\beta_2}} \frac{1}{1-\frac{\beta_1}{\sqrt{\beta_2}}}\right)^2\right].
\end{aligned}$$

Recall we have $2\left(\sqrt{T}-\sqrt{t_0-1}\right) \leq \sum_{k=t_0}^{T} \frac{1}{\sqrt{k}}, \sum_{k=t_0}^{T} \frac{1}{k} \leq \log \frac{T+1}{t_0}$. Further, since $\|\cdot\|_1 \geq\|\cdot\|_2$, we get the following relation when $t_0=1$.

$$\begin{aligned}
&\min_{k \in[1, T]} \mathbb{E}\left[\min\left\{\sqrt{\frac{2 D_1 d}{D_0}}\|\nabla f(x_{k,0})\|_2^2, \|\nabla f(x_{k,0})\|_2\right\}\right] \\
&\leq \frac{1}{\sqrt{T}} \frac{d \sqrt{10 D_1 d n}}{2 \eta_0}\left[\mathbb{E} f\left(x_{1,0}\right)-f^*+\log (T+1)\left(\frac{L d n}{2}\left(\eta_0 \frac{(1-\beta_1)}{\sqrt{1-\beta_2}} \frac{1}{1-\frac{\beta_1}{\sqrt{\beta_2}}}\right)^2+H_2\right)\right]+F_5,
\end{aligned} \tag{69}$$

We specify all the constant as follows. For all the following constants, We keep the same notation as their appearance in their corresponding lemmas.

$F_5 := \sqrt{\frac{D_0}{D_1 d}} \frac{1}{\sqrt{10 D_1 d}}$;

$H_2 := \frac{\eta_0(G_2+d F_1)}{\sqrt{n}}$;

$F_1 := \triangle_1 n^2 \sqrt{n} \frac{32 \sqrt{2}}{(1-\beta_2)^n \beta_2^n} \frac{1-\beta_1}{\sqrt{1-\beta_2}} \frac{1}{1-\frac{\beta_1}{\sqrt{\beta_2}}} n$;

$G_2 := \max\left\{\frac{\left(4 \sqrt{2} \frac{\triangle_1}{(1-\beta_2) \sqrt{D_1 n d}}\right)^2}{\sqrt{5 D_0}}, \frac{4 \sqrt{2} \triangle_1}{(1-\beta_2) \sqrt{D_1 n d} \sqrt{10 D_1 d}}\right\}+G_1$;

$G_1 := F_2+4 \sqrt{2} \frac{\triangle_1}{(1-\beta_2) \sqrt{D_1 n d} \sqrt{10 D_1 d}}$;

$F_2 := \delta_1 \sqrt{\frac{2 \rho_3^2}{\beta_2^n}}\left[\frac{d(n+1) n^{\frac{3}{2}}}{2} \triangle_1+\frac{d 2 \sqrt{2} \sqrt{n} \triangle_1}{1-\beta_1}+\sqrt{2} n \beta_1^n \sum_{i=0}^{n-1}\|\nabla f_i(x_{1,0})\|_1\right]+G_4+G_5+G_6$;

$$G_5 = d\sqrt{\frac{2\rho_3^2}{\beta_2^n}}\left(\frac{\beta_1^{2n}2n^3\triangle_1\sqrt{2}}{\sqrt{n}}\frac{1-\beta_1}{(1-\beta_1^n)^2} + n\left(1-\beta_1^{n-1}\right)\sum_{i=0}^{n-1}\mathbb{E}|\partial_\alpha f_i(x_{1,0})|\frac{(1-\beta_1)\beta_1^n\sqrt{2}}{1-\beta_1^n}\right);$$

$$G_4 = d\sqrt{\frac{2\rho_3^2}{\beta_2^n}}\beta_1^n\sqrt{2}n(n-1)\sum_{i=0}^{n-1}\mathbb{E}\left(|\partial_\alpha f_i(x_{1,0})|\right);$$

$$\begin{aligned}
G_6 \quad := \quad & \beta_1^n(1-\beta_1)\sqrt{2}\,|J_1|\sqrt{\frac{2\rho_3^2}{\beta_2^n}}\mathbb{E}\left[\sum_{l=1}^{d}\left|\mathbb{I}_1\sum_{i=0}^{n-1}\partial_l f_i(x_{1,0})\right|\right] + \frac{\triangle_1}{\sqrt{n}}\delta_2 d\sqrt{\frac{2\rho_3^2}{\beta_2^n}}(1-\beta_1)n^3 \\
& +d(1-\beta_1)|J_1|\frac{1}{1-\frac{1}{\sqrt{\beta_2^n}}}n^2\sqrt{\frac{2}{n\beta_2^n}}\frac{\triangle_1\delta_2}{\sqrt{n}} \\
& +d(1-\beta_1)|J_1|n^2\left(\sqrt{\frac{2\rho_3^2}{\beta_2^n}}\frac{1}{\left(1-\frac{(1-\beta_2)4n\rho_2}{\beta_2^n}\right)}\delta_1\right)\frac{1+\beta_1^n}{(1-\beta_1^n)^3}\frac{\triangle_1\sqrt{2}}{\sqrt{n}} \\
& +2(1-\beta_1)d\sqrt{\frac{2\rho_3^2}{\beta_2^n}}|J_1|n^2\frac{\triangle_1\delta_2\sqrt{2}}{\sqrt{n}} - 5(1-\beta_1)d\sqrt{\frac{2\rho_3^2}{\beta_2^n}}|J_1|n\frac{1}{(1-\beta_1^n)^2}\Delta_1 n\sqrt{n}\frac{32\sqrt{2}}{(1-\beta_2)^n\,\beta_2^n} \\
& +d\left(\frac{1}{1-\frac{1}{\sqrt{\beta_2^n}}}\sqrt{\frac{2}{n\beta_2^n}}\right)(1-\beta_1)(\beta_1+\beta_1^n)n^3\frac{\triangle_1}{\sqrt{n}}\delta_2 \\
& +d\sqrt{\frac{2\rho_3^2}{\beta_2^n}}\frac{1}{\left(1-\frac{(1-\beta_2)4n\rho_2}{\beta_2^n}\right)}\delta_1(1-\beta_1)(\beta_1+\beta_1^n)n^3\frac{1+\beta_1^n}{(1-\beta_1^n)^3}\frac{\triangle_1\delta_2\sqrt{2}}{\sqrt{n}} \\
& +2d\sqrt{\frac{2\rho_3^2}{\beta_2^n}}(1-\beta_1)(\beta_1+\beta_1^n)n^2\frac{1}{\beta_1^n(1-\beta_1^n)^2}\Delta_1 n\sqrt{n}\frac{32\sqrt{2}}{(1-\beta_2)^n\,\beta_2^n} \\
& +d\sqrt{\frac{2\rho_3^2}{\beta_2^n}}(1-\beta_1)\left(\beta_1+\beta_1^n\right)n^3\frac{\triangle_1}{\sqrt{n}}\delta_2,
\end{aligned}$$

$\Delta_1 := \eta_0\frac{L\sqrt{d}}{\sqrt{1-\beta_2}}\frac{1-\beta_1}{1-\frac{\beta_1}{\sqrt{\beta_2}}}$;

$\delta_1 := \frac{(1-\beta_2)4n\rho_2}{\beta_2^n} + \left(\frac{1}{\sqrt{\beta_2^n}} - 1\right)$;

where $J_1 = \left(-\frac{1}{n}\beta_1 - \frac{2}{n}\beta_1^2 - \cdots - \frac{n-1}{n}\beta_1^{n-1}\right)$, $\delta_2 = \lim_{k\to\infty}\sum_{j=1}^{k-1}(\beta_1^n)^j\sqrt{\frac{k}{k-j}} = \frac{\beta_1}{1-\beta_1}$. If needed, we can further bound J_1 by n for simplicity.

Further, ρ_1, ρ_2, ρ_3 are constants satisfying the following conditions for $\forall l = 1, \cdots, d$. Usually, these constants can be different for different problems. In the worst case, we have $0 \le \rho_3 \le \sqrt{n}\rho_1 \le n$. ρ_3 is larger when $\partial_l f_i(x_{k,0})$ are more aligned.

$\rho_1 \ge \frac{\sum_{i=1}^n|\partial_l f_i(x_{k,0})|}{\sqrt{\sum_{i=1}^n|\partial_l f_i(x_{k,0})|^2}}$;

$\rho_2 \ge \frac{|\max_i \partial_l f_i(x_{k,0})|^2}{\frac{1}{n}\sum_{i=1}^n|\partial_l f_i(x_{k,0})|^2}$;

$\rho_3 \ge \frac{\left|\sum_{i=1}^n \partial_l f_i(x_{k,0})\right|}{\sqrt{\frac{1}{n}\sum_{i=1}^n|\partial_l f_i(x_{k,0})|^2}}$.

The proof of Lemma G.9 is now completed. This also concludes the whole proof of Theorem 3.1.